THE ROLE OF UBIQUITINATION IN THE REGULATED TRAFFICKING OF GLUT4: A STUDY WITH YEAST AND ADIPOCYTES

A thesis submitted to the
FACULTY OF BIOMEDICAL AND LIFE SCIENCES

For the degree of
DOCTOR OF PHILOSOPHY

By Rebecca K McCann

Division of Biochemistry and Molecular Biology
Institute of Biomedical and Life Sciences
University of Glasgow

September 2007

Abstract

It has become increasingly apparent that, besides targeting proteins for proteasomal degradation, ubiquitination has a role in regulating the trafficking of proteins between intracellular compartments. One well-documented example of this is the nitrogen-regulated trafficking of the general amino acid permease, Gap1p, through the endosomal system of the yeast *Saccharomyces cerevisiae*. It has previously been noted that the nitrogen-regulated trafficking of Gap1p bears similarity to the insulin-regulated trafficking of the glucose transporter, GLUT4, in fat and muscle cells. Both proteins move from an intracellular location to the cell surface in response to an extrinsic trigger. In this thesis, I show that human GLUT4 is subject to nitrogen-regulated trafficking when expressed in yeast. Furthermore, I demonstrate that, like Gap1p trafficking in yeast, the regulated trafficking of GLUT4, both in yeast and in the insulin-sensitive cell line 3T3-L1 adipocytes, requires the ubiquitination of the transporter. A model in which ubiquitination is required for the sorting of GLUT4 into the insulin-responsive pool, from where it is mobilised to the cell surface in response to insulin, is presented and discussed.

Table of Contents

List of Tables

List of Figures

Acknowledgements

Firstly, I would like to thank my supervisor Dr. Nia Bryant for all of the support, advice and encouragement given throughout my PhD, but particularly for putting up with my *occasional* 'freak out' moments during the 'writing up' stage. :-) ;-) :-)

I would also like to thank Prof. David James and the rest of the James lab for making my time in Sydney so enjoyable, but would particularly like to thank Jacky Stoeckli for all of her help and for taking me through some of the techniques I used while there.

I thank all of the members of Lab 241 for any helpful comments, for making work in the lab so enjoyable, and of course for the essential stress-relief (pub) sessions. I'd particularly like to mention my colleagues, and now good friends, Jenny and Fiona, who have taught me the value of enjoying things in *moderation*, especially with respect to red wine.

I'd also like to thank the Bryant lab, Maz, Scott, Curly Chris and Tall Chris for all of the giggling and craziness and dress-up Fridays.

And to my labmate-in-crime, Lindsay Cog, thank-you for all of the 'time-out' Tinderbox trips, for introducing me to circwits, (for the singing, for the confidence boosts – BTW these two can stop now), and for being a best bud.

Finally, a huge loving thanks to my parental unit (and Iona) for the unending support, encouragement and for all of the reassurance that 'I'll get there'.

TA

Abbreviations

~	approximately
ABC	ATP-binding cassette
ADP	adenosine 5' diphosphate
ALP	alkaline phosphatase
AP	adaptor protein complex
APNE	*N*-acetyl-DL-phenylalanine β-naphthyl ester
AQP2	aquaporin-2
ARF	ADP ribosylation factor
AS160	Akt substrate of 160kDa
ATP	adenosine 5' triphosphate
AVP	arginine vasopressin
β-Me	β-mercaptoethanol
BSA	bovine serum albumin
°C	degrees celsius
CD-MPR	cation-dependent mannose-6-phosphate receptor
CEN	centromeric
CI-MPR	cation-independent mannose-6-phosphate receptor
cm	centimetre
CPY	carboxypeptidase Y
C-terminal	carboxyl terminal
$CuSO_4$	copper sulphate
Cu-MT	copper metallothionein
ddH_2O	double distilled water
DMEM	Dulbecco's modified Eagle's medium
DMF	dimethyl formamide
DMSO	dimethyl sulfoxide
DNA	deoxyribonucleic acid
DTT	dithiothreitol
DUB	deubiquitinating enzyme
E1	ubiquitin activating enzyme
E2	ubiquitin conjugating enzyme
E3	ubiquitin ligase
E.coli	*Escherichia coli*
ECL	enhanced chemiluminescence
EDTA	ethylenediaminetetraacetic acid
EEA1	early endosome antigen 1
ER	endoplasmic reticulum
FCS	foetal calf serum
FM4-64	N-(3-triethylammoniumpropyl)-4-(p-diethylaminophenyl-hexatrienyl) pyridium dibromide
5-FOA	5 fluoroorotic acid
g	gram
g	gravitational force
Gap1p	general amino acid permease
GAE	γ-adaptin ear
GAT	GGA and TOM
GFP	*aequorea victoria* green fluorescent protein
GGA	golgi localised γ-ear containing ARF binding protein

GLUT	glucose transporter protein isoform
GSC	GLUT4 storage compartment
GST	glutathione S-transferase
GSV	GLUT4 storage vesicle
H_2O_2	hydrogen peroxide
HA	influenza hemagglutinin epitope tag
HCl	hydrochloric acid
HDM	high-density microsome
HECT	homologous to the E6-AP carboxyl terminus
HEPES	2-[4-(2-Hydroxyethyl)-1-piperazine]ethanesulfonic acid
HES	HEPES, sucrose, EDTA
hr	hour
HRP	horseradish peroxidase
IgG	immunoglobulin G
IP	immunoprecipitation
IPTG	isopropyl-β-D-thiogalactopyranoside
IRS	insulin-receptor substrate
kb	kilobase of DNA
kDa	kiloDalton (atomic mass)
KCl	potassium chloride
K_2HPO_4	dipotassium hydrogen orthophosphate
KH_2PO_4	potassium dihydrogen orthophosphate
k_m	Michaelis constants
KOAc	potassium acetate
KOH	potassium hydroxide
KPi	potassium phosphates buffer,
L	litre
LDM	low density microsome
LiOAc	lithium acetate
LSB	laemmli sample buffer
μ	micro
M	molar
mA	milliamp
mg	milligram
$MgCl_2$	magnesium chloride
$MgSO_4$	magnesium sulphate
MHC II	major histocompatibility complex class II molecule
min	minute
MIU	motif interacting with ubiquitin
ml	millilitre
mM	millimolar
M/N	mitochondria/nuclei
MVB	multivesicular body
n	nano
NaCl	sodium chloride
Na_2HPO_4	disodium hydrogen orthophosphate
NaOH	sodium hydroxide
NCS	newborn calf serum
NEM	N-ethylmaleimide
NH_4^+	ammonium

NIDD	non-insulin dependent diabetes
NSF	N-ethylmaleimide-sensitive factor
OD_{600}	optical density at 600nm
OMP	orotine-5'-monophosphate
ORF	open reading frame
PBS	phosphate-buffered saline
PBST	0.1% (v/v) Tween-20 in PBS
PCR	polymerase chain reaction
PFA	paraformaldehyde
PI	phosphatidylinositol
PIPES	1,4-Piperazinediethanesulfonic acid
PKB	protein kinase B
PKC	protein kinase C
PM	plasma membrane
PMSF	phenylmethylsulphonyl fluoride
PTB	phosphotyrosine binding
PrA	protein A
PVC	prevacuolar compartment
Rab-GAP	Rab-GTPase activating protein
RING	really interesting new gene
RS-ALP	retention sequence ALP
rpm	revolutions per minute
S.cerevisiae	*Saccharomyces cerevisiae*
SD	yeast synthetic media, dextrose
SDM	site-directed mutagenesis
SDS	sodium dodecyl sulphate
SDS-PAGE	sodium dodecyl sulphate polyacrylamide gel electrophoresis
SH2	Src-homology-2
SM	yeast synthetic media, maltose
SNARE	soluble NSF attachment protein receptor
SOEing PCR	splicing by overlap extension polymerase chain reaction
SUMO	small ubiquitin-like modifier
TAE	tris-acetic acid-EDTA
TE	tris-EDTA
TEMED	N,N,N',N', - tetramethyl ethylene diamine
TfR	transferrin receptor
TGN	*trans*-Golgi network
t-SNARE	target-SNARE
TOM	target of MyB
Tris	2-amino-2-(hydroxymethyl)-1,3-propanediol
Ub	ubiquitin
UBA	ubiquitin associated domain
Ubc	ubiquitin conjugating enzyme
UBD	ubiquitin-binding domains
Ubl	ubiquitin-like
UBM	ubiquitin-binding motif
UEV	ubc E2 varient
UIM	ubiquitin-interacting motif
UTR	untranslated region
VAMP2	vesicle associated membrane protein

VHS	Vps27, Hrs, Stam
VPS	vacuolar protein sorting
v-SNARE	vesicle-SNARE
v/v	units volume per unit volume
w/v	units weight per unit volume
YPD	yeast extract, peptone, dextrose
YPM	yeast extract, peptone, maltose
YT	yeast extract, tryptone, NaCl
ZnF	zinc-finger domain

Chapter 1: Introduction

Chapter 1: Introduction

1.1. Type-2 Diabetes

Diabetes mellitus is characterised by persistent hyperglycemia (Saltiel and Kahn, 2001). In normal individuals, plasma glucose levels are maintained within a narrow range between 4 and 7mM (Saltiel and Kahn, 2001). This level rises following a carbohydrate meal due to the absorption of glucose from the intestine. The pancreatic β-cells sense this increase and respond by secreting insulin, which acts to lower the elevated plasma glucose levels in a number of ways, including, inhibiting hepatic glucose production, and increasing the uptake of glucose into fat and muscle tissues (Saltiel and Kahn, 2001). Conversely, under conditions of hypoglycemia, glucagons (secreted by the α-cells of the pancreas) raise plasma glucose levels by, for example, stimulating the breakdown of glycogen stored in the liver, and by activating gluconeogenesis (Figure 1.1 - taken from http://health.howstuffworks.com/diabetes1.htm).

In the disease state of diabetes, insulin fails to bring about the aforementioned decrease in plasma glucose levels (Saltiel and Kahn, 2001). Type-1 diabetes is characterised by the autoimmune-mediated destruction of pancreatic β-cell islets, leading to a failure of insulin production and/or insulin secretion (Zimmet et al., 2001). Type-1 diabetic sufferers must therefore take exogenous insulin for survival (Zimmet et al., 2001). Type-2 diabetes (also known as non-insulin-dependent diabetes, NIDD) is characterised by an underlying insulin resistance: a failure of normally insulin sensitive tissues, such as muscle and adipose, to respond to insulin and increase their glucose uptake (Zimmet et al., 2001). Hyperinsulinaemia often precedes the development of Type 2 diabetes as a compensatory response to insulin resistance, indicating that insulin resistance, rather than impaired insulin secretion, is involved in the development of Type 2 diabetes (DeFronzo, 1992). This, combined with an oversupply of glucose from the liver, results in high circulating plasma glucose levels, causing many of the complications associated with Type-2 diabetes, including eye, nerve, kidney and heart disease (Brownlee, 2001).

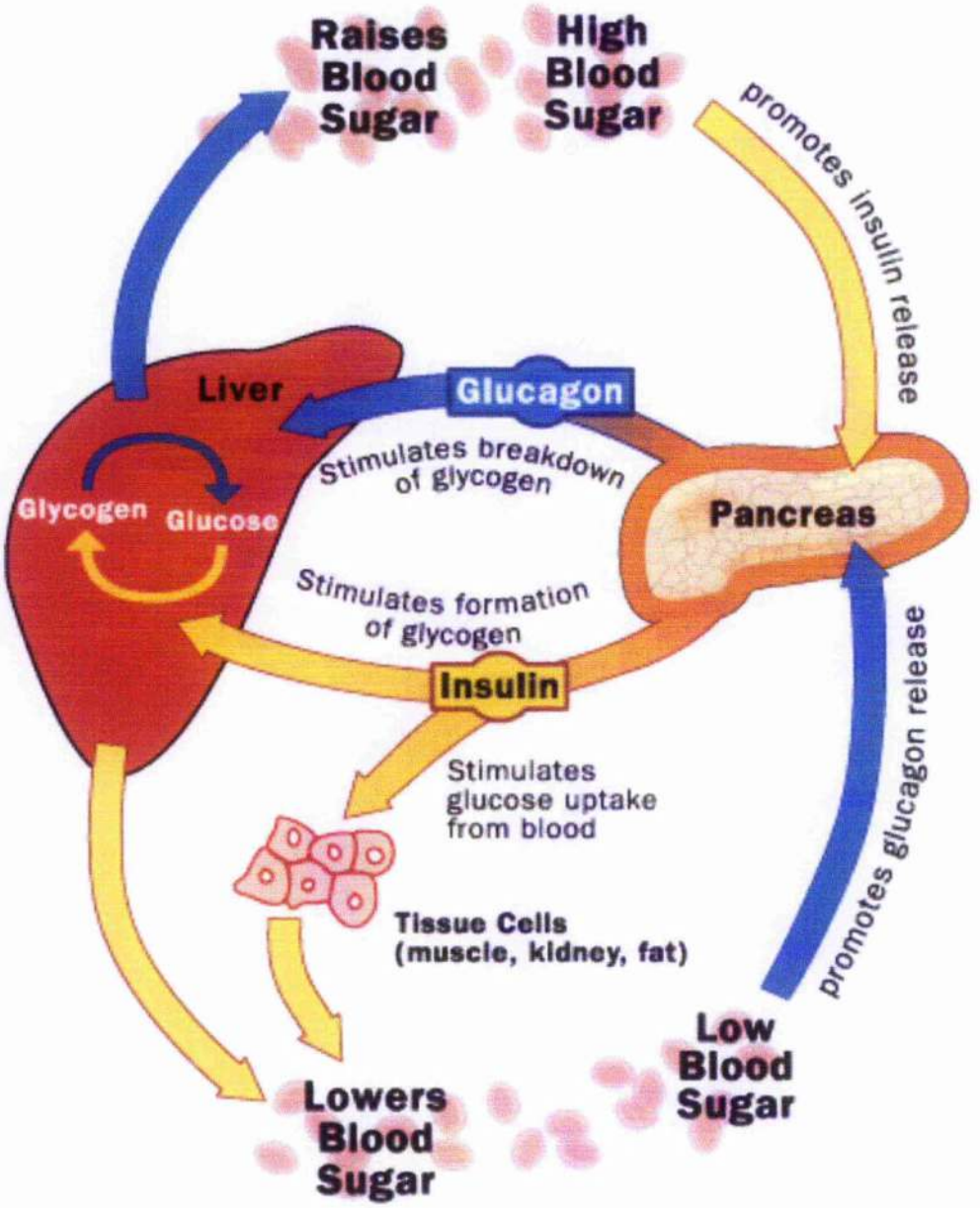

Figure 1.1. Schematic diagram showing factors that maintain blood sugar homeostasis

(taken from http://health.howstuffworks.com/diabetes1.htm)

The recent explosive increase in the number of people, worldwide, diagnosed with diabetes has led to the conviction that *diabetes mellitus* is now one of the major threats to human health in the 21st century (Zimmet et al., 2001). Globally, the incidence of diabetes has been estimated to increase from the present value of around 150 million, to 220 million by 2010; and this figure has been projected to increase further to 300 million by 2025 (Amos et al., 1997; King et al., 1998).

Although Type-1 diabetes is more commonly detected among children, its frequency among the general population is relatively low when compared to Type-2 diabetes, which accounts for over 90% of diabetic cases globally (Zimmet et al., 2001). Its increased prevalence among children and adolescents in various countries, including the UK, has underlined a serious new aspect of this epidemic, which is strongly associated with obesity and an inactive lifestyle (Zimmet et al., 2001). As a multifactorial disease, understanding Type-2 diabetes is an overwhelming task. It is not clear, for example, why the disease is particularly pronounced in certain ethnic groups, such as, Pacific and Indian Ocean Islanders, groups in India and Australian Aboriginal communities (Zimmet et al., 2001). What is clear is that insulin-resistance and Type-2 diabetes are disease states that constitute an enormous healthcare problem in both the developed and developing world. Understanding the actions of insulin will go a long way towards arming us to tackle this epidemic and this represents the overall goal of the work presented in this thesis.

1.2. Insulin Action

Following its secretion from the pancreas, insulin binds to its receptor on the surface of insulin-sensitive cells in its primary targets, skeletal muscle, adipose tissue and liver (Lee and Pilch, 1994; Sesti, 2006). The insulin receptor is a cell-surface heterotetrameric tyrosine kinase consisting of two extracellular α-subunits, which bind insulin, and two transmembrane β-subunits with tyrosine kinase activity (Lee and Pilch, 1994). The binding of insulin to the α-subunits of the receptor induces the transphosphorylation of one of the β-subunits by the other which, in turn, results in the increased catalytic activity of the kinase (Saltiel and Pessin, 2003; Watson et al., 2004a). The activated insulin receptor catalyses the tyrosine phosphorylation of a number of intracellular substrates, including members of the insulin-receptor substrate (IRS) family, IRS1/2, Shc, Cbl and APS (Saltiel and Kahn, 2001). The phosphorylated tyrosines of these substrates act as docking sites for

signalling proteins containing Src-homology-2 (SH2) or phosphotyrosine binding (PTB) domains (Czech and Corvera, 1999; Saltiel and Kahn, 2001), triggering a series of signalling cascades that regulate a plethora of cellular processes; including vesicle trafficking, protein synthesis, enzyme activation and inactivation, and gene expression (Czech and Corvera, 1999; Saltiel and Kahn, 2001). The IRS family of proteins are the best-characterised intracellular substrates to be phosphorylated by the insulin receptor. They interact with a variety of SH2 domain containing effector molecules, but perhaps most importantly with the p85 regulatory subunit of phosphatidylinositol (PI) 3-kinase, which has an essential role in insulin-stimulated glucose uptake and GLUT4 translocation, likely through its downstream targets, the serine/threonine kinase Akt/protein kinase B (PKB) and the atypical protein kinase C (PKC) isoform PKCζ (Czech and Corvera, 1999). The exact mechanism(s) by which PKB and PKCζ regulate glucose transport remains undefined but one particular downstream target of Akt/PKB, the protein Akt substrate of 160kDa (AS160), has the potential in providing a functional link between the insulin signalling cascade and glucose uptake (Watson and Pessin, 2006). AS160 contains multiple Akt/PKB phosphorylation sites in addition to a Rab-GTPase activating protein (Rab-GAP) domain (Sano et al., 2003). As Rab proteins regulate several steps of membrane transport, such as vesicle budding, motility, tethering and fusion (Zerial and McBride, 2001), AS160 could translate the information carried by the insulin-signalling cascade into molecular events that result in glucose uptake (Watson and Pessin, 2006).

One of the major consequences of insulin binding to its receptor on fat and muscle cells is the translocation of the facilitative glucose transporter 4 (GLUT4) from an intracellular store to the plasma membrane (reviewed in (Bryant et al., 2002) Figure 1.2). Following this translocation, GLUT4 proteins transport glucose across the plasma membrane according to a model of alternate conformation (Mueckler, 1994). This model predicts that the transporter exposes a single substrate binding site toward the outside of the cell. The binding of glucose to this site provokes a conformational change associated with transport, and releases glucose to the other side of the membrane (Mueckler, 1994). This allows the rapid movement of glucose, down its concentration gradient, from the interstitial fluid into the fat or muscle cell, thereby increasing the uptake of glucose into muscle and adipose tissue and reducing the levels of plasma glucose (Bryant et al., 2002).

Insulin resistance is associated with insufficient recruitment of GLUT4 to the plasma membrane, despite there being normal GLUT4 expression (Bjornholm and Zierath, 2005). Therefore, understanding the precise molecular mechanisms that control the insulin-regulated translocation of GLUT4 is a major focus of current research. Understanding this process could provide specific therapeutic targets to help treat and/or prevent Type-2 diabetes.

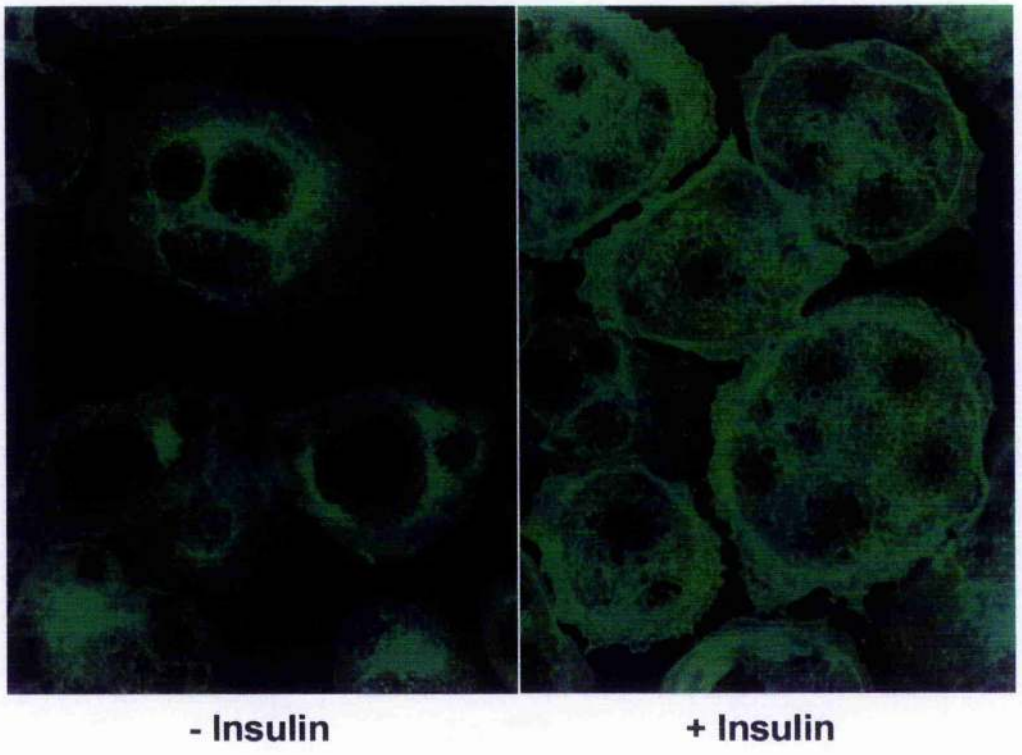

Figure 1.2. GLUT4 translocation in 3T3-L1 adipocytes.

A confocal image of 3T3-L1 adipocytes either treated with 100nM insulin for 15 mins (right panel), or not (left panel). GLUT4 localisation was visualised using an antibody that specifically recognizes the transporter and a secondary antibody conjugated to alexa-488 (green). Taken from (Bryant et al., 2002)).

1.3. GLUT4

GLUT4 is a member of a large family of facilitative sugar transporters, known as GLUTs, which distribute glucose throughout various tissues of the body (Gould and Bell, 1990; Mueckler, 1994; Olson and Pessin, 1996). GLUTs are highly related proteins, each predicted to span the membrane twelve times with both their amino- and carboxyl- termini located in the cytosol (Figure 1.3) (Joost and Thorens, 2001).

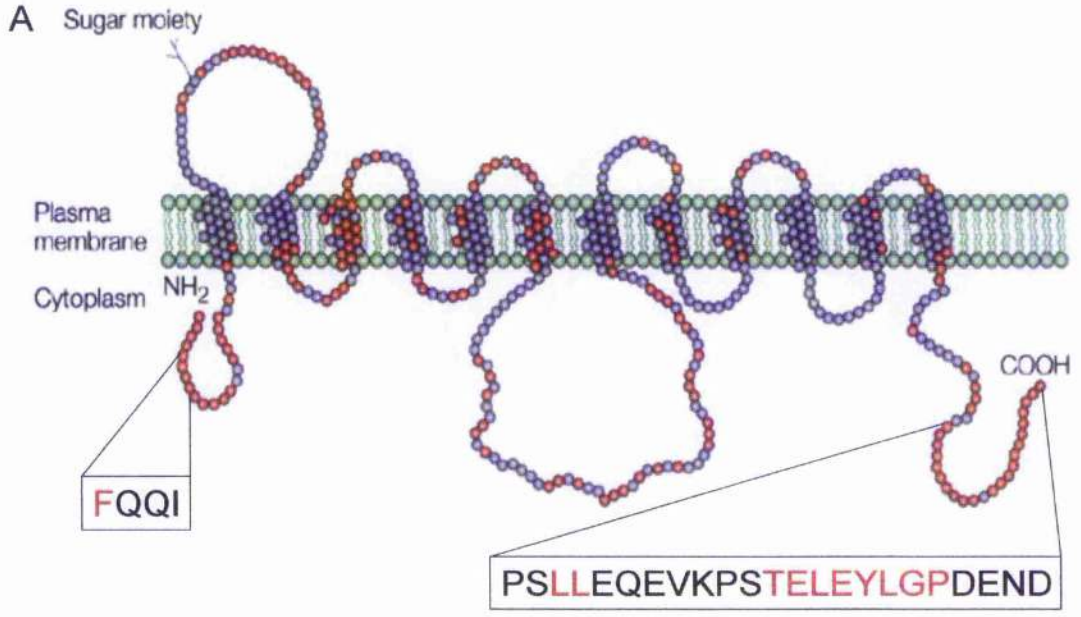

Figure 1.3. Targeting motifs of GLUT4 and Gap1p

A) Schematic diagram of the predicted membrane topology of GLUT4 indicating of the position of the targeting motifs (highlighted in red) (discussed in Section 1.5 (adapted from (Bryant et al., 2002)). B) Sequence of the C-terminal tail of Gap1p (residues 570-601), indicating important targeting motifs (highlighted in red) (discussed in Section 1.8 (adapted from (Hein and Andre, 1997)).

As facilitative carriers, GLUT proteins act as shuttles to transport glucose down its concentration gradient in an energy-independent manner (Watson et al., 2004a). There are

thirteen known members of the GLUT family, each of which differ in their tissue distribution and kinetic properties as well as in their intracellular localization: together, these allow for the acute regulation of glucose transport into various body tissues under various physiological conditions (Gould and Bell, 1990; Mueckler, 1994; Olson and Pessin, 1996). For example, mammalian tissues such as the brain, which require a constant supply of glucose, contain glucose transporters with a high affinity for glucose that are constitutively targeted to the cell surface, a property specific to GLUT1 and GLUT3 (Thorens, 1996). High affinity transporters such as GLUT1, GLUT3 and GLUT4 have Michaelis constants (K_m) well below the normal blood glucose concentration, and so their levels of cell surface expression determines the flux of glucose into the cell (Thorens, 1996). Certain tissues, such as muscle and adipose, require a more regulated glucose transport system and have adapted methods to rapidly up-regulate their glucose transport rates in response to an extracellular stimulus (Bryant et al., 2002). Such systems enable the body to control the large fluctuations in blood glucose levels after a meal and supply skeletal muscle with the extra glucose it requires during exercise (Bryant et al., 2002). GLUT4, primarily expressed in skeletal muscle and adipose tissue is responsible for the insulin-stimulated transport of glucose into fat and muscle cells and for the increased transport of glucose into skeletal muscle during exercise (Bryant et al., 2002; Olson and Pessin, 1996; Watson et al., 2004a). Under basal conditions, in the absence of insulin, GLUT4 is retained intracellularly, but is mobilised (translocated) to the plasma membrane in response to insulin (Bryant et al., 2002; Watson et al., 2004a). This translocation of GLUT4 to the plasma membrane accounts for the increased transport of glucose into fat and muscle cells in response to insulin (Bryant et al., 2002; Watson et al., 2004a).

Despite the fact that the intracellular trafficking of GLUT4 has been intensely studied for nearly 20 years, two fundamental questions remain largely unanswered (Bryant et al., 2002).

- How does insulin cause the release of GLUT4 from the intracellular compartment(s) that it occupies under basal conditions?

- How is GLUT4 sorted into the location from which it is released in response to insulin?

1.4. Intracellular trafficking of GLUT4

As noted above (Section 1.3 and Figure 1.2) GLUT4 is almost entirely sequestered within intracellular compartments and excluded from the plasma membrane of adipocytes in the absence of insulin (reviewed in (Bryant et al., 2002)). GLUT4 has been localised to a variety of intracellular organelles, including, sorting and recycling endosomes, the *trans*-Golgi network (TGN), the plasma membrane and vesicles that mediate transport between these compartments. This range of intracellular localisations for GLUT4 indicates a complex intracellular trafficking itinerary that adds to the complexity surrounding the debate regarding GLUT4 intracellular trafficking (reviewed in (Bryant et al., 2002)).

Although GLUT4 clearly overlaps to some extent with endocytic markers such as the transferrin receptor (TfR), a significant proportion of GLUT4 does not co-localise with the TfR, suggesting that endosomes do not represent the major storage compartment of GLUT4 in adipocytes (Livingstone et al., 1996). Furthermore, detailed analysis of GLUT4 traffic to and from the cell surface in non-insulin-stimulated adipocytes highlights that the rate of GLUT4 exocytosis is approximately 10-fold slower than that of the TfR (which is regarded as one of the most well studied constitutive recycling proteins in mammalian cells) (Holman et al., 1994; Tanner and Lienhard, 1987). This indicates that GLUT4 must be selectively retained either within a more static secretory pool, or involved in a dynamic cycle that is distinct from recycling endosomes. In support of this, chemical ablation of endosomes upon the uptake of horseradish peroxidase (HRP) conjugated transferrin not only demonstrated that only 30-40% of intracellular GLUT4 is subject to ablation (Livingstone et al., 1996; Martin et al., 1996), but also that chemical ablation of endosomes does not affect the insulin-stimulated translocation of GLUT4 in adipocytes (Martin et al., 1998).

Immunogold labelling of GLUT4 identified a proportion of GLUT4 (~13% of total GLUT4 distribution in basal cells), that is present in the TGN of both muscle and fat cells (Slot et al., 1991a; Slot et al., 1991b). Furthermore, GLUT4 co-localises significantly with proteins known to traffic between the TGN and endosomes, including the cation-dependent mannose 6-phosphate receptor (CD-MPR) (Martin et al., 2000b), the cation-independent mannose 6-phosphate receptor (CI-MPR) (Kandror and Pilch, 1996b) and adaptor protein complex-1 (AP-1) (Martin et al., 2000b). This suggests the possibility of a recycling

pathway for GLUT4 between the TGN and endosomes. Following internalised GLUT4 from the adipocyte cell surface (Palacios et al., 2001) demonstrated that GLUT4 transits through endosomes (localising with the early endosomal marker EEA1 at early time points) to the TGN (localising with the SNARE proteins syntaxin 6 and syntaxin 16 at later time points after internalisation) (Shewan et al., 2003).

As well as there being evidence to support the intracellular retention of GLUT4 within a recycling loop between endosomes and the TGN (discussed above), the use of both morphological and biochemical techniques identified a discrete portion of small (50nm diameter) GLUT4-containing vesicles (Hashiramoto and James, 2000; Kandror and Pilch, 1996a; Ramm et al., 2000), supporting the presence of a pool of GLUT4-containing membranes, devoid of GLUT1 and other non-insulin regulated cargo, that move directly to the plasma membrane in response to insulin. This population of, somewhat ill-defined, vesicles are highly responsive to insulin and are often referred to as GLUT4 storage vesicles (GSVs) (Rea and James, 1997). GSVs have been found to exclude other recycling proteins, such as the TfR and the CD-MPR, but importantly, do contain the v-SNARE, vesicle associated membrane protein (VAMP2) (Ramm et al., 2000), which has previously been shown to facilitate the exocytosis of synaptic vesicles to the plasma membrane. VAMP2 forms a functional SNARE complex with the t-SNAREs Syntaxin 4 and SNAP23 (Kawanishi et al., 2000), which are highly enriched at the plasma membrane of fat and muscle cells (Thurmond and Pessin, 2001). Formation of a SNARE complex between VAMP2 present in GSVs and Syntaxin 4/SNAP23 at the cell surface likely results in the delivery of GLUT4 from GSVs to the plasma membrane.

It is worth noting that the two models of intracellular sequestration of GLUT4 discussed here are not mutually exclusive. In the absence of insulin, GSVs are likely to represent a dynamic storage pool of GLUT4, in constant movement between the TGN and endosomes (Bryant et al., 2002). Otherwise, the endosomal and TGN pools would become depleted of GLUT4; to account for this models in which, in the absence of insulin, GSVs constantly re-enter the endosomal system have been proposed (Bryant et al., 2002).

1.5. GLUT4 Targeting Motifs

A variety of studies have been focussed on the goal of identifying specific targeting motifs in the primary sequence of GLUT4. By examining the subcellular distribution of either GLUT4 point mutants, or chimeras comprised of different portions of GLUT4 and GLUT1 (the glucose transporter isoform constitutively targeted to the cell surface), two distinct trafficking motifs in the cytosolic amino and carboxyl termini were identified in GLUT4 (Marshall et al., 1993; Piper et al., 1992; Verhey et al., 1993); a phenylalanine-based motif, $FQQI^{5-8}$, located in the N-terminus and a dileucine motif, $LL^{489-490}$, in the C-terminus (Figure 1.3). These motifs fall into two categories of structurally unrelated transport motifs (so called phenylalanine/tyrosine and dileucine based motifs) that are shared by a variety of other membrane proteins (Lalioti et al., 2001). These motifs have the ability to recruit clathrin adaptors (such as AP1 and AP2) to membranes and thereby facilitate in the packaging of membrane proteins into clathrin-coated vesicles for further transport (Lalioti et al., 2001). Originally, the $FQQI^{5-8}$ and $LL^{489-490}$ motifs in GLUT4 were shown to function as internalisation motifs in the process of endocytosis (Garippa et al., 1996; Garippa et al., 1994; Kao et al., 1998; Piper et al., 1993; Verhey et al., 1995); at the cell surface, GLUT4 is localised to AP-2/clathrin coated pits and is endocytosed via a clathrin-mediated process (Kao et al., 1998; Robinson et al., 1992), this process was shown to be regulated by the N-terminal $FQQI^{5-8}$ and C-terminal $LL^{489-490}$ motifs (Garippa et al., 1996; Garippa et al., 1994; Marsh et al., 1995; Piper et al., 1993; Verhey et al., 1995). However, further analysis revealed additional roles for these motifs in the intracellular sorting and sequestration of GLUT4 and they have been proposed to function at distinct intracellular sorting steps (Melvin et al., 1999).

Mutation of the phenylalanine^5 (Phe^5) residue of GLUT4 causes the transporter to accumulate at the cell surface of unstimulated adipocytes (Marsh et al., 1995). This mutant also displays an enhanced susceptibility to endosomal ablation with Tfn-HRP as compared to the wild type GLUT4 (Melvin et al., 1999). By following the internalisation of GLUT4 from the adipocyte cell surface, it was also found that Phe^5 mutagenesis inhibits the recycling of endocytosed GLUT4 to the GLUT4 storage compartment and results in its mis-targeting to late endosomes/lysosomes (co-localising with the late endosomal/lysosomal marker, LIMPIII) where it undergoes rapid degradation (Palacios et al., 2001). These data indicate a role for Phe^5 of GLUT4 in regulating its intracellular

sorting at the levels of both endocytosis and entry into the GLUT4 storage compartment. Examination of the trafficking of newly synthesised GLUT4 (studied at short time intervals within 2-12hr post-transfection), indicates that the transporter moves from the TGN directly to the GLUT4 storage compartment, without first transiting the plasma membrane (Watson et al., 2004b). Analyses of a variety of GLUT4/GLUT1 chimera proteins indicate that this transport step relies upon sequences in both the amino terminus and the large cytoplasmic loop, between transmembrane domains 6 and 7 (Khan et al., 2004).

A role for the dileucine$^{489-490}$ (diLeu$^{489-490}$) motif in the intracellular sorting of GLUT4 was recognised when diLeu$^{489-490}$/AA mutants were found to show increased resistance to endosomal ablation (Melvin et al., 1999), and exhibit increased cell surface distribution in basal adipocytes at high levels of expression (Marsh et al., 1995). This indicates a role for the diLeu$^{489-490}$ motif, most likely at the TGN, as endosomal ablation does not significantly affect this compartment (Livingstone et al., 1996). Moreover, it was found that diLeu$^{489-490}$ mutants were retained in the TGN, leading to their exclusion from the GLUT4 storage compartment (Martinez-Arca et al., 2000). A major phosphorylation site in GLUT4, serine^{488}, which resides adjacent to the diLeu$^{489\ 490}$ motif, may play a role in the intracellular sorting of GLUT4 at the TGN, as the co-localisation of GLUT4 and the clathrin adaptor protein AP1 in intracellular vesicles is enhanced when this residue is mutated (Marsh et al., 1998).

Additional analyses of chimeric transporter proteins in insulin-responsive cells led to the suggestion of there being additional targeting information, besides the diLeu$^{489-490}$ motif, in the C-terminus of GLUT4 (Haney et al., 1995; Verhey et al., 1995). A C-terminal truncation mutant of GLUT4, lacking the last five residues, is mis-targeted to late endosomes following trafficking through the TGN of fibroblasts (Martinez-Arca et al., 2000), and mutation of the diLeu$^{489-490}$ motif in the context of this GLUT4 truncation mutant reveals a role in sorting to the GLUT4 storage compartment from the TGN (Martinez-Arca et al., 2000). In addition, mutagenesis of a potential protein tyrosine kinase and phosphatase substrate, tyrosine^{502}, within the truncation mutant, was shown to control the exit of GLUT4 from the GLUT4 storage compartment (Martinez-Arca et al., 2000). Further evidence to indicate the importance of the extreme C-terminus of GLUT4 in intracellular targeting was highlighted by the disruption of the acidic motif,

TELEYLGP[498-505], distal to the diLeu[489-490] motif, resulting in mutants being more susceptible to endosomal ablation, implying a role for this motif in the endocytic sorting of GLUT4 (Shewan et al., 2000). Given that GLUT4 was shown to traffic rapidly from the cell surface, via the early endosomal system, to a perinuclear compartment enriched in the TGN t-SNAREs, Syntaxin 6 and 16 (Shewan et al., 2003), SNAREs previously implicated in the trafficking of material between endosomes and the TGN (Mallard et al., 2002), these data suggest that this C-terminal acidic targeting domain regulates the trafficking of GLUT4 to this perinuclear Syntaxin 6/16-positive compartment (Shewan et al., 2003).

1.6. A model for GLUT4 transport

The apparent complexity that surrounds the intracellular trafficking itinerary of GLUT4 is highlighted by the finding that under basal conditions GLUT4 can be found distributed, to varying degrees, throughout the majority of intracellular membrane systems. The numerous studies outlined in Section 1.4 led to the proposal of a working model that could accommodate many of the apparently contradictory observations (Figure 1.4) (Bryant et al., 2002). This model suggests that GLUT4 is selectively targeted into an intracellular transport loop between the TGN and endosomes (cycle 2, Figure 1.4) in a seemingly futile cycle, which serves to exclude GLUT4 from the cell-surface recycling pathway (cycle 1, Figure1.4). Contained within this intracellular transport loop is the intracellular store of GLUT4, which, in the absence of insulin, moves slowly from the TGN to fuse with endosomes. In the presence of insulin, however, this intracellular store is released from the cycle and able to fuse directly with the plasma membrane. There are several lines of evidence that support the existence of a unique pool of GLUT4 vesicles that can fuse directly with the plasma membrane in response to insulin. However, in the absence of insulin, this population of vesicles is highly unlikely to remain a static body (as discussed before, at the end of Section 1.4). If this were the case, the endosomal and TGN stores of GLUT4 would soon become depleted and all the GLUT4 would be present in GSVs. Therefore, it seems likely that GSVs slowly fuse with endosomes, thus allowing GLUT4 to re-enter the endosomal system.

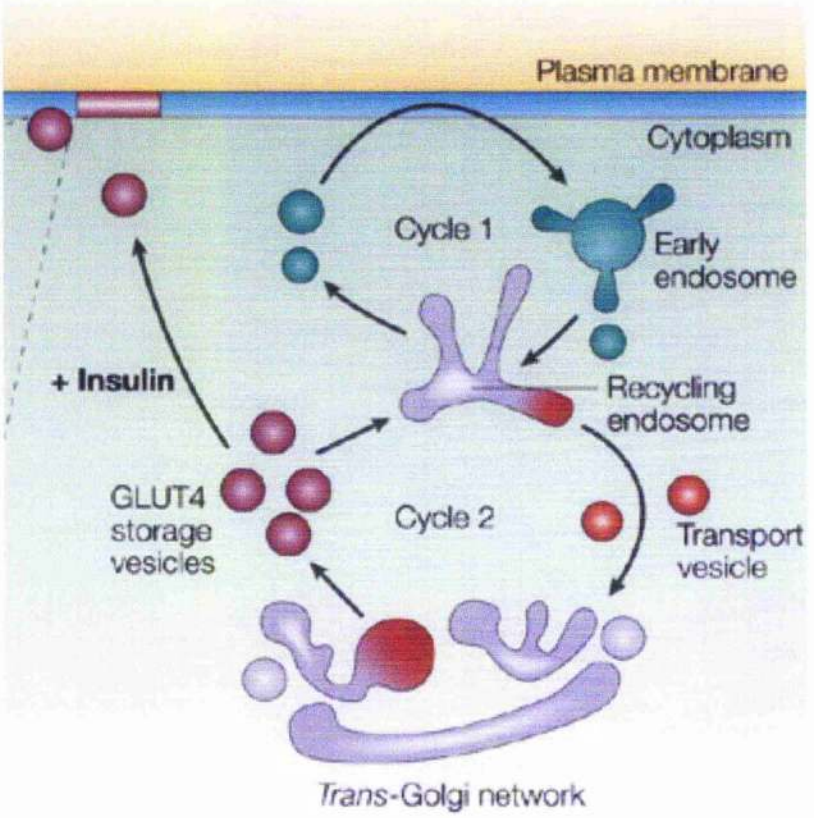

Figure 1.4. A model depicting the insulin-regulated trafficking of GLUT4
Details are described in Section 1.6. Taken from (Bryant et al., 2002).

One of the major problems with the study of insulin-regulated GLUT4 trafficking is that, as terminally differentiated cells, fat and muscle are hard to work with experimentally (Quon et al., 1993). For example, they are notoriously difficult to transfect, giving inefficient and irreproducible results (Quon et al., 1993). As a consequence of this, the expression of exogenous constructs requires the use of viral expression vectors (Hertzel et al., 2000). This is an expensive and time-consuming process, and therefore not one to be taken lightly. A common approach used to circumvent such a problem is to use an experimentally tractable eukaryote system, such as the budding yeast *Saccharomyces cerevisiae* (Baker's yeast) (Broach et al., 1991; Guthrie and Fink, 1991). However, since yeast neither responds to insulin, nor express GLUT4, it is not the immediately obvious model system in which to study the insulin-regulated trafficking of GLUT4.

1.7. Yeast as a system to study GLUT4 trafficking

S. cerevisiae is a well-established and powerful tool that has greatly furthered the knowledge of many aspects of cell biology, including membrane trafficking (Broach et al., 1991; Guthrie and Fink, 1991). Until recently, it was thought that yeast are not subject to regulated membrane trafficking events akin to the insulin-regulated trafficking of GLUT4. It is now clear that yeast do indeed possess a regulated membrane trafficking step that bears remarkable similarity to the insulin-regulated trafficking of GLUT4; that is the nitrogen regulated trafficking of the general amino acid permease Gap1p. The general amino acid permease Gap1p is stored intracellularly under nutrient rich conditions (Roberg et al., 1997). However, when nutrients are limited, Gap1p is trafficked to the plasma membrane where it facilitates the uptake of amino acids from the extracellular media (illustrated in Figure 1.5b) (Roberg et al., 1997). This regulated trafficking bears many striking similarities to that of GLUT4 in insulin-sensitive cells and accounts for the increase in levels of Gap1p on the cell surface of yeast in response to nitrogen availability (Roberg et al., 1997). On preferred sources of nitrogen, such as glutamate, Gap1p is transported to the yeast endosomal system (Figure 1.5b) (Roberg et al., 1997). In contrast, when cells are grown on non-preferred sources of nitrogen, such as proline, Gap1p is sorted from an intracellular storage pool to the cell surface, where it allows amino acids into the cell for use as a nitrogen source (Figure 1.5b) (Roberg et al., 1997).

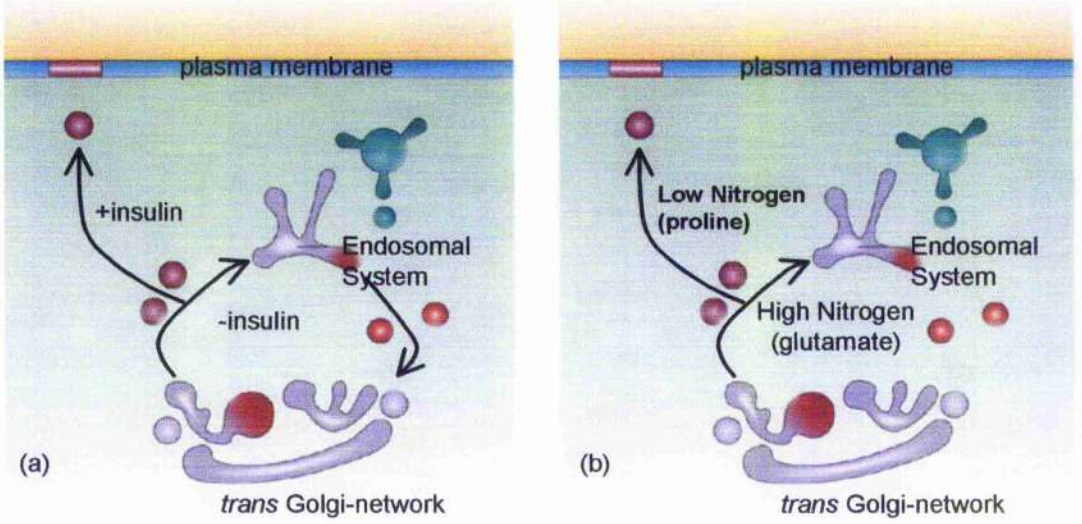

Figure 1.5. Comparison of insulin-regulated GLUT4 trafficking in adipocytes (a) with nitrogen-regulated Gap1p trafficking in S.cerevisiae (b)

(adapted from (Bryant et al., 2002))

Like GLUT4, Gap1p is predicted to span the membrane twelve times (Jauniaux and Grenson, 1990) and, intriguingly, contains motifs in the cytosolic carboxyl-terminal domain that are analogous to those involved in GLUT4 trafficking (Hein and Andre, 1997). The carboxyl-terminal tail of GLUT4 contains several motifs required for its insulin-regulated trafficking (Lalioti et al., 2001) (outlined in Section 1.5) that, when mutated, result in a loss of insulin-stimulated translocation (Lalioti et al., 2001). When the carboxyl-terminal tail of GLUT4 is replaced with the equivalent region from the yeast protein Gap1p, resulting in a GLUT4/Gap1p chimeric protein, the chimera exhibits a similar trafficking response to insulin as endogenous GLUT4 (Figure 1.6, Nia Bryant and David James; unpublished results). In the absence of insulin, the chimera, like endogenous GLUT4, co-localises with the TGN marker, TGN38 (Figure 1.6a). Upon insulin stimulation, again like GLUT4 itself, the chimera translocates to the plasma membrane (Figure 1.6a). Fractionation of 3T3-L1 adipocytes (shown in Figure 1.6b, Nia Bryant and David James; unpublished results) also shows an insulin-dependent movement of the chimera out of the intracellular membrane (LDM) fraction to the plasma membrane (PM) fraction. The transferrin receptor (TfR), however, remained unaffected in these same cells. These data indicate that the targeting motifs and the molecular machinery that control the regulated trafficking of Gap1p and GLUT4 is conserved throughout evolution.

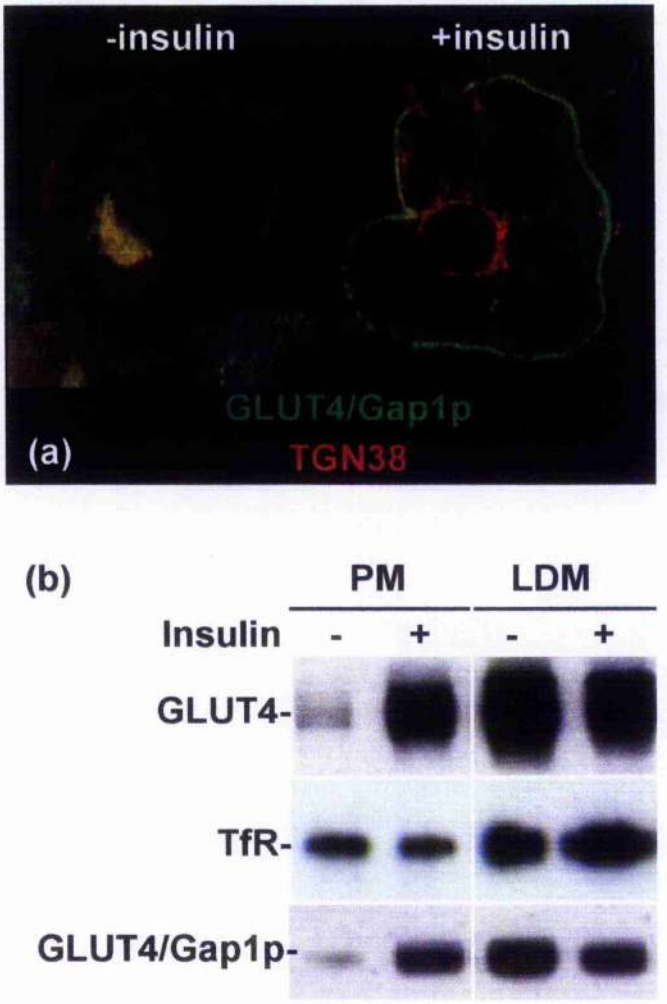

Figure 1.6. The C-terminal tail of Gap1p directs GLUT4 to the plasma membrane in an insulin-dependent manner

(unpublished data; Nia Bryant and David James).

A chimeric protein in which the C-terminal tail of GLUT4 was replaced with the analogous region from the yeast protein, Gap1p (GLUT4/Gap1p) carrying an HA-tag, was expressed in 3T3-L1 adipocytes using a retroviral expression vector. Cells were either treated with 10nM insulin (+insulin) or vehicle alone (-insulin), before the following procedures were performed: (a) indirect immunofluorescence microscopy using an anti-HA antibody was used to visualise the chimera. (b) differential centrifugation was used to generate fractions enriched in either plasma membrane (PM) or intracellular GLUT4 membranes (LDM; low density microsomes). These fractions were subjected to SDS-PAGE and immunoblot analysis.

1.8. The general amino acid permease, Gap1p

The *S. cerevisiae* genome encodes a family of around twenty related amino acid permeases, which are delivered by the secretory pathway to the plasma membrane and function to allow amino acids into the cell for use in protein synthesis and as a source of nitrogen (Andre, 1995). These permeases can be divided into two distinct classes according to their regulation and function (Sophianopoulou and Diallinas, 1995). Constitutive permeases are usually high affinity permeases that transport either specific amino acids, or a set of chemically related compounds, and are expressed in yeast regardless of the nitrogen conditions (Horak, 1986). Included within this class of permeases are the histidine permease, Hip1p (Tanaka and Fink, 1985) and the lysine permease, Lyp1p (Sychrova and Chevallier, 1993). This class of permeases are thought to transport amino acids primarily for use in protein synthesis (Andre, 1995). It is the second class of permeases, regulated permeases, that includes the general amino acid permease, Gap1p, (which can transport all naturally occurring amino acids) (Grenson et al., 1970; Jauniaux and Grenson, 1990) and Put4p (which transports proline) (Lasko and Brandriss, 1981; Vandenbol et al., 1989). Regulated permeases are induced by growth on poor nitrogen sources and Gap1p is thought to play a pivotal role in the control of nitrogen metabolism, since it transports amino acids that are both substrates for, and inducers of, amino acid utilisation pathways (Magasanik and Kaiser, 2002).

S.cerevisiae has the ability to utilise a variety of nitrogen-containing compounds as its sole source of nitrogen (Magasanik and Kaiser, 2002). Inside the cell, a range of enzymes catalyse the metabolism of these assorted compounds to generate ammonia, which then feeds into a common set of reactions that ultimately produce glutamate and glutamine (Magasanik and Kaiser, 2002). The amino nitrogen of glutamate and the amide group of glutamine serve as the basis of total cellular nitrogen in yeast and are donors for all of the amino acid and nucleotide biosynthesis pathways in the cell (Magasanik and Kaiser, 2002). When provided with a mixture of nitrogen sources in the growth medium, *S.cerevisiae* will show preference for the utilisation of particular nitrogen sources (Chen and Kaiser, 2002). Preferred nitrogen sources such as glutamine are used by the cell first and only once these are depleted will the cell then use the non-preferred nitrogen sources such as proline (Chen and Kaiser, 2002). In the laboratory, glutamine, glutamate and asparagine are commonly provided as preferable sources of nitrogen, while proline is mostly used as the non-

preferable source; other non-preferred sources include ornithine, allantoin and urea (Magasanik and Kaiser, 2002).

Gap1p activity is strictly regulated by nitrogen availability, to some extent at a transcriptional level, but largely by posttranslational means (Magasanik and Kaiser, 2002). The GATA-type transcription factors Gln3p and Gat1p/Nil1p and the cytoplasmic factor Ure2p co-ordinately control the transcription of a variety of nitrogen-responsive genes, which includes the expression of *GAP1* (Stanbrough et al., 1995). Gln3p and Gat1p/Nil1p positively regulate *GAP1* expression in cells grown on urea or glutamate as the nitrogen source, but when cells are grown on glutamine, Ure2p represses *GAP1* expression (Stanbrough and Magasanik, 1995). However, it became apparent that posttranslational modifications of Gap1p were also involved in its regulation (Stanbrough and Magasanik, 1995): a comparison between Gap1p protein levels and permease activity on different nitrogen sources indicated that Gap1p protein levels were similar in cells grown either on glutamate or urea, but that Gap1p activity in cells grown on urea was 100-fold higher than that of cells grown on glutamate (Stanbrough and Magasanik, 1995). Therefore, although expression of *GAP1* was comparable in cells grown on either urea or glutamate, indicated by the similar protein levels, the Gap1p protein must be regulated at another point to account for the differences in permease activity (Stanbrough and Magasanik, 1995).

Cell fractionation experiments localised Gap1p to the Golgi/endosomal system in cells grown on rich sources of nitrogen (Roberg et al., 1997) such as in the presence of glutamate. Despite displaying steady state localisation to the endosomal system, Gap1p is eventually transported directly to the vacuole where it is degraded, without transiting through the plasma membrane (Roberg et al., 1997). When cells are then transferred to urea medium (an unfavourable source of nitrogen) the activity of Gap1p increases, as it redistributes to the plasma membrane (Roberg et al., 1997). It has been suggested that Gap1p is engaged within an intracellular recycling loop between the Golgi and prevacuolar compartment (PVC) that acts as an internal store of Gap1p, which is ready to be mobilised to the plasma membrane in response to the quality of the nitrogen source (Magasanik and Kaiser, 2002). This strengthens the parallels noted between the nitrogen-regulated pathway of Gap1p and the insulin-regulated trafficking pathway of GLUT4.

The exposure of cells to ammonia results in an increase in ubiquitinated forms of Gap1p (Springael and Andre, 1998). The products of the *NPI1* and *NPI2* genes are required for the nitrogen-regulated inactivation and degradation of Gap1p (Grenson, 1983a; Grenson, 1983b). *NPI1* is an essential gene that encodes the E3 ubiquitin ligase, Rsp5p, which catalyses the addition of a ubiquitin moiety to lysine residues in target proteins (Huibregtse et al., 1995; Springael and Andre, 1998) and *NPI2* encodes the ubiquitin hydrolase Doa4p/Ubp4p/Ssv7p (Springael et al., 1999), further suggesting that the ubiquitin pathway is involved in the turnover regulation of Gap1p (Hein et al., 1995). In *npi1* mutant cells, where the levels of the Npi1/Rsp5 ubiquitin ligase are significantly reduced, and in *npi2* mutant cells, where the amount of free monomeric ubiquitin is around four times lower than in wild type cells, Gap1p ubiquitination is impaired, and the permease remains stable at the plasma membrane (Springael and Andre, 1998; Springael et al., 1999). This is because the monoubiquitination of Gap1p, like many cell surface proteins, is required for the internalisation step of endocytosis (Hicke and Dunn, 2003). However, the role of ubiquitination in Gap1p traffic is more complicated than this. For instance, overexpression of Bul1p or Bul2p proteins, which form a complex with Rsp5p (Yashiroda et al., 1998; Yashiroda et al., 1996), cause Gap1p to be sorted to the vacuole for degradation regardless of the nitrogen source (Helliwell et al., 2001). Bul1p and Bul2p, together with Rsp5p, specify the polyubiquitination of Gap1p, which is required for its intracellular targeting from the TGN to the vacuole (Helliwell et al., 2001). Therefore, ubiquitination of Gap1p is required, not only for the endocytosis and eventual down-regulation of Gap1p that has pre-accumulated at the cell surface, but also for the direct sorting of neosynthesised Gap1p from the late secretory pathway to the vacuole (Helliwell et al., 2001).

The carboxy- terminal tail of Gap1p plays an essential role in its nitrogen regulated down-regulation, as mutations within the last eleven amino acids of Gap1p or within a di-leucine peptide or glutamate residue located in a putative α-helix of the carboxy- terminal tail, protects the permease against NH_4^+ induced inactivation (Figure 1.3) (Hein and Andre, 1997; Springael and Andre, 1998). However, these mutant permeases are still modified by the addition of ubiquitin moeities (Springael and Andre, 1998). Gap1p is poly-ubiquitinated at two lysine acceptor sites, with the ubiquitin moieties being attached to Lys^{63} of the preceding ubiquitin, creating Lys^{63}-linked polyubiquitin chains (Springael et

al., 1999). Specifically Lys^9 and Lys^{16} of the amino-terminal cytosolic domain of Gap1p are poly-ubiquitinated with chains of at least two ubiquitin moieties (Soetens et al., 2001).

1.9. Ubiquitination

Ubiquitination is the post-translational conjugation of the small protein, ubiquitin, to specific lysine residues on a target protein (Hicke and Dunn, 2003). Ubiquitin is a 76 amino acid polypeptide whose C-terminal glycine carboxyl group forms an isopeptide bond with either the ε-amino group of specific lysine residues or, less commonly, with the amino group at the amino-terminus of a substrate protein (Hicke and Dunn, 2003). The conjugation of ubiquitin to a target protein can regulate a wide assortment of cellular processes including protein degradation and quality control, endocytosis and vesicular trafficking, cell-cycle control, stress response, DNA repair, signalling, transcription and gene silencing (Hicke and Dunn, 2003).

The covalent attachment of ubiquitin to target lysine residues in a substrate protein occurs following the sequential action of three different enzymes (outlined in Figure 1.7) (Weissman, 2001). A ubiquitin-activating enzyme (E1) adenylates the carboxyl terminus of ubiquitin before forming a high-energy thiolester bond between ubiquitin and a cysteinyl side-chain, in an ATP-dependent reaction (Hershko and Ciechanover, 1998; Schwartz and Hochstrasser, 2003; Weissman, 2001). The activated ubiquitin is then transferred onto a cysteinyl group on one of the twenty known ubiquitin-conjugating enzymes (E2) by transthiolation, which, usually in cooperation with a ubiquitin ligase (E3), then transfers the ubiquitin moiety onto the lysine side chain of a target protein (Hershko and Ciechanover, 1998; Hicke and Dunn, 2003; Schwartz and Hochstrasser, 2003; Weissman, 2001). The substrate specificity and timing of the ubiquitination reaction is determined largely by the E3 ubiquitin ligase, which is therefore often regarded as the key regulatory determinant of the process (Hicke and Dunn, 2003). E3 ligases can either themselves form a thioester bond with ubiquitin before transferring it onto a substrate protein or can function as a bridge between an activated E2 enzyme and the substrate protein; with the ubiquitin molecule transferring directly from the E2 enzyme to the substrate (Schwartz and Hochstrasser, 2003). This depends on whether the E3 enzyme contains a HECT (homologous to the E6-AP carboxyl terminus) domain or RING (really interesting new gene) related domain, respectively (Hicke et al., 2005; Schwartz and

Hochstrasser, 2003). De-ubiquitinating enzymes (DUBs) can trim or remove ubiquitin signals and are necessary to process ubiquitin precursors in order to generate a Gly-Gly sequence at their carboxy- terminal, which is the site of attachment to target molecules (Schwartz and Hochstrasser, 2003).

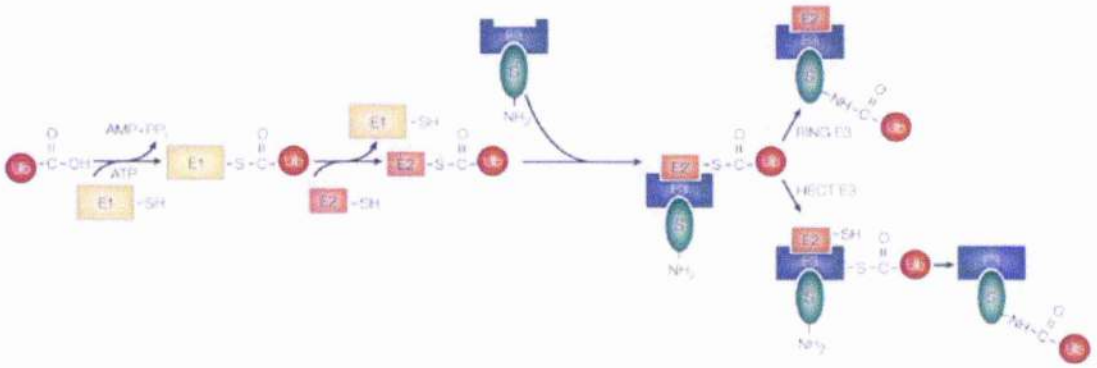

Figure 1.7. The ubiquitination pathway

(Weissman, 2001).

Different types of ubiquitin modification are associated with distinct cellular functions (Hicke and Dunn, 2003). Protein modification by a single ubiquitin molecule on one or more of its lysine residues is referred to as monoubiquitination or multi-monoubiquitination, respectively (Hicke and Dunn, 2003). However, at least three lysines within ubiquitin itself, Lys^{29}, Lys^{48}, and Lys^{63}, can themselves be ubiquitinated, thus forming chains of ubiquitination (Arnason and Ellison, 1994). This is referred to as polyubiquitination (Arnason and Ellison, 1994). A polyubiquitin chain of at least four ubiquitin moieties linked through Lys^{48} of ubiquitin has been shown to regulate a large number of nuclear, cytosolic and ER membrane proteins by targeting them for degradation by the 26S proteasome (Chau et al., 1989; Thrower et al., 2000), a large barrel-shaped multicatalytic protease complex (Hershko and Ciechanover, 1998). Polyubiquitin chains linked through Lys^{48} facilitate the binding of substrate proteins to this complex (Thrower et al., 2000). This role for ubiquitin dominated early discussion as to ubiquitin function; however, it has become increasingly apparent that ubiquitin also has a distinct role in regulating the transport of proteins between intracellular membrane compartments (Horak, 2003). Short di- or tri- chains of Lys^{63} linked polyubiquitin have been associated with regulating the endocytosis of some plasma membrane proteins and their subsequent

delivery to the mammalian lysosome or yeast vacuole where they undergo eventual proteolysis (Fisk and Yaffe, 1999; Galan and Haguenauer-Tsapis, 1997; Hoege et al., 2002). Monoubiquitination has been identified as a sorting signal throughout the endocytic pathway (Hicke, 2001; Hoege et al., 2002; Salghetti et al., 2001) and, in fact, fusion of a single ubiquitin moiety in-frame to many plasma membrane proteins is a sufficient signal for their internalisation (Dupre et al., 2004; Hicke and Dunn, 2003).

1.9a. The role of ubiquitin in protein transport

There are at least two distinct mechanisms by which ubiquitin can regulate protein transport; ubiquitin can either modify the activity of the protein transport machinery, or can serve as a sorting signal to direct the movement of transmembrane proteins between different intracellular compartments (Hicke and Dunn, 2003). For example, monoubiquitin acts as a signal to sort transmembrane proteins, from both endocytic and biosynthetic pathways, into vesicles that bud into the lumen of a late endosomal compartment known as the multivesicular body (MVB) (Katzmann et al., 2002). The MVB fuses with the mammalian lysosome or the yeast vacuole, which results in the eventual proteolysis of the MVB contents (Katzmann et al., 2002).

1.9b. Ubiquitin Binding Domains

The method by which a ubiquitin signal can regulate various cellular events has been attributed to the recently discovered collection of modular protein domains that non-covalently bind to ubiquitin, known as ubiquitin-binding domains (UBDs) (Hicke et al., 2005; Hurley et al., 2006). These motifs allow ubiquitin to function as a signalling connection in the regulation of various cellular proteins and processes in a manner similar to that controlled by phsophorylation/dephosphorylation of proteins (Hicke et al., 2005; Hurley et al., 2006). For example, multiple ubiquitin-binding proteins containing a wide variety of UBDs function to deliver ubiquitinated proteins into the budding luminal vesicles of MVBs (Katzmann et al., 2002) by recognising two hydrophobic patches on the surface of the ubiquitin molecule (Di Fiore et al., 2003). UBDs are generally small (20-150 amino acid residues), independently folded motifs that recognise various surfaces on ubiquitin, which allows them to interact directly with monoubiquitin and/or polyubiquitin chains (Hicke et al., 2005). At least sixteen structurally diverse UBDs have been identified thus far, which are found in a wide variety of proteins with differing structural features and

biological functions (reviewed in (Hicke et al., 2005; Hurley et al., 2006)). The largest class of ubiquitin-binding domains are α-helical domains and include, the ubiquitin-associated domain (UBA), the ubiquitin-interacting motif (UIM), the double-sided UIM (DUIM), the motif interacting with ubiquitin (MIU), the GAT domain (GGA (Golgi-localised, gamma-ear-containing, ADP-ribosylation-factor-binding protein) and TOM (target of Myb)) and the CUE (similar to Cue1) domain (Hurley et al., 2006). All of the above are known to interact with a hydrophobic patch on ubiquitin that includes the residue Ile^{44} (Hurley et al., 2006). Zinc-finger domains (ZnF's) make up the second largest class of UBDs and offer more diversity with respect to recognition and binding affinity when compared to helical domains, largely due to the fact they recognise three different regions on the surface of ubiquitin (Hurley et al., 2006). Other UBDs include, amongst others (as reviewed in (Hurley et al., 2006)), the Ubc (ubiquitin-conjugating enzyme) E2 variant (UEV) domain which contains an α/β fold that contacts both the Ile^{44} hydrophobic patch and a hydrophilic site centred around Gln^{62} of ubiquitin and the ubiquitin-binding motif (UBM), which is centred around Leu^{8} of ubiquitin (Hurley et al., 2006).

1.9c. Ubiquitination as a signal in regulated traffic

During the conversion of immature mouse dendritic cells to mature mouse dendritic cells, the major histocompatibility complex class II molecules (MHC II) are redistributed from late endosomal and lysosomal compartments to the plasma membrane (Shin et al., 2006). The MHC II β-chain cytoplasmic tail is ubiquitinated in immature dendritic cells, resulting in its endocytosis (Shin et al., 2006). This ubiquitination ceases upon cell maturation, allowing for the accumulation of MHC II at the plasma membrane (Shin et al., 2006). A ubiquitination-deficient mutant of MHC II, where the single lysine residue in the β-chain is replaced by an arginine residue, is retained at the plasma membrane in immature dendritic cells (Shin et al., 2006). This effect is reversed upon the addition of a single ubiquitin moiety to the cytoplasmic tail of this mutant, creating a constitutively ubiquitinated MHC II molecule that is retained intracellularly (Shin et al., 2006).

The short-chain ubiquitination of renal aquaporin-2 (AQP2) water channels provides a recently described example of ubiquitination regulating the endocytosis and subsequent targeting of a membrane protein into MVBs (Kamsteeg et al., 2006). Transmembrane water transport, and consequently water homeostasis, is controlled by the insertion and

retrieval of water channels, such as AQP2, to and from the cell surface (Kamsteeg et al., 2006). Arginine-vasopressin (AVP) induces the phosphorylation of AQP2 at Ser^{256}, causing its redistribution from intracellular vesicles to the apical membrane of kidney cells (Kamsteeg et al., 2006), thus allowing an increase in the water permeability of the kidney-collecting duct. Upon AVP removal or PKC activation, AQP2 is ubiquitinated at the apical membrane, with one Lys^{63}-linked chain at Lys^{270} (Kamsteeg et al., 2006). Internalisation kinetic studies between wild type and a ubiquitination-deficient (K270R) AQP2 mutant revealed that ubiquitination enhanced AQP2 endocytosis (Kamsteeg et al., 2006). Electron microscopy localised the ubiquitin-deficient mutant to the apical membrane, early endosomes, and the limiting membrane of MVBs, in contrast to a constitutively ubiquitinated form of AQP2 (AQP2-Ub) that localised primarily to the internal vesicles of MVBs (Kamsteeg et al., 2006). Furthermore, lysosomal degradation was found to be extensive for AQP2-Ub, low for AQP2-K270R, and intermediate for AQP2-wt, indicating that the short-chain ubiquitination of AQP2 has a role in its endocytosis, MVB sorting, and consequently, its lysosomal degradation (Kamsteeg et al., 2006).

1.10. A role for ubiquitination in the insulin-regulated trafficking of GLUT4?

Although GLUT4 has not previously been shown to be ubiquitinated, the small ubiquitin-like modifier protein, SUMO (also called sentrin), has been shown to modify GLUT4 (Lalioti et al., 2002). Additionally, the SUMO-conjugating enzyme, mUbc9 was identified in a yeast two-hybrid screen to identify proteins that interact with the C-terminal tail of GLUT4 in insulin-sensitive cells (Giorgino et al., 2000). SUMO is related to ubiquitin and may also regulate protein transport, either by acting as a signal, or by competing with ubiquitin for lysine modification sites (Hay, 2005). Little is known about the interaction of mUbc9 with GLUT4, although several observations indicate that it has an important role in regulating the transporter: for example, expression of a dominant-negative version of mUbc9 causes the degradation of GLUT4 and a decrease in the insulin-stimulated glucose transport in L6-myoblasts (Giorgino et al., 2000). A role for ubiquitin in GLUT4 trafficking has also been implicated by the identification of a protein harbouring two ubiquitin-like (Ubl) domains as being involved in the intracellular retention of GLUT4 in adipocytes in the absence of insulin (Bogan et al., 2003). This protein, TUG, is found in a complex with GLUT4 in basal adipocytes, but this association is lost following insulin-

stimulation (Bogan et al., 2003). Furthermore, TUG disruption results in enhanced translocation of GLUT4, along with increased glucose uptake (Yu et al., 2007). These data support a model in which GLUT4-containing vesicles are tethered and thus retained intracellularly through interaction with TUG (Bogan et al., 2003). Insulin would then stimulate the release of tethered GLUT4, allowing its delivery to the plasma membrane (Bogan et al., 2003).

As discussed above in Section 1.8, the nitrogen-regulated trafficking of Gap1p in yeast is controlled by ubiquitination of the transporter, which occurs when cells are grown under nutrient-rich conditions (Helliwell et al., 2001). This ubiquitination facilitates the binding of Gap1p to the GAT domain of the GGA (Golgi-localised, γ-ear-containing, ARF-binding) adaptor proteins (Scott et al., 2004). The GGA proteins are a family of ubiquitously expressed, monomeric clathrin adaptors that facilitate protein sorting in the TGN/endosomal system (Bonifacino, 2004; Pelham, 2004). They have a conserved modular arrangement consisting of four distinct domains: the Vps27, Hrs, Stam (VHS) domain interacts with acidic di-leucine sorting signals found in the mannose-6-phosphate receptors; the GGA and TOM (GAT) domain binds Arf:GTP and ubiquitin; the hinge region recruits clathrin; and finally, the γ-adaptin ear (GAE) domain (which has sequence similarity to the ear region of γ-adaptin) binds a number of accessory factors (Figure 1.8) (Bonifacino, 2004; Pelham, 2004). GGA proteins are recruited to the TGN by the Arf1 GTPase and therefore have the ability to select cargo destined for endosomes by recruiting ubiquitinated proteins and incorporating into clathrin-coated vesicles (Pelham, 2004).

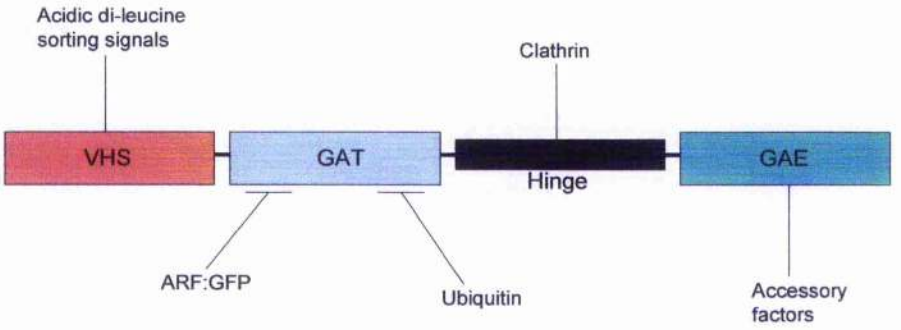

Figure 1.8. Domains and interactions of a typical GGA protein *(Pelham, 2004).*

Gga proteins are essential for the nitrogen-regulated trafficking of Gap1p in yeast (Scott et al., 2004). The interaction between ubiquitin moieties on Gap1p and the GAT domain of the Gga proteins is an absolute requirement, as yeast cells carrying the *gga2ΔGAT* allele as the sole *GGA* gene are unable to sort Gap1p in this regulated manner (Scott et al., 2004).

GGA proteins have also been implicated in regulating the entry of GLUT4 into its insulin-responsive location in 3T3-L1 adipocytes (Li and Kandror, 2005; Watson et al., 2004b). Initial studies expressing a 'dominant-negative' GGA mutant (containing only the VHS and GAT domains) blocked the entry of newly synthesized GLUT4 into its insulin-sensitive pool in 3T3-L1 adipocytes (Watson et al., 2004b) and selectively inhibited the *in vitro* budding of GLUT4-containing vesicles (while having no effect on the generation of vesicles containing GLUT1 and/or the transferrin receptor) (Watson et al., 2004b). Furthermore, in adipocytes, the GGA2 isoform shows significant colocalisation with GLUT4 in the perinuclear region of the cell (Li and Kandror, 2005).

The involvement of GGA proteins in the regulated sorting of both Gap1p (in yeast) and GLUT4 (in adipocytes) underscores the parallels between these two systems and makes it tempting to speculate that ubiquitination may be involved in the biogenesis of the insulin-sensitive pool of GLUT4, perhaps utilising the GGA proteins to do so.

1.11. Aims of project

As with many studies looking at the insulin-regulated trafficking of GLUT4, investigations into the role of ubiquitin in the process of GLUT4 trafficking have been hampered by the difficulties involved with using terminally differentiated fat and muscle cells. This study set out to overcome such issues by taking advantage of the easily manipulated, genetically tractable model eukaryote *Saccharomyces cerevisiae* in order to investigate the role of ubiquitination in the insulin-regulated trafficking of GLUT4.

Chapter 2: Materials and Methods

Chapter 2: Materials and Methods

2.1. Materials

2.1.1. General reagents and enzymes

All chemicals reagents were obtained from Sigma-Aldrich (Poole, UK), VWR (Poole, UK) or Fisher Scientific (Leicester, UK). Acrylamide was obtained from Severn Biotech Ltd (Kidderminster, UK). Media components were from Melford Laboratories Ltd (Suffolk, UK), FORMEDIUM (Norwich, UK) or Difco Laboratories Inc (Appleton Woods Laboratory Equipment and Consumables, Birmingham, UK). Solutions for enhanced chemiluminescence (ECL) and secondary antibodies for immunoblotting were from Amersham Biosciences (Buckinghamshire, UK). DNA restriction enzymes, T4 DNA ligase, *Taq*® polymerase and *Pfu*® polymerase were obtained from Promega (Southampton, UK). Platinum *Pfx*® polymerase was obtained from Invitrogen (Paisley, UK). Broad range protein markers from Biorad (Hertfordshire, UK) were used for protein electrophoresis. Yeast lytic enzyme was from MP Biomedicals (Aurora, USA)

2.1.2. Bacterial and yeast strains

The strains of *E.coli* and *S.cerevisiae* used in this study are listed in Table 2.1. Plasmids were routinely propagated in the *E.coli* host strain XL-1 Blue (Stratagene); recombinant proteins were produced in the *E.coli* host strain BL-21 (DE3) (Invitrogen).

2.1.3. Media

Yeast cultures were grown in either rich medium (YPD; containing 1% (w/v) yeast extract, 2% (w/v) peptone and 2% (w/v) glucose) or standard minimal (selective) medium (SD; containing 0.67% (w/v) yeast nitrogen base without amino acids, 2% (w/v) glucose and supplemented with synthetic complete amino acid dropout supplements as required) (ForMedium; Norwich, UK) (Sherman, 1986). Where stated, maltose was added as the sole carbon source in place of glucose to make YPM and SM. When solid medium was required micro agar was added to 2% (w/v).

Bacterial cultures were grown in standard 2YT medium (containing 1.6% (w/v) tryptone, 1% (w/v) yeast extract and 0.5% (w/v) NaCl) supplemented with 100μg/ml ampicillin. For solid plates, micro agar was added to 2% (w/v). For the production of recombinant

proteins, bacterial strains were grown in nutrient enriched Terrific Broth medium (Melford Laboratories Ltd; 1.2% (w/v) tryptone, 2.4% (w/v) yeast extract, 0.4% (v/v) glycerol, 0.017M KH_2PO_4, 0.072M K_2HPO_4), supplemented with 100μg/ml ampicillin.

2.1.4. Antibodies

Rabbit polyclonal antiserum that specifically recognises the carboxyl-terminal fourteen amino acids of hGLUT4 (Brant et al., 1992) were made in-house and used at a 1:1000 dilution for immunoblotting or a 1:100 dilution for immunofluorescence. Rat monoclonal antibodies (clone 3F10; 100µg/ml) that specifically recognise the epitope YPYDVPDYA (derived from the human influenza hemagglutinin (HA) protein) were purchased from Roche (Mannheim) and used at a 1:2000 dilution for immunoblotting or a 1:100 dilution for immunofluorescence. Rabbit polyclonal anti-Vti1p antibodies have been previously described (Coe et al., 1999); antiserum was used at a 1:30000 dilution for immunoblotting. Mouse monoclonal antibodies (3-5µg/µl) that specifically recognise ubiquitin were purchased from Covance (Cambridge Bioscience Ltd, UK) and used at a 1:1000 dilution for immunoblotting. Living Colors® A.v. mouse monoclonal antibody (JL-8) that recognises *Aequorea victoria* green fluorescent protein (GFP; 100µg/ml) was used at a concentration of 1:3000 for immunoblotting and purchased from Clontech Laboratories, Inc (California, USA). Rabbit polyclonal antibody (1µg/µl) specifically recognising the carboxyl-terminal fourteen amino acid peptide YASINFQKQPEDRQ of rat liver IRS-1 was from Upstate (New York, USA) and used at a concentration of 1:1000 for immunoblotting. Rabbit polyclonal antiserum, raised against the cytoplasmic domain of rat Syntaxin 4 was used at a concentration of 1:1000 for immunoblotting and obtained from Synaptic Systems (Goettingen, Germany). Antibodies against EEA1, Syntaxin16 and a mouse monoclonal antibody that recognises the C-terminus of hGLUT4 (1F8) (James et al., 1988) were kindly provided by Professor David James (Garvan Institute of Medical Research, Australia).

2.2. Methods

2.2.1. DNA manipulations

Plasmid DNA was routinely isolated from bacterial cultures using the Promega Wizard® Plus SV Miniprep kit. Oligonucleotides used in polymerase chain reaction (PCR) amplification or site-directed mutagenesis (SDM) of DNA sequences (listed in Table 2.2)

were manufactured by either Yorkshire Bioscience Ltd (York, UK) or Vhbio Ltd (Gateshead, UK) and diluted in nuclease free water to a final concentration of 50pmol/µl. The high fidelity polymerase Platinum *Pfx*® (Invitrogen) was used for PCR amplification of DNA sequences.

The following indicates a typical recipe for the PCR:

10mM dNTPs	5µl
50mM $MgSO_4$	5µl
10X *Pfx* buffer	5µl
Enhancer	5µl
ddH_2O	26µl
Forward primer (50pmol/µl stock)	1µl
Reverse primer (50pmol/µl stock)	1µl
Purified plasmid DNA	1µl
Pfx DNA polymerase	1µl

Generally, the PCR was completed with the following conditions:

95°C	1min	
94°C	1min30secs	30 cycles
55°C	1min	
68°C	(1min/kb)	
68°C	10min	
4°C	hold	

DNA manipulation techniques were performed using standard procedures (Sambrook, 2001). DNA fragments were resolved electrophoretically through 0.8% (w/v) agarose in tris-acetate (TAE) buffer (0.04M Tris-acetate, 0.001M EDTA). SDM of DNA sequences was carried out with *Pfu*® polymerase according to the QuikChange® method (Stratagene). The exchange of one amino acid residue for another was performed with the use of synthetic oligonucleotides, designed with the desired mutation at the centre of the oligonucleotide. 1µl (10 units) *Dpn*I was added to the reaction mixture following completion of the SDM reaction, and further incubated for 1hr at 37°C in order to digest the parental DNA. Mutations were confirmed by DNA sequencing.

The following indicates a typical recipe for the SDM reaction:

10X *Pfu* buffer	5µl
10mM dNTPs	1µl
Pfu polymerase	1µl
ddH_2O to final volume of	50µl
Purified plasmid DNA	50ng
Primer 1	125ng
Primer 2	125ng

Typically, the following conditions were used to complete the SDM reaction:

95°C	1min	
95°C	50secs	} 18 cycles
60°C	50secs	
68°C	(2min/kb)	
68°C	7min	
4°C	hold	

2.2.2. Plasmid construction

All plasmids constructed and used in this study are listed in Table 2.3. pRM1 was constructed by subcloning a *Bam*HI-*Pst*I fragment, containing sequence encoding HA-tagged ubiquitin downstream of the *CUP1* promoter, from Yep112 (Hochstrasser et al., 1991) into pRS315 (Sikorski and Hieter, 1989).

pWTG4 (pRM2) was constructed by amplifying the human GLUT4 ORF from a cDNA (provided by Professor Gwyn Gould) by PCR using oligos 1 and 2 (Table 2.2) to generate the GLUT4 ORF flanked by sequences homologous to the 3' end of the *CUP1* promoter and the proximal end of the *PHO8 3'UTR*. This plasmid was then used to repair a gapped pNB701 (constructed by Nia Bryant and based on pRS316 (Sikorski and Hieter, 1989)), which contains the ORF encoding the protein RS-ALP (retention sequence-ALP) (Bryant et al., 1998b) under control of the *CUP1* promoter, followed by the 3'*UTR* of *PHO8*.

pG47KR (pRM3) was constructed from pWTG4 (pRM2) by using SDM to sequentially mutate the codons for the 7 lysine residues (at positions 109, 242, 245, 261, 264, 266 and 495) to codons for arginine residues. The pairs of oligonucleotides used (61 and 62, 73 and 74, 85 and 86, 77 and 78, 117 and 118, 119 and 120, 121 and 122), and the 'intermediate' plasmids created (pRM5, pRM11, pRM12, pRM13, pRM14, pRM15 and pRM3) in the process of making the final plasmid pG47KR (pRM3) are listed in Tables 2.2 and 2.3, respectively.

Plasmids pRM5, pRM6, pRM7, pRM8, pRM9, pRM10 and pRM16 were constructed from pWTG4 (pRM2) by using SDM to individually mutate the codons for the 7 lysine residues (at positions 495, 242, 245, 261, 264, 266 and 109, respectively) to codons for arginine residues. The pairs of oligonucleotides used in each SDM reaction (61 and 62, 85 and 86, 87 and 88, 89 and 90, 91 and 92, 93 and 94, 73 and 74) are listed in Table 2.2.

Plasmids pRM17, pRM18, pRM19, pRM20, pRM21, pRM22 and pRM23 were constructed from pG47KR (pRM3) by using SDM to individually mutate the codons for the 7 arginine residues (at positions 242, 261, 109, 245, 264, 266 and 495, respectively) to codons for lysine residues. The pairs of oligonucleotides used in each SDM reaction (233 and 234, 237 and 238, 231 and 232, 235 and 236, 239 and 240, 241 and 242, 243 and 244) are listed in Table 2.2.

pRM34 was constructed using oligos 365 and 366 (Table 2.2) to generate a PCR product from pGO36 (Odorizzi et al., 2003) encoding GFP(S65T) flanked by sequences homologous to the 3' end of the GLUT4 ORF and the proximal end of the *PHO8 3'UTR*. Homologous recombination was used to insert the GFP(S65T) ORF immediately after the last codon of GLUT4 by repairing a version of pRM2 in which the GLUT4 STOP codon was replaced by an *Sph*I site (by SDM using oligos 343 and 344; Table 2.2) and subsequently linearised using this site.

pG47KRHAUb (pRM24) was constructed using oligos 185 and 186 (Table 2.2) to generate a PCR product from pRM1 encoding HA-tagged ubiquitin flanked by sequences homologous to the 3' ends of the GLUT4-7K/R ORF and the proximal end of the *PHO8* 3'*UTR*. Homologous recombination was used in insert the HA-tagged ubiquitin ORF

immediately after the last codon of GLUT4-7K/R by repairing a version of pRM3 in which the GLUT4-7K/R STOP codon was replaced by an *Sph*I site (by SDM using oligos 183 and 184; Table 2.2) and subsequently linearised using this site.

pRM4 was constructed using the pairs of oligos 260, 263 and 261, 264 (Table 2.2) to generate two PCR products encoding amino acid residues 1 to 75 of wild type HA-GLUT4 (with the exofacial HA-tag between residues 67 and 68) and amino acid residues 69 to 509 of the hGLUT4-7K/R mutant, respectively, using pMEXHAGLUT4 (Benito et al., 1991; Shewan et al., 2000) and pRM3 as templates,. These two PCR products were 'spliced' together in a PCR using oligos 260 and 261 (Table 2.2) and subcloned as an *Eco*RI-*Sal*I fragment into the pBABE-puro retroviral expression vector (Morgenstern and Land, 1990).

pRM25 was constructed using oligos 260 and 262 (Table 2.2) to generate a PCR product from pRM24 encoding GLUT4-7K/R-HA-Ub with *Eco*RI and *Sal*I restriction sites at the 5' and 3' ends, respectively. This PCR product was then subcloned into pBABE-puro retroviral expression vector (Morgenstern and Land, 1990).

pRM30 and pRM31 were constructed using oligos 149 and 153 (Table 2.2) to generate a PCR product from p1839 (Piper et al., 1997) encoding *LEU2* and regions of ~600bp upstream and downstream of the *LEU2* gene. This PCR product was used to replace the *URA3* gene of pRM2 and pRM3 with the *LEU2* gene, by homologous recombination.

pCAL1 was constructed by using SDM to mutate the codons for Met^{342} and Phe^{344} of Dsk2p in the context of the plasmid encoding the GST-UBA fusion protein (Funakoshi et al., 2002) to codons for arginine and alanine respectively, using oligos 352 and 353 (Table 2.2) (this was performed by Chris Lamb, a placement student in the lab).

2.2.3. DNA sequencing

All plasmids constructed for use in this study were verified by DNA sequencing, which was performed by The Sequencing Service (School of Life Sciences, University of Dundee, Scotland) using Applied Biosystems Big-Dye Ver 3.1 chemistry on an Applied Biosystems model 3730 automated capillary DNA sequencer.

2.2.4. Transformation of E. coli and S. cerevisiae

Bacterial transformations were carried out as described (Hanahan, 1983). Yeast cells were made competent and transformed according to lithium acetate method, as described (Ito et al., 1983).

2.2.5. APNE assay

Yeast cells were patched onto solid rich media (YPD) and overlaid with ~8ml reaction media (RxM; 0.2M Tris-HCl pH7.4, 0.2mg/ml N-acetyl-phenylalanine-p-naphthyl-ester (APNE) in dimethylformamide (DMF), 0.8mg/ml Fast Garnet GBC salt and 0.7% (w/v) micro agar). Overlaid RxM was allowed to solidify and colour development of patched yeast was observed over time. *PEP4* strains turn red, *pep4-3* strains remain white.

2.2.6. Isolation of yeast chromosomal DNA

Yeast cells were grown to stationary phase in 10ml of rich medium, harvested and washed in 1ml 1.0M sorbitol, 0.1M EDTA (pH7.5). Cells were resuspended in 0.4ml 1.0M sorbitol, 0.1M EDTA (pH7.5) and transferred to a 1.5ml microcentrifuge tube. 15μl of 15mg/ml yeast lytic enzyme (in 50mM Tris-HCl pH7.7, 1mM EDTA, 50% (v/v) glycerol) was added to the cells prior to a 30min incubation at 37°C. The resulting spheroplasts were harvested in a microcentrifuge at 1840 *g* for 2mins and resuspended in 500μl TE (10mM Tris-HCl pH8.0, 1mM EDTA pH8.0). To lyse spheroplasts, 90μl of lysis solution (0.25M EDTA pH8.0, 0.4M Tris-HCl pH8.0, 2% SDS (w/v)) was added, prior to a brief (2 sec) period of vortexing and a 30 min incubation at 65°C. After spheroplast lysis, 80μl of 5M KOAc was added to the lysates, and the samples left on ice for a minimum of 2hours. Precipitated matter, including insoluble potassium dodecyl sulphate and denatured proteins, was pelleted in a 15 min spin at top speed at 4°C in a microcentrifuge. Supernatants were transferred to fresh 1.5ml microcentrifuge tubes and DNA was precipitated by the addition of an equivalent volume of ice-cold 100% ethanol. Precipitated DNA was harvested in a 15 min spin at top speed at 4°C in a microcentrifuge. The DNA pellets were washed with 70% ethanol (v/v), recovered in another 15 min spin at top speed at 4°C in a microcentrifuge, air-dried at 25°C, and resuspended in 100μl TE (10mM Tris-HCl pH8.0, 1mM EDTA pH8.0). 1μl was routinely used as a template for PCR in a 50µl reaction.

2.2.7. Plasmid rescue from yeast

Yeast cells were grown to stationary phase in 10ml selective media and 5 OD_{600} equivalents of cells were harvested in a microcentifuge at 3610 *g* for 2mins. Cells were resuspended in 0.5ml buffer S (100mM K_2HPO_4 pH7.2, 10mM EDTA, 50mM β-Mercaptoethanol, 50µg/ml yeast lytic enzyme (in 50mM Tris-HCl pH7.7, 1mM EDTA, 50% (v/v) glycerol)) and incubated at 37°C for 30mins. The resulting spheroplasts were harvested using centrifugation in a microfuge and lysed by resuspension and trituration in 100µl lysis buffer (25mM Tris-HCl pH7.5, 25mM EDTA and 2.5% (w/v) SDS) and incubation at 65°C for 30mins. 166µl 3M KOAc was added before incubation on ice for 10mins. Lysates were subject to centrifugation at top speed in a microcentrifuge for 10mins at 4°C. Supernatants were transferred to fresh microcentifuge tubes, and 0.8ml 100% cold ethanol was added. Samples were left on ice for 10mins before being subject to centrifugation at top speed in a microcentrifuge. Precipitated DNA was washed with 70% ethanol (v/v), air dried, and resuspended in 40µl dH_2O. 20µl was commonly used to transform XL-1 Blue cells.

2.2.8. Tissue culture techniques

2.2.8a. Cell culture of 3T3-L1 murine fibroblasts and adipocytes

3T3-L1 fibroblasts were cultured in Dulbecco's modified Eagle's medium (DMEM) supplemented with 10% (v/v) newborn calf serum (NCS) and 1% (v/v) penicillin and streptomycin. Fibroblasts were maintained as sub-confluent cultures at 37°C in a 10% CO_2 humidified incubator. Differentiation into adipocytes was initiated 1 to 3 days post-confluency by the addition of DMEM containing 10% (v/v) foetal calf serum (FCS), 1% (v/v) penicillin and streptomycin, 0.25µM dexamethasone, 0.5mM 3-isobutyl-1-methylxanthine and 1µg/ml insulin. After 3 days, the differentiation medium was replaced with fresh DMEM supplemented with 10% (v/v) FCS, 1% (v/v) penicillin and streptomycin and 1µg/ml insulin. Adipocytes were re-fed with DMEM supplemented with 10% (v/v) FCS and 1% (v/v) penicillin and streptomycin every 3 days and utilised for experiments at least 8-12 days following the initiation of differentiation.

2.2.8b. Cell culture of Plat-E cells

Plat-E cells were cultured in DMEM supplemented with 10% (v/v) foetal calf serum (FCS), 1% (v/v) penicillin and streptomycin, 1µg/ml puromycin (Sigma) and 10µg/ml

blasticidin (Invitrogen). Plat-E cells were maintained as sub-confluent cultures at 37°C in a 5% CO_2 humidified incubator.

2.2.8c. Preparation of virus using Plat-E cells

cDNA constructs subcloned into the pBABE-puro retroviral expression vector were transfected into Plat-E cells (plated at a density of $5x10^6$ cells/10cm plate 24hr prior in DMEM with 10% (v/v) FCS) using Lipofectamine™ 2000 reagent (Invitrogen) according to the manufacturer's protocol. Transfection medium was replaced after 3hr with 8ml DMEM with 10% (v/v) FCS. After a further 24hr at 37°C this media was replaced with 6ml DMEM with 10% (v/v) FCS to increase retroviral titre and following another 24hr at 37°C, cells were transferred to 32°C for 24hr before harvesting the media, which was filtered through a 0.45μm syringe filter (Millipore) and stored at -80°C until required.

2.2.8d. Infection of fibroblasts with retrovirus

To generate 3T3-L1 adipocytes stably expressing each construct, 3T3-L1 fibroblasts (plated into 10cm dishes to achieve 40% confluence) were infected with the relevant retrovirus for 12hr in the presence of 10μg/ml Polybrene® (Sigma). Infected cells were selected in DMEM containing 10% (v/v) FCS, 1% (v/v) penicillin and streptomycin supplemented with 2μg/ml puromycin (Sigma). These infected fibroblasts were then grown to confluence and differentiated into adipocytes exactly as outlined in Section 2.2.8a except always with 2μg/ml puromycin added to the medium.

2.2.9. Electrophoretic separation of proteins

Electrophoretic separation of proteins was performed using discontinuous SDS polyacrylamide gels (SDS-PAGE) following the basic procedures outlined by (Laemmli, 1970). Proteins were separated using gels composed of a stacking region (5% acrylamide in stacking buffer; 0.25M Tris-HCl (pH6.8), 0.2% (w/v) SDS) and a separating region (routinely 10% acrylamide in separating buffer; 0.75M Tris-HCl (pH8.8), 0.2% (w/v) SDS). A 30% acrlyamide-bisacrylamide mixture (37.5:1 ratio; Severn Biotech Ltd, Worcestershire) was used. Gels were run in tris-glycine electrophoresis buffer (25mM Tris-HCl, 250mM glycine, 0.1% (w/v) SDS).

Resolved proteins were visualised by agitating gels in Coomassie Brilliant Blue solution (0.25g Coomassie Brilliant Blue R250 in methanol: H_2O: glacial acetic acid (4.5:4.5:1 v/v/v)) for 1 hour, followed by agitation in destain solution (5% (v/v) methanol, 10% (v/v) glacial acetic acid) until bands were clearly visible (generally overnight).

2.2.10. Transfer of proteins onto nitrocellulose

A Bio-Rad Trans-Blot® SD cell was to transfer proteins from polyacrylamide gels onto nitrocellulose membranes (Protran, 0.45µ pore size). Gels and membranes were sandwiched between 6 pieces of Whatman 3MM paper, presoaked in semi-dry transfer buffer (50mM Tris-HCl, 40mM glycine, 0.037% (w/v) SDS, 10% methanol) prior to the application of constant 180mA current, which was routinely applied for anywhere between 35 min (for one gel) up to 60 min (for four gels).

2.2.11. Immunoblot analysis

Following protein transfer, unfilled sites on the nitrocellulose membrane were blocked with 5% (w/v) non-fat dried milk in PBST (0.1% (v/v) Tween-20 in phosphate buffered saline (PBS; 140mM NaCl, 3mM KCl, 1.5mM KH_2PO_4, 8mM Na_2HPO_4)) by gentle agitation for at least 30 min at room temperature. The membranes were then exposed to primary antibody for either 2 hours at room temperature, or overnight at 4°C, with gentle agitation. Antibody preparations were diluted as described in Section 2.1.4 in 1% (w/v) non-fat dried milk in PBST. Following exposure to primary antibody, the membrane was washed with PBST, 6 times for 5 min each, before exposure to secondary antibody for 1 hour at room temperature [routinely, α-rabbit (at a 1:5000 dilution), α-rat (at a 1:2000 dilution), or α-mouse (at a 1:2000 dilution) IgG-HRP conjugate; Amersham Biosciences, Bucks, UK] in 5% (w/v) non-fat dried milk in PBST. Following another 6 washes of 5 min each in PBST, protein bands were visualised using ECL.

2.2.12. Preparation of yeast cell extracts for immunoblot analysis

To assess the steady-state levels of proteins in yeast whole cell extracts, cells were harvested (by centrifugation for 5 min at 660 *g* on a bench top centrifuge) from yeast cultures that had grown to mid-log phase (OD_{600} between 0.6-1.0), washed once in distilled water and resuspended to 100 OD units/ml in Twirl buffer (50mM Tris (pH 6.8), 8M urea, 10% (v/v) glycerol, 5% (w/v) SDS and 0.2% (w/v) bromophenol blue, 10% (v/v) β-

mercaptoethanol). Cell extracts were generated by a 10 min incubation at 65°C, followed by brief vortexing. The denatured proteins contained within 15µl of cell extract were resolved by SDS-PAGE, transferred to nitrocellulose membrane, and subjected to immunoblot analysis.

2.2.13. Microscopic Analysis

2.2.13a. Direct fluorescence with yeast

Yeast cells harbouring GFP-expressing plasmids were grown in selective medium containing 100μM $CuSO_4$ to an OD_{600} of 0.6-1.0. For labelling with FM4-64 (Molecular Probes, Oregon, USA), cells were labelled for 1hr at 30°C with 200nM FM4-64 in selective medium (SD). Cells were then washed at least twice before incubating for at least 30min at 30°C in selective media (SD). To ensure that the GFP protein was kept at the optimal pH level for fluorescence detection, cells were finally resuspended in 200µl 1M Tris-HCl (pH8).

2.2.13b. Indirect immunofluorescence with yeast

Cells were grown in selective medium (SD) containing 100μM $CuSO_4$ to an OD_{600} of 0.6-1.0. Cells were pre-fixed in 3.7% formaldehyde for 1hr at room temperature before fixation in 45μM NaOH, 4% (w/v) paraformaldehyde, 0.1M KH_2PO_4 for 16hrs at room temperature. Cells were converted to spheroplasts using 150μg/ml yeast lytic enzyme in 1.2M sorbitol, 50mM KPi (pH7.3), 1mM $MgCl_2$ at 30°C for 30min and permeabilised by treatment with 1% (w/v) SDS in 1.2M sorbitol for 1min. Cells were then allowed to adhere to poly-L-lysine coated multiwell slides. Nonspecific antibody binding was blocked by incubation of cells in PBS containing 5mg/ml BSA and 0.1% (v/v) normal donkey serum. Primary antibody incubations were performed at room temperature in a humid chamber for 2 hr. Antibodies against hGLUT4 and the HA epitope tag were pre-absorbed to yeast proteins (to remove non-specific binding) by incubating with cells harbouring either pTC2 (a plasmid with a similar background to pWTG4) or cells without an HA-tagged protein, respectively. Cells were double labelled for hGLUT4 and hemagglutinin epitope (HA) tagged Kex2p by including both antibodies in the primary antibody solution. All antibodies were diluted in PBS containing 5mg/ml BSA, which was also used for all washes. Cells were then washed at least 7 times before undergoing a 1 hr incubation with the appropriate secondary antibodies diluted in PBS containing 5mg/ml

BSA, which were conjugated to either Alexa Fluor-488 or Alexa Fluor-568 (Molecular Probes, USA). Cells were again washed at least 7 times before being coverslipped with immunomount (Thermo Shandon, USA). Cells were visualised through a 100x oil immersion objective on a Zeiss Axiovert fluorescence microscope (Carl Zeiss, Germany) equipped with a Zeiss LSM410 laser confocal imaging system. Image sets were processed and overlaid using Adobe Photoshop™.

2.2.13c. Indirect immunofluorescence with 3T3-L1 adipocytes

Cells were grown on coverslips (previously autoclaved and coated with gelatine) in 24-well plates and were washed twice with PBS prior to being fixed with 200µl of 3% (w/v) paraformaldehyde (PFA) in PBS for 30 min at room temperature. After another two washes with PBS, free aldehyde groups were neutralised by washing twice with 20mM glycine in PBS. Non-specific binding sites were blocked and cells permeabilised by incubating with 200µl 0.1% (w/v) saponin in 2% (w/v) BSA in 20mM glycine in PBS for 20 min. Cells undergoing staining to detect hemagglutinin epitope (HA) at the cell surface were not permeabilised but were incubated in 2% (w/v) BSA in 20mM glycine in PBS for 20 mins to block non-specific binding sites. Incubation with primary antibodies was achieved by placing a 40µl drop of antibody preparation onto parafilm. Coverslips were removed from wells, the edges dried, and placed on top of the drop of antibody, cell side down. Cells were double labelled for HA-tagged GLUT4 and endogenous Syntaxin16 or EEA1 by including both antibodies in 0.1% (w/v) saponin in 2% (w/v) BSA in 20mM glycine in PBS. For cell surface labelling of HA-tagged GLUT4, primary antibody was prepared in 2% (w/v) BSA in 20mM glycine in PBS. After a 45 min incubation, the coverslips were washed 4 times with either 0.1% (w/v) saponin in 2% (w/v) BSA in 20mM glycine in PBS or 2% (w/v) BSA in 20mM glycine in PBS. Secondary antibodies Alexa Fluor-488 (Molecular Probes) and Cy3-conjugated antibody (Jackson Immunoresearch) were applied in a manner similar to that of the primary antibody but with a 30 min incubation time. After a further 4 washes, the coverslips were embedded in immunomount onto microscope slides and stored overnight in the dark at 4°C. Mounted coverslips were analysed using a 63x oil immersion objective fitted to a Zeiss Axiovert fluorescence microscope, equipped with a Bio-Rad MRC-600 confocal imaging system. Image sets were processed and overlaid using Adobe Photoshop™.

2.2.14. Immunoprecipitation from yeast cell lysates

Yeast strains harbouring the appropriate plasmids were grown to mid-log phase (OD_{600} between 0.6-1.0) in 500ml of suitable selective media containing 100μM $CuSO_4$ to induce expression from the *CUP1* promoter as required. Cells were harvested (by centrifugation for 30 min at 1060 *g* in a bench top centrifuge) and resuspended in 5ml YPD-sorb (50% (v/v) YPD, 50% (v/v) 1.2M sorbitol), to which 50μl of a 15mg/ml stock of yeast lytic enzyme (in 50mM Tris-HCl pH7.7, 1mM EDTA, 50% (v/v) glycerol) and 15μl β-mercaptoethanol were added. Cells were converted to spheroplasts during a 1 hr incubation, with shaking, at 30°C. Spheroplasts were then layered onto 10ml of 1.2M sucrose (to cushion spheroplasts during centrifugation) before being harvested at 660 *g* for 5min in a bench top centrifuge and transferred to ice. Spheroplasts were disrupted by vortexing briefly in 5ml ice-cold lysis buffer (200mM sorbitol, 100mM KoAc, 1% (v/v) Triton X-100, 50mM KCl, 20mM PIPES (pH6.8)). Cell debris was removed by a 5 min spin at 660 *g* at 4°C in a bench top centrifuge before the cleared lysate was separated into aliquots of 1.2ml into screw-capped tubes. To reduce non-specific binding, 50μl of PrA-Agarose (50% slurry; Sigma-Aldrich) was added to the lysates, which were then briefly vortexed and incubated on ice for 15 min. PrA-Agarose was then removed by centrifugation for 5 min at 7370 *g* at 4°C in a bench top centrifuge. A small aliquot (10μl) of cell lysate was reserved for SDS-PAGE analysis before 1ml of lysate was transferred to a fresh tube. To each tube, the appropriate primary antiserum (10μl αGLUT4 (Brant et al., 1992)) was added. After brief vortexing, lysates and antibodies were mixed by rotation for 2 hr at 4°C, prior to the addition of 50μl PrA-Agarose and a subsequent additional hour of rotation at 4°C. PrA-Agarose with bound antibody and associated proteins were pelleted in a 1 min spin at 7370 *g* at 4°C in a bench top centrifuge, and pellets washed 3 times in 1ml lysis buffer. Bound proteins were eluted in 20μl LSB (100mM Tris-HCl (pH6.8), 4% (w/v) SDS, 20% (v/v) glycerol, 0.2% (w/v) bromophenol blue, 10% (v/v) β-mercaptoethanol) and denatured by incubation for 5 min at 65°C. PrA-Agarose was pelleted in a 5 min spin at top speed in a microcentrifuge and immunoprecipitated proteins resolved by SDS-PAGE, transferred to nitrocellulose membrane, and subjected to immunoblot analysis.

2.2.15. Preparation of 3T3-L1 adipocytes lysate

3T3-L1 adipocytes cultured on 10cm dishes were washed once and incubated at 37°C in serum-free DMEM for 2 hr. Following the transfer of plates onto ice, the cells were washed 3 times with cold PBS. All subsequent steps were performed on ice unless indicated otherwise. Cells were scraped from the plate into 0.25ml/plate lysis buffer (50mM sodium HEPES (pH7.5), 150mM sodium chloride, 5mM EDTA, 1mM sodium vanadate, 6μM MG132, 1mM N-ethylmaleimide (NEM), 1% (v/v) Triton X-100, 0.1mM phenylmethylsulphonyl fluoride (PMSF), 10μg/ml soybean trypsin inhibitor, 10μg/ml benzamidine and EDTA-free complete protease inhibitor mix (1 tablet (Roche) / 50ml lysis buffer). Pooled cells were homogenised by passing the cell suspension through a 24XG needle 10 times and twice through a 26XG needle. In order to remove lipid droplets, homogenized cells were centrifuged at 500 *g* for 10 min at 4°C in a bench top centrifuge and the lysate removed from underneath the floating layer of lipid.

2.2.16. Immunoprecipitation from 3T3-L1 adipocytes lysate

1ml adipocyte lysate (prepared as described in Section 2.2.15) was incubated at 4°C for 1 hr with rotation before centrifugation at 12470 *g* for 15 min at 4°C in a bench top centrifuge to pellet insoluble material. To reduce non-specific binding, 50μl of PrA-Agarose (50% slurry; Sigma-Aldrich) was added to the lysates, which were then briefly vortexed and incubated on ice for 15 min. PrA-Agarose was then removed by centrifugation for 5 min at 7370 *g* at 4°C. A 10μl aliquot of cell lysate was reserved for SDS-PAGE analysis before 1ml of lysate was transferred to a fresh tube. To each tube, the appropriate primary antisera (e.g. 10μl αGLUT4 (Brant et al., 1992)) was added. After brief vortexing, lysates and antibodies were mixed by rotation for 2 hr at 4°C, prior to the addition of 50μl PrA-Agarose (50%slurry; Sigma-aldrich) and a subsequent additional hour of rotation at 4°C. PrA-Agarose with bound antibody and associated proteins were pelleted in a 1 min spin at 7370 *g* at 4°C in a bench top centrifuge, and pellets washed 3 times in 1ml lysis buffer. Bound proteins were eluted in 20μl LSB (100mM Tris-HCl (pH6.8), 4% (w/v) SDS, 20% (v/v) glycerol, 0.2% (w/v) bromophenol blue, 10% (v/v) β-mercaptoethanol) and denatured by incubating for 5 min at 65°C. PrA-Agarose was pelleted in a 5 min spin at top speed in a microcentrifuge and immunoprecipitated proteins resolved by SDS-PAGE, transferred to nitrocellulose membrane, and subjected to immunoblot analysis.

2.2.17. GST fusion protein expression and purification

Chemically competent BL-21(DE3) cells (Invitrogen) were transformed with plasmids driving the production of the appropriate GST fusion protein. Overnight cultures of transformed cells were diluted into 400ml Terrific Broth medium (with appropriate antibiotics) and incubated, with shaking, at 37°C until an OD_{600} of ~0.6 was reached. Expression of the recombinant fusion proteins was then induced with 1mM isopropyl-β-D-thiogalactopyranoside (IPTG) for 4 hr. Cells were harvested by centrifugation in a Beckman Coulter SX4750 rotor at 3,273 *g* for 20 min. Cell pellets were resuspended in 19.5ml PBS before transfer to 50ml falcon tubes and incubation with lysozyme (at a final concentration of 1mg/ml) for 30 min on ice. Cells were lysed by immersing the probe of a Sanyo Soniprep 150 in the suspension and sonicating for 5 x 30 sec pulses, with 30 sec cooling periods on ice separating the pulses of sonication. Cell lysates were centrifuged in a Beckman JA-20 rotor for 30 min at 4°C at 48,400 *g* to remove insoluble material. To recover fusion proteins, glutathione-Sepharose (Amersham Biosciences) was pre-equilibrated (as per the manufacturer's instructions) and made up to a 50% slurry in PBS. An aliquot of glutathione -Sepharose slurry was added to the cleared bacterial lysate containing the GST- (glutathione S- transferase) tagged fusion proteins. Generally, ~0.5ml glutathione-Sepharose slurry was used. Lysates and glutathione-sepharose resin were then mixed, with rotation, for at least 1 hr at 4°C. Beads loaded with recombinant proteins were routinely harvested in a 2 min spin at 500 *g* at 4°C, followed by at least 3 washes in cold PBS (generally ~1ml) to remove non-specifically bound proteins. Beads were resuspended in PBS supplemented with protease inhibitors (1 tablet complete inhibitor cocktail (Roche)/ 50ml PBS) at a bead:buffer ratio of 1:1.

2.2.18. GST fusion protein pull down assays from adipocyte cell lysates

Recombinant GST fusion proteins were purified from transformed *E.coli* BL21(DE3) cultures as outlined above in Section 2.2.17. For pull-down assays, 3T3-L1 adipocytes cultured on 10cm dishes were washed once and incubated at 37°C in serum-free DMEM for 2 hr. Following the transfer of plates onto ice, the cells were washed 3 times with cold PBS. All subsequent steps were performed on ice unless indicated otherwise. Adipocyte cell lysates (prepared as described in Section 2.2.15) was then incubated at 4°C for 1 hr with rotation before centrifugation at 12470 *g* for 15 min at 4°C in a bench top centrifuge

to pellet insoluble material. A 10µl aliquot of cell lysate was reserved for SDS-PAGE analysis before the lysate was split equally amongst the various GST fusion proteins (10µg/sample) immobilised to glutathione-Sepharose beads and incubated with rotation at 4°C for 2 hr. Beads were recovered by a brief 20 sec centrifugation and washed 3 times with lysis buffer prior to the elution of bound proteins by the addition of 20µl LSB and incubation at 65°C for 15 min. Samples were subject to SDS-PAGE and immunoblot analysis.

2.2.19. GST fusion protein pull down of yeast cell lysates

Yeast strains harbouring the appropriate plasmids were grown to mid-log phase (OD_{600} between 0.6-1.0) in 50ml of suitable selective media containing 100µM $CuSO_4$ to induce expression from the *CUP1* promoter as required. Cells were harvested (by centrifugation for 5 min at 900 *g* in a bench-top centrifuge) and resuspended in 5ml YPD-sorb (50% (v/v) YPD, 50% (v/v) 2.4M sorbitol), to which 50µl of a 15mg/ml stock of yeast lytic enzyme (in 50mM Tris-HCl pH7.7, 1mM EDTA, 50% (v/v) glycerol) and 15µl β-mercaptoethanol were added. Cells were converted to spheroplasts during a 1 hr incubation, with shaking, at 30°C. Spheroplasts were collected by centrifuging at 660 *g* for 5 min in a bench top centrifuge and resuspended in 250µl pull-down lysis buffer (50mM sodium HEPES (pH7.5), 150mM sodium chloride, 5mM EDTA, 1mM sodium vanadate, 6µM MG132, 1mM N-ethylmaleimide (NEM), 1% (v/v) Triton X-100, 0.1mM phenylmethylsulphonyl fluoride (PMSF), 10µg/ml soybean trypsin inhibitor, 10µg/ml benzamidine and EDTA-free complete protease inhibitor mix (1 tablet (Roche) / 50ml lysis buffer) before transferring to a 1.5ml microfuge tube. Cell lysate was then incubated at 4°C for 1 hr with rotation before centrifugation at 12470 *g* for 15 min at 4°C in a bench top centrifuge to pellet insoluble material. Samples were equalised for protein concentration by Bradford assay and a small aliquot of cell lysate reserved for SDS-PAGE analysis before the lysate was split equally amongst the various GST fusion proteins (10µg/sample) immobilised to glutathione Sepharose beads and incubated with rotation at 4°C for 2 hr. Beads were recovered by a brief 20 sec centrifugation and washed 3 times with lysis buffer prior to the elution of bound proteins by the addition of 20µl LSB and incubation at 65°C for 15 min. Samples were subject to SDS-PAGE and immunoblot analysis.

2.2.20. Subcellular membrane fractionation of 3T3-L1 adipocytes

3T3-L1 adipocytes cultured on 10cm dishes were washed once and incubated at 37°C in serum-free DMEM for 2 hr, prior to incubation with 200nM insulin for 15 mins. Following the transfer of plates onto ice, the cells were washed 3 times with cold PBS. All subsequent steps were performed on ice unless indicated otherwise. Cells were scraped from the plate into 1ml/plate HES+PI (250mM sucrose, 20mM HEPES (pH7.4), 1mM EDTA and 1 protease inhibitor tablet (Roche)/ 50ml HES buffer). Pooled cells were homogenised by passing the cell suspension through a 25XG needle 10 times and twice through a 27XG needle. In order to remove lipid droplets, homogenized cells were centrifuged at 500 *g* for 10 min at 4°C in a bench top centrifuge and the homogenate removed from underneath the floating layer of lipid. Homogenate was subject to differential centrifugation to prepare subcellular membrane fractions. This protocol yields four membrane fractions designated as high-density microsomes (HDM), low-density microsomes (LDM), plasma membrane (PM) and mitochondria/nuclei (M/N). All centrifugation steps were carried out at 4°C. The homogenates were initially centrifuged for 12 mins at 12000rpm in an 80Ti rotor (Beckman, Palo Alto, CA, USA) to pellet PM and M/N. This pellet was resuspended in 10ml of HES+PI and recentrifuged for 12 mins at 12000rpm in an 80Ti rotor, the washed pellet was resuspended in 1ml HES+PI and layered onto 10ml high sucrose HES (1.12M sucrose, 1mM EDTA, 20mM HEPES (pH7.4)) and centrifuged for 60mins at 25000rpm using a SW41Ti rotor (Beckman, Palo Alto, CA, USA). The pellet obtained from this step represents the M/N. The PM fraction was removed from the interface, HES added to a final volume of 12ml and the membranes collected by centrifugation for 15 mins at 15000rpm in an 80Ti rotor. The supernatant from the initial 80Ti centrifugation, comprising LDM, HDM and cytosol was subjected to centrifugation for 17 mins at 15000rpm in an 80Ti rotor to isolate the HDM fraction. The resulting supernatant was then subject to centrifugation for 75mins at 50000rpm using an 80Ti rotor to yield the LDM fraction. Membrane fractions were resuspended in HES+PI and stored at -20°C.

***E.coli* strains used in this study:**		
Strain	**Genotype**	**Source**
BL-21 (DE3)	F⁻ *ompT* *hsdS*$_B$($r_B^-m_B^-$) *gal dcm* (DE3)	Invitrogen
XL-1 Blue	*recA1 endA1 gyrA96 thi-1 hsdR17 supE44 relA1 lac* [F' *proAB lacI*^{q}ZΔ*M15* Tn10 (Tet^r)]	Stratagene

***S.cerevisiae* strains used in this study:**				
	Strain	**Genotype**	**Construction**	**Source**
1	SF838-9Dα	*MATα leu2-3,112 ura3-52 his4-519 ade6 gal2 pep4-3*		(Rothman et al., 1989)
2	RPY10	*MATα leu2-3,112 ura3-52 his4-519 ade6 gal2*		(Piper et al., 1994)
7	MC996A	*MATa ura3-52 his3-11,15 leu2-3,112 MAL2 SUC2 GAL MEL*		(Reifenberger et al., 1995)
8	KY73	*MATa ura3-52 his3-11,15 leu2-3,112 MAL2 SUC2 GAL MEL hxt1Δ::HIS3::Δhxt4 hxt5::LEU2 hxt2Δ::HIS3 hxt3Δ::LEU2::Δhxt6 hxt7::HIS3*		(Reifenberger et al., 1995)
10	SEY6210	*MATα ura3-52 his3-Δ200 leu2-3,112 lys2-801 trp1-Δ901 suc2-Δ9 ade2-101*		(Robinson et al., 1988)
20	RMY1	KY73 with *pep4-3*	pLO2010 (Nothwehr et al., 1995) linearised with *Eco*RI was used to disrupt *PEP4* in KY73	This study
21	RMY2	MC996A with *pep4-3*	pLO2010 (Nothwehr et al., 1995) linearised with *Eco*RI was used to disrupt *PEP4* in MC996A	This study
77	SGY73	*leu2-3,112 ura3-52 his4-519 ade6 pep4-3 Δvps27::LEU2*		(Gerrard et al., 2000)
88	MBY004	*MATα ura3-52 his3-Δ200 leu2-3,112 lys2-801 trp1-Δ901 suc2Δ9gga1::HIS5spLgga2::TRP1*		(Black and Pelham, 2000)

Table 2.1. E.coli and S.cerevisiae strains used in this study

Oligo	Description	Sequence (5'⇒ 3')
1	*CUP1*hGLUT4	GATATTAAGAAAAACAAACTGTACAATCA ATCAATCAATCATCACATAAAATGCCGTC GGGCTTCCAACAGATA
2	*3'UTR*hGLUT4	ATTATAACGTATTAAATAATATGTGAAAA AAGAGGGAGAGTTAGATAGGATCAGTCG TTCTCATCTGGCCCTAA
61	hGLUT4K495RhGLUT4	CTTTTAGAGCAGGAGGTGCGACCCAGCAC AGAACTTG
62	reverse compliment of 61	CAAGTTCTGTGCTGGGTCGCACCTCCTGC TCTAAAAG
73	hGLUT4K109RhGLUT4	CAGTGGCTTGGAAGGCGAAGGGCCATGCT GGTC
74	reverse compliment of 73	GACCAGCATGGCCCTTCGCCTTCCAAGCC ACTG
85	hGLUT4K242RhGLUT4	CGAGGGGCCTGCCAGACGAAGTCTGAAG CGCCTGAC
86	reverse compliment of 85	GTCAGGCGCTTCAGACTTCGTCTGGCAGG CCCCTCG
87	hGLUT4K245RhGLUT4	CTGCCAGAAAGAGTCTGCGACGCCTGACA GGCTGGG
88	reverse compliment of 87	CCCAGCCTGTCAGGCGTCGCAGACTCTTT CTGGCAG
89	hGLUT4K261RhGLUT4	GAGTGCTGGCTGAGCTGCGAGATGAGAA GCGGAAGC
90	reverse compliment of 89	GCTTCCGCTTCTCATCTCGCAGCTCAGCCA GCACTC
91	hGLUT4K264RhGLUT4	CTGAGCTGAAGGATGAGCGACGGAAGCT GGAGCGTG
92	reverse compliment of 91	CACGCTCCAGCTTCCGTCGCTCATCCTTCA GCTCAG
93	hGLUT4K266RhGLUT4	GAAGGATGAGAAGCGGCGACTGGAGCGT GAGCGGC
94	reverse compliment of 93	GCCGCTCACGCTCCAGTGCCCGCTTCTCA TCCTTC
117	hGLUT4K109RK242RK245 RhGLUT4K109RK242R	CTGCCAGACGAAGTCTGCGACGCCTGACA GGCTGGG
118	reverse compliment of 117	CCCAGCCTGTCAGGCGTCGCAGACTTCGT CTGGCAG
119	hGLUT4K109RK242RK245 RK261RK264RhGLUT4K10 9RK242RK245RK261R	CTGAGCTGCGAGATGAGCGACGGAAGCT GGAGCGTG
120	reverse compliment of 119	CACGCTCCAGCTTCCGTCGCTCATCTCGC AGCTCAG
121	hGLUT4K109RK242RK245 RK261RK264RK266RhGL UT4K109RK242RK245RK2 61RK264R	GCGAGATGAGCGACGGCGACTGGAGCGT GAGCGGC

122	reverse compliment of 121	GCCGCTCACGCTCCAGTCGCCGTCGCTCA TCTCGC
149	LEU23'	GGTTAAAAAATGAGCTGATTTAAC
153	LEU25'	GGAGACGGTCACAGCTTGTC
183	hGLUT47KR*Sph*I3'UTR	GGGCCAGATGAGAACGACGCATGCTCCTA TCTAACTCTCCCTC
184	reverse compliment of 183	GAGGGAGAGTTAGATAGGAGCATGCGTC GTTCTCATCTGGCCC
185	3'UTR*Sph*IUb	ATTATAACGTATTAAATAATATGTGAAAA AAGAGGGAGAGTTAGATAGGAGCATGCT TAACCTCCACGCAGACGCAAGACCAA
186	hGLUT47KR*Sph*IHA-Ub	GGAGGTGCGACCCAGCACAGAACTTGAG TATTTAGGGCCAGATGAGAACGACGCATG CATGAAATACCCATACGATGTT
231	hGLUT47KRR109KhGLUT 47KR	CAGTGGCTTGGAAGGAAAAGGGCCATGC TGGTC
232	reverse compliment of 231	GACCAGCATGGCCCTTTTCCTTCCAAGCC ACTG
233	hGLUT47KRR242KhGLUT 47KR	GAGGGGCCTGCCAGAAAGAGTCTGCGAC GCCTG
234	reverse compliment of 233	CAGGCGTCGCAGACTCTTTCTGGCAGGCC CCTC
235	hGLUT47KRR245KhGLUT 47KR	GCCAGACGAAGTCTGAAGCGCCTGACAG GCTGG
236	reverse compliment of 235	CCAGCCTGTCAGGCGCTTCAGACTTCGTC TGGC
237	hGLUT47KRR261KhGLUT 47KR	GTGCTGGCTGAGCTGAAGGATGAGCGAC GGCGA
238	reverse compliment of 237	TCGCCGTCGCTCATCCTTCAGCTCAGCCA GCAC
239	hGLUT47KRR264KhGLUT 47KR	GAGCTGCGAGATGAGAAGCGGCGACTGG AGCGTG
240	reverse compliment of 239	CACGCTCCAGTCGCCGCTTCTCATCTCGC AGCTC
241	hGLUT47KRR266KhGLUT 47KR	CGAGATGAGCGACGGAAGCTGGAGCGTG AGCGG
242	reverse compliment of 241	CCGCTCACGCTCCAGCTTCCGTCGCTCATC TCG
243	hGLUT47KRR495KhGLUT 47KR	CTTTTAGAGCAGGAGGTGAAACCCAGCAC AGAACTTG
244	reverse compliment of 243	CAAGTTCTGTGCTGGGTTTCACCTCCTGCT CTAAAAG
260	*Eco*RIhGLUT4	GGAATTCATGCCGTCGGGCTTCCAACAG
261	*Sal*IhGLUT4	AGGGTCGACTCAGTCGTTCTCATCTGGCC C
262	*Sal*IUb	AGGGTCGACTTAACCTCCACGCAGACGCA AG
263	3'hGLUT4 from residue 69	GCCTGGAGGGATGGAGCTGGG
264	5'hGLUT4 from residue 69	CCCAGCTCCATCCCTCCAGGC

343	hGLUT4*Sph*I3'UTR (removing stop)	GCCAGATGAGAACGACGCATGCTATCTAA CTCTCCCTC
344	reverse compliment of 343	GAGGGAGAGTTAGATAGCATGCGTCGTTC TCATCTGGC
352	DSK2M342RF344ADSK2	GACAACTAAACGACAGGGGCGCCTTCGAT TTCGATAGAAAC
353	reverse compliment of 352	GTTTCTATCGAAATCGAAGGCGCCCCTGT CGTTTATTGGTC
365	hGLUT4*Sph*IGFP	GGAGGTGCGACCCAGCACAGAACTTGAG TATTTAGGGCCAGATGAGAACGACGCATG CATGGGTAAAGGAGAAGAACTTTTC
366	3'UTR*Sph*IGFP	ATTATAACGTATTAAATAATATGTGAAAA AAGAGGGAGAGTTAGATAGGAGCATGCT TACTTGTATAGTTCATCCATGCCATG

Table 2.2. Oligonucleotides used in this study

	Plasmid	Description	Reference
1	pLO2010	*pep4-ΔH3* in pRS306	(Nothwehr et al., 1995)
33	pRM2	Yeast expression plasmid (*CEN, URA3*) encoding human GLUT4 from the *CUP1*promoter	This study
66	pRM1	Yeast expression plasmid (*CEN, LEU2*) encoding HA-tagged ubiquitin from the *CUP1*promoter	This study
133	pTC2	Yeast expression plasmid (*CEN, URA3*) encoding *PHO8* under control of *CUP1*promoter	This study (constructed by Tom Carr)
155	pRM5	Yeast expression plasmid (*CEN, URA3*) encoding human GLUT4 with the point mutation K495R from the *CUP1* promoter	This study
174	pRM6	Yeast expression plasmid (*CEN, URA3*) encoding human GLUT4 with the point mutation K242R from the *CUP1* promoter	This study
175	pRM7	Yeast expression plasmid (*CEN, URA3*) encoding human GLUT4 with the point mutation K245R from the *CUP1* promoter	This study
176	pRM8	Yeast expression plasmid (*CEN, URA3*) encoding human GLUT4 with the point mutation K261R from the *CUP1* promoter	This study
187	p1839	Yeast expression plasmid (CEN, LEU2) encoding PHO8 from the GAL promoter	(Piper et al., 1997)
190	pRM9	Yeast expression plasmid (*CEN, URA3*) encoding human GLUT4 with the point mutation K264R from the *CUP1* promoter	This study
191	pRM10	Yeast expression plasmid (*CEN, URA3*) encoding human GLUT4 with the point mutation K266R from the *CUP1* promoter	This study
197	pRM11	Yeast expression plasmid (*CEN, URA3*) encoding human GLUT4 with the point mutations K495R and K242R from the *CUP1* promoter	This study
198	pRM12	Yeast expression plasmid (*CEN, URA3*) encoding human GLUT4 with the point mutations K495R, K242R and K245R from the *CUP1* promoter	This study
203	pRM13	Yeast expression plasmid (*CEN, URA3*) encoding human GLUT4 with the point mutations K495R, K242R, K245R and K261R from the *CUP1* promoter	This study
204	pRM14	Yeast expression plasmid (*CEN, URA3*) encoding human GLUT4 with the point mutations K495R, K242R, K245R, K261R and K264R from the *CUP1* promoter	This study
205	pRM15	Yeast expression plasmid (*CEN, URA3*) encoding human GLUT4 with the point mutations K495R, K242R, K245R, K261R, K264R and K266R from the *CUP1* promoter	This study

206	pRM3	Yeast expression plasmid (*CEN, URA3*) encoding human GLUT4 with lysines 109, 242, 245, 261, 264, 266, 495 mutated to arginine residues (GLUT4-7K/R) from the *CUP1* promoter	This study
230	pRM16	Yeast expression plasmid (*CEN, URA3*) encoding human GLUT4 with the point mutation K109R from the *CUP1* promoter	This study
269	p2313	Yeast expression plasmid (*CEN, URA3*) encoding GFP-tagged Gap1p from the *CUP1* promoter	(Scott et al., 2004)
305	pRM17	Yeast expression plasmid (*CEN, URA3*) encoding human GLUT4-7K/R with the point mutation R242K from the *CUP1* promoter	This study
306	pRM18	Yeast expression plasmid (*CEN, URA3*) encoding human GLUT4-7K/R with the point mutation R261K from the *CUP1* promoter	This study
311	pRM19	Yeast expression plasmid (*CEN, URA3*) encoding human GLUT4-7K/R with the point mutation R109K from the *CUP1* promoter	This study
312	pRM20	Yeast expression plasmid (*CEN, URA3*) encoding human GLUT4-7K/R with the point mutation R245K from the *CUP1* promoter	This study
313	pRM21	Yeast expression plasmid (*CEN, URA3*) encoding human GLUT4-7K/R with the point mutation R264K from the *CUP1* promoter	This study
314	pRM22	Yeast expression plasmid (*CEN, URA3*) encoding human GLUT4-7K/R with the point mutation R266K from the *CUP1* promoter	This study
315	pRM23	Yeast expression plasmid (*CEN, URA3*) encoding human GLUT4-7K/R with the point mutation R495K from the *CUP1* promoter	This study
316	pRM24	Yeast expression plasmid (*CEN, URA3*) encoding GLUT4-7K/R-HAUb from the *CUP1* promoter	This study
320	pRM25	Retroviral expression vector encoding GLUT4-7K/R-HAUb	This study
321	pRM4	Retroviral expression vector encoding HA-tagged GLUT4-7K/R	This study
332	pSN222	Yeast expression plasmid (*CEN, LEU2*) encoding HA-tagged Kex2p	(Nothwehr et al., 1995)
346	pRM30	Yeast expression plasmid (*CEN, LEU2*) encoding human GLUT4 from the *CUP1*promoter	This study
347	pRM31	Yeast expression plasmid (*CEN, LEU2*) encoding GLUT4-7K/R from the *CUP1*promoter	This study
358	pHA-GLUT4	Retroviral expression vector encoding HA-tagged GLUT4	(Shewan et al., 2000)
359	pGEX-DSK_{UBA}	*E.coli* expression vector encoding GST-UBA (the UBA domain, residues 328-373 fused to the C-terminus of GST), based on pGEX	(Funakoshi et al., 2002)
390	pCAL1	*E.coli* expression vector encoding GST-UBA_{mut} (as pGEX-DSK_{UBA} but with two point mutations,	This study (constructed by

		M342R and F344A in the UBA domain)	Chris Lamb)
398	GST-GGA1-VHS-GAT	*E.coli* expression vector encoding the VHS and GAT domains of GGA1, based on pGEX	(Mattera et al., 2004)
399	GST-GGA3-VHS-GAT	*E.coli* expression vector encoding the VHS and GAT domains of GGA3, based on pGEX	(Mattera et al., 2004)
405	2256	Yeast expression plasmid (*CEN, URA3*) encoding HA-tagged GGA2	(Scott et al., 2004)
406	2309	Yeast expression plasmid (*CEN, URA3*) encoding HA-tagged GGA2gatΔ	(Scott et al., 2004)
421	pRM34	Yeast expression plasmid (*CEN, URA3*) encoding human GLUT4 tagged with GFP(S65T) from the *CUP1* promoter	This study

Table 2.3. Plasmids used in this study

Chapter 3: Investigation of GLUT4 trafficking in yeast Saccharomyces cerevisiae

Chapter 3: Investigation of GLUT4 trafficking in yeast Saccharomyces cerevisiae.

3.1. Introduction

Kaiser and colleagues first noted that yeast possess a regulated membrane trafficking step that bears remarkable similarity to the insulin-regulated trafficking of GLUT4; that is the nitrogen-regulated trafficking of the general amino acid permease Gap1p (Roberg et al., 1997). Fat and muscle cells increase their capacity to take up glucose in response to insulin by delivering the GLUT4 transporter to the cell surface from an intracellular storage compartment. Likewise, the general amino acid permease Gap1p is stored intracellularly under nutrient rich conditions but when nutrients are limited, Gap1p is trafficked to the plasma membrane where it facilitates the uptake of amino acids from the extracellular media (Roberg et al., 1997).

Given the parallels that exist between the insulin-regulated trafficking of GLUT4 in fat and muscle cells and the nitrogen-regulated trafficking of Gap1p in *S. cerevisiae,* a chimeric protein was constructed, in which the carboxyl terminal tail of GLUT4 was replaced with the analogous portion of Gap1p. When expressed in adipocytes, this GLUT4/Gap1p chimera localises to the TGN, like endogenous GLUT4 (unpublished data; Nia Bryant and David James, Figure 1.6). Additionally, like GLUT4 itself, the GLUT4/Gap1p chimera translocates to the cell surface of adipocytes upon insulin stimulation (unpublished data; Nia Bryant and David James, Figure 1.6). To build on this observation, I set out to further explore the parallels between GLUT4 and Gap1p regulated trafficking by testing the hypothesis that mammalian GLUT4 would traffic in a nitrogen-regulated manner if expressed in the *S. cerevisiae* (yeast).

To this end, I expressed human GLUT4 (hGLUT4) in yeast. This chapter describes how this was achieved and also presents data consistent with the above hypothesis.

3.2. Expression of hGLUT4 in yeast Saccharomyces cerevisiae.

Previous studies expressing mammalian GLUT4 in yeast have reported that the transporter is retained intracellularly, localising to the endoplasmic reticulum (ER) (Kasahara and Kasahara, 1997; Wieczorke et al., 2003). This ER localisation may be due to the high

levels of expression used in these studies as they expressed GLUT4 at very high levels from the *GAL1-10* promoter. In order to produce GLUT4 at more modest levels in yeast, I undertook to express the transporter from the regulatable *CUP1* promoter.

The yeast *CUP1* promoter is derived from the copper metallothionein protein (Cu-MT); a low molecular weight, cysteine-rich protein that binds copper and whose induction in response to the addition of copper to yeast cells results in their copper resistance (Butt et al., 1984). One advantage of using the *CUP1* promoter for heterologous gene expression is that it is titratable, allowing gene expression to be tightly modulated (Mascorro-Gallardo et al., 1996). This can prevent the masking of certain phenotypes that would otherwise occur with gene overexpression. The expression features of the *CUP1* promoter contrast with that of the *GAL1-10* promoter from which GLUT4 has previously been expressed in yeast (Kasahara and Kasahara, 1997; Wieczorke et al., 2003), which, in the presence of galactose and absence of glucose, induces a 1000-fold increase in gene expression (Adams, 1972; Douglas and Hawthorne, 1964). This high level of expression from the *GAL1-10* promoter is either switched 'on' or 'off' and lacks the advantages of being more tightly controlled.

In order to place the GLUT4 ORF under *CUP1* control, the strategy outlined in Figure 3.1 was adopted to construct plasmid pWTG4 (pRM2) (harbouring hGLUT4 under control of the *CUP1* promoter).

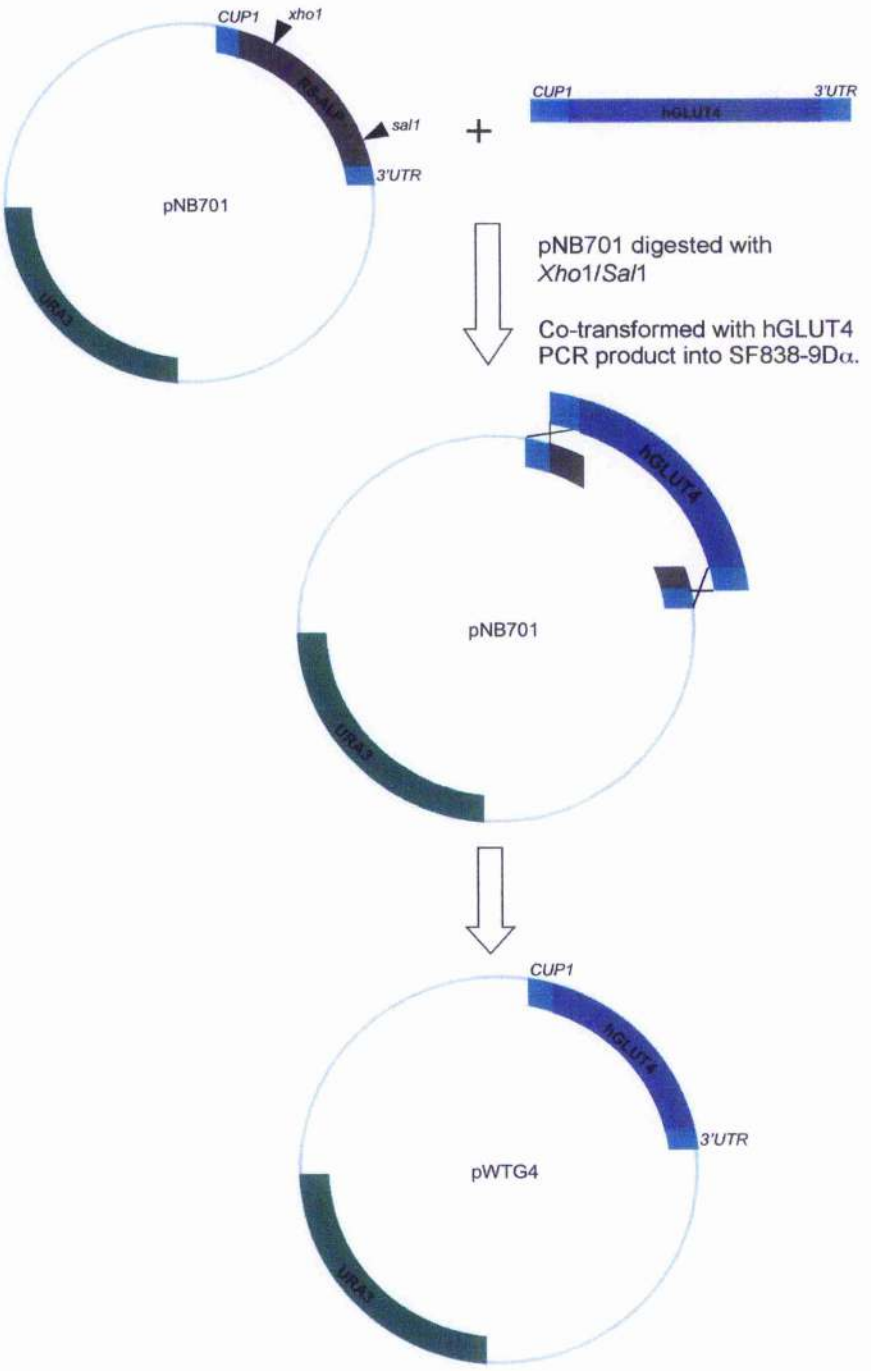

Figure 3.1. Schematic of pWTG4 (pRM2) construction

(details as described in text. Please note that the XhoI and SalI sites indicated in pNB701 are unique).

Plasmid pNB701 (based on pRS316 (Sikorski and Hieter, 1989), and constructed by Nia Bryant) contains the ORF encoding the protein RS-ALP (retention sequence-ALP) (Bryant et al., 1998b) under control of the *CUP1* promoter, followed by the 3'*UTR* of *PHO8* (a region often containing important regulatory sequences (Mazumder et al., 2003)). Homologous recombination was used to replace the RS-ALP ORF of pNB701 with the ORF for hGLUT4. To this end, PCR was used to amplify hGLUT4 from a plasmid carrying human GLUT4 cDNA (provided by Professor Gwyn Gould) using hGLUT4 oligos 1 and 2 (Figure 3.2 and Table 2.2). These primers were designed to produce a fragment of DNA, encoding human GLUT4, with ends homologous to the *CUP1* promoter and *PHO8* 3'*UTR*. The majority of the ORF for RS-ALP was removed from pNB701 by digestion with restriction enzymes *Xho*I and *Sal*I and the resulting linear plasmid, along with the hGLUT4 PCR fragment, was used to co-transform SF838-9Dα yeast cells. Homologous recombination between the ends of the PCR product and the linearised plasmid (as illustrated in Figure 3.1) allowed the hGLUT4 PCR product to repair the gap created in pNB701, thereby creating pWTG4 (pRM2).

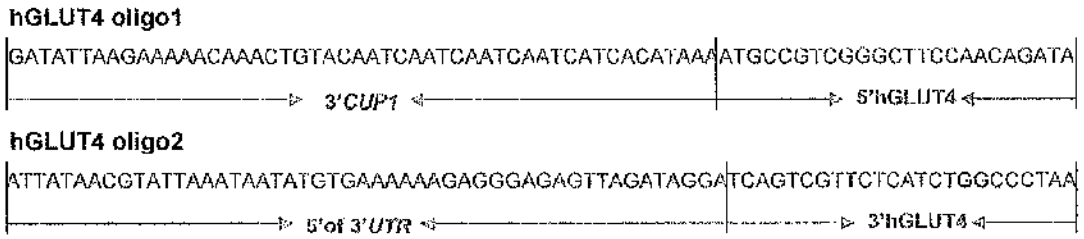

Figure 3.2. hGLUT4 primer sequences

Following the co-transformation reaction, colonies were selected on media lacking uracil (any cells that did not repair the gapped plasmid would not be able to grow as the linearised plasmid would not be able to propagate). Colonies were picked from this plate and patched onto media lacking uracil and containing 150μM $CuSO_4$. Immunoblot analysis was performed to identify colonies that were expressing human GLUT4. This was performed by Nia Bryant and is therefore not presented in this thesis. Plasmid was rescued from colonies identified as expressing GLUT4 and these were subsequently transformed into 'fresh' SF838-9Dα yeast cells to check for expression of GLUT4. Having obtained plasmid DNA that drives the expression of human GLUT4 from the *CUP1* promoter, I confirmed that no errors had been introduced into the GLUT4 ORF using DNA

sequencing. The plasmid thus obtained was subsequently used to characterize the expression of human GLUT4 in yeast.

The ability of plasmid pWTG4 (pRM2) to drive the expression of hGLUT4 in yeast was characterised using immunoblot analysis. pWTG4 (pRM2) was used to transform into SF838-9Dα yeast cells and the resulting transformants were grown in selective media (SD) either containing 100μM $CuSO_4$, or not, (as indicated; Figure 3.3). Proteins contained in lysates prepared from 10 OD_{600} equivalents of cells were separated using SDS-PAGE prior to immunoblot analysis using an antibody that specifically recognises the carboxyl-terminal fourteen amino acids of GLUT4 (Brant et al., 1992).

An immunoreactive band with an apparent molecular weight of ~42KDa was detected in cells grown in the presence of copper but missing from those cells grown in the absence of copper, indicating that this band is a result of expression from the *CUP1* promoter. No such band was detected in SF838-9Dα cells harbouring pTC2 (a plasmid harbouring *PHO8* under the *CUP1* promoter instead of hGLUT4, from Tom Carr) indicating the band was specific to cells carrying pWTG4. Lysate from 3T3-L1 adipocytes was used as a positive control for the presence of mammalian GLUT4. Although the predicted molecular weight of hGLUT4 is 55kDa (Fukumoto et al., 1989) typically a lower molecular weight of around 48kDa is detected by SDS-PAGE analysis, as seen with the 3T3-L1 adipocyte lysate in Figure 3.3. Hydrophobic proteins bind SDS at a higher ratio, therefore it is common for highly hydrophobic proteins like mammalian glucose transporters to migrate faster on SDS-PAGE gels (Birnbaum et al., 1986; Mueckler et al., 1985; Thorens et al., 1988) and so this lower molecular weight value for hGLUT4 is not unexpected.

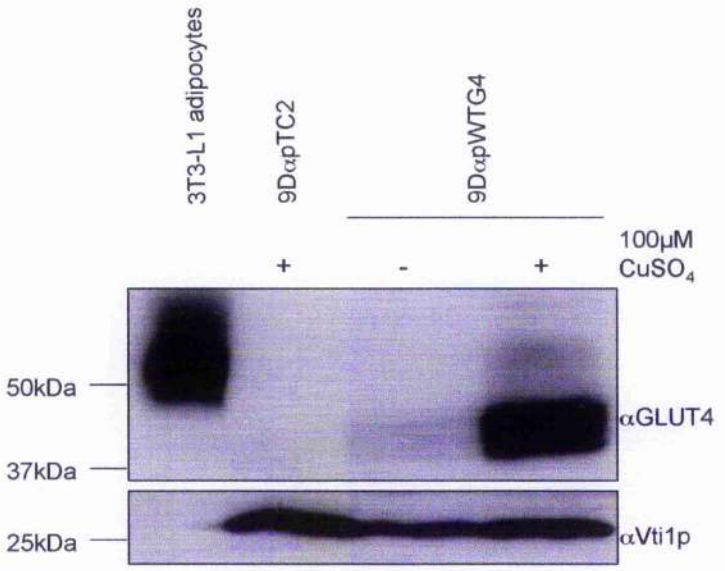

Figure 3.3. Expression of hGLUT4 in SF838-9Dα cells.

SF838-9Dα yeast cells harbouring pWTG4 (hGLUT4 under CUP1 promoter) or pTC2 (empty vector) were grown in selective media either with or without 100μM $CuSO_4$ as indicated above. The amount of hGLUT4 in 10 OD_{600} of cells was assessed using immunoblot analysis. Lysate from 3T3-L1 adipocytes was included in the immunoblot as a positive control (the amount of the v-SNARE Vti1p in each sample was similarly assessed to control for equal loading).

Figure 3.3 indicates a discrepancy between the molecular weight of hGLUT4 detected in the yeast lysate with that of the adipocyte lysate (approximately 42 and 48kDa respectively). The heterologous expression of ratGLUT1 in yeast cells showed a similar reduction in molecular weight of around 5kDa between ratGLUT1 expressed in yeast (40kDa) compared to that expressed in animal cells (varies from 44 to 55kDa depending on tissue and cell type) (Kasahara and Kasahara, 1996). In this case, the glycosylation of GLUT1 was examined. Treatment of human erythrocyte GLUT1 with *N*-glycosidase F treatment (a deglycosylation enzyme) saw a reduction in molecular mass from 50 to 40kDa. With the molecular mass of GLUT1 in yeast also being 40kDa this indicates yeast-made GLUT1 is not N-glycosylated to the same extent as it is in mammalian cells (Kasahara and Kasahara, 1996). GLUT4 contains a single N-glycosylation site in its first extracellular loop (Pessin and Bell, 1992) and is processed by *N*-linked glycosylation to form the mature transporter in L6 muscle cells (Mitsumoto and Klip, 1992). It is therefore

likely that, like ratGLUT1, the hGLUT4 expressed in yeast lacks glycosylation. In Figure 3.3, the majority of hGLUT4 detected in yeast is found at 42kDa (indicating unglycosylated hGLUT4) but a small minority of hGLUT4 can be detected at 50kDa that would indicate glycosylated hGLUT4. Glycosylated proteins often migrate as diffuse bands by SDS-PAGE, as indicated with adipocyte lysate, but less so in the yeast lysate.

As discussed above, a major advantage of using the *CUP1* promoter is that it is titratable, allowing gene expression to be tightly modulated (Mascorro-Gallardo et al., 1996). The expression characteristics of pWTG4 were established by growing SF838-9Dα cells harbouring pWTG4 in selective media (SD) containing increasing amounts of $CuSO_4$ (Figure 3.4). Proteins contained in lysates prepared from 10 OD_{600} equivalents of cells grown in these media were separated using SDS-PAGE. Immunoblot analysis with α-GLUT4 antibody shows that an increase of $CuSO_4$ in the media is related to an increase in the expression of hGLUT4.

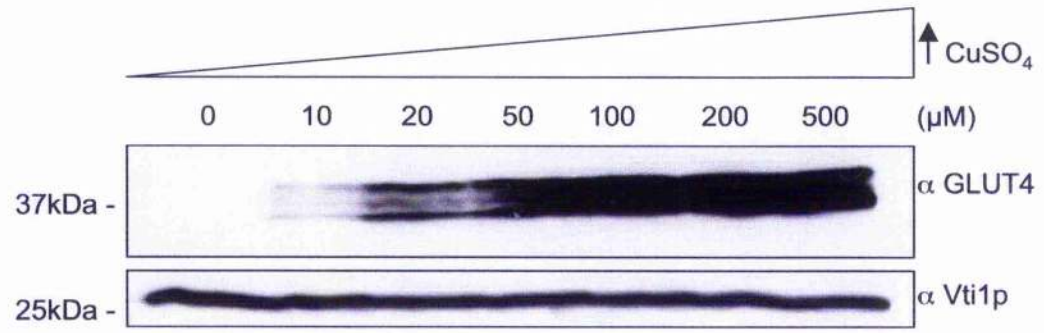

Figure 3.4. hGLUT4 expression increases in relation to $CuSO_4$ in media.
SF838-9Dα yeast cells harbouring pWTG4 (hGLUT4 under CUP1 promoter) were grown in selective media (SD) with increasing amounts of $CuSO_4$, as indicated above. The amount of hGLUT4 in 10 OD_{600} of cells was assessed using immunoblot analysis (the amount of Vti1p in each sample was similarly assessed to control for equal loading.

3.3. hGLUT4 is stabilised in yeast cells that lack active vacuolar proteases.

The *PEP4* gene encodes the vacuolar aspartyl protease, proteinase A which promotes the activation of mature vacuolar hydrolases from their inactive precursors (Ammerer et al., 1986; Woolford et al., 1986). The yeast strain SF838-9Dα contains a *pep4-3* mutation that makes it deficient in active vacuolar protease activity (Rothman et al., 1989) and,

consequently, allows the stabilisation of proteins that are targeted to the lumen of the vacuole or to the proteolytically active endosomal system.

pWTG4 was expressed in the yeast strain SF838-9Dα (*pep4-3*) and the congenic *PEP4* strain, RPY10 (Piper et al., 1995; Piper et al., 1994) and proteins contained in lysates prepared from 10 OD_{600} equivalents of cells were separated using SDS-PAGE prior to immunoblot analysis performed with anti-GLUT4 antibody. hGLUT4 was detected when expressed in the *pep4-3* strain (SF838-9Dα) but not when expressed in the congenic *PEP4* strain (RPY10), suggesting that hGLUT4 is stabilised in strains that lack active vacuolar proteases (Figure 3.5).

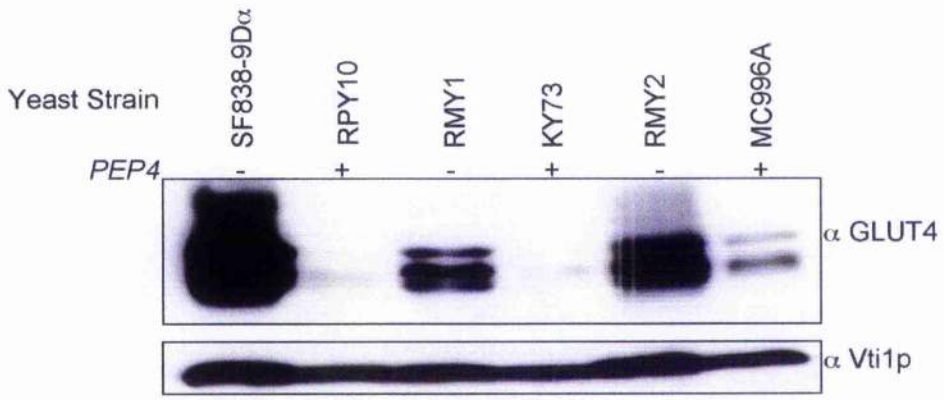

Figure 3.5. hGLUT4 is stabilised in yeast lacking active vacuolar proteases
SF838-9Dα, RPY10, KY73, RMY1, MC996A and RMY2 yeast cells (PEP4 or pep4-3, as indicated above) harbouring pWTG4 (hGLUT4 under CUP1 promoter) were grown in selective media (SM) with 100μM $CuSO_4$. The amount of hGLUT4 in 10 OD_{600} of cells was assessed using immunoblot analysis (the amount of Vti1p in each sample was similarly assessed to control for equal loading). SF838-9Dα, RMY1 and RMY2 are congenic to RPY10, KY73 and MC996A respectively; in each case the congenic pairs differ only at the PEP4 locus, with the latter being wild-type and the former null mutant.

To investigate this further, the *PEP4* gene was disrupted in strains KY73 and MC996A to create the congenic strains RMY1 and RMY2 respectively. The *PEP4* gene was disrupted in strains KY73 and MC996A using the loop in/loop out gene disruption method with the plasmid pLO2010 (Nothwehr et al., 1995). This involved transforming strains KY73 and

MC996A with plasmid pLO2010 linearised following digestion with *Eco*R1. pLO2010 contains the *URA3* selectable marker flanked by homologous sequences to *PEP4* (Nothwehr et al., 1995). The *PEP4* gene was replaced by the *URA3* containing fragment following its integration by homologous recombination and cells with the *URA3* disruption were selected by growth on SD-URA solid media. The *URA3* marker is also flanked by sequences of DNA that enable the *URA3* marker to 'loop-out' by homologous recombination. Cells successful in looping out *URA3* were selected by growth on media containing 5-fluoroorotic acid (5-FOA) (Nothwehr et al., 1995). The *URA3* gene encodes orotine-5'-monophosphate (OMP) dicarboxylase, which converts the non-toxic 5-FOA to fluorodeoxyuridine (Boeke et al., 1987). Fluorodeoxyuridine is toxic to cells and so, only those strains lacking the *URA3* gene can grow in the presence of 5-FOA (Boeke et al., 1987). Finally, the N-acetyl-phenylalanine-p-naphthyl-ester (APNE) overlay assay (Wolf and Fink, 1975) was used to confirm the *pep4-3* mutant colonies and their lack of vacuolar protease activity. The APNE overlay assay detects the activity of carboxypeptidase Y (CPY) (Wolf and Fink, 1975), which is activated by proteinase A, the *PEP4* gene product. CPY mediates the release of β-naphthol from APNE, which is detected in the APNE overlay assay from its reaction with the Fast Garnet GBC salt and the resulting formation of an insoluble red dye. *PEP4* strains therefore turn red, whereas *pep4-3* strains (with their lack of active CPY) remain white.

Immunoblot analysis using anti-GLUT4 antibody with cells harbouring pWTG4 (grown on copper-containing media) detects hGLUT4 in the strains lacking active vacuolar proteases (*pep4* mutants; SF838-9Dα, RMY1 and RMY2, Figure 3.5) but not in the congenic parent strains (wild-type *PEP4*; RPY10, KY73 and MC996A, Figure 3.5). These data indicate that, when expressed in yeast, hGLUT4 is delivered to a proteolytically active compartment.

3.4. hGLUT4 localises to the Golgi in yeast.

In order to determine the subcellular distribution of hGLUT4 in yeast, SF838-9Dα cells harbouring pWTG4 (expressing hGLUT4) and pSN222 (which drives expression of HA-tagged Kex2p) were visualised using indirect immunofluorescence microscopy (Figure 3.6). Kex2p is a well-characterised endoprotease in *S.cerevisiae*, which cleaves the precursors of several proteins, such as the mating pheromone α-factor (Fuller et al., 1989),

in the late Golgi compartment of yeast cells, likely the yeast equivalent of the mammalian TGN (Bryant and Boyd, 1993; Redding et al., 1991; Wilcox and Fuller, 1991; Wilcox et al., 1992). Figure 3.6 shows an intracellular punctate staining of hGLUT4, which co-localises significantly with that of the TGN marker Kex2p. This Golgi-localised punctate staining seen for hGLUT4 (Figure 3.6) is in contrast to that previously described (Kasahara and Kasahara, 1997; Wieczorke et al., 2003), where it was reported that mammalian GLUT4, when expressed in yeast, localised to the ER. However, as noted earlier, this is likely due to the fact that in these studies GLUT4 was expressed at very high levels from the GAL1-10 promoter, perhaps resulting in GLUT4 misfolding and failing to leave the ER.

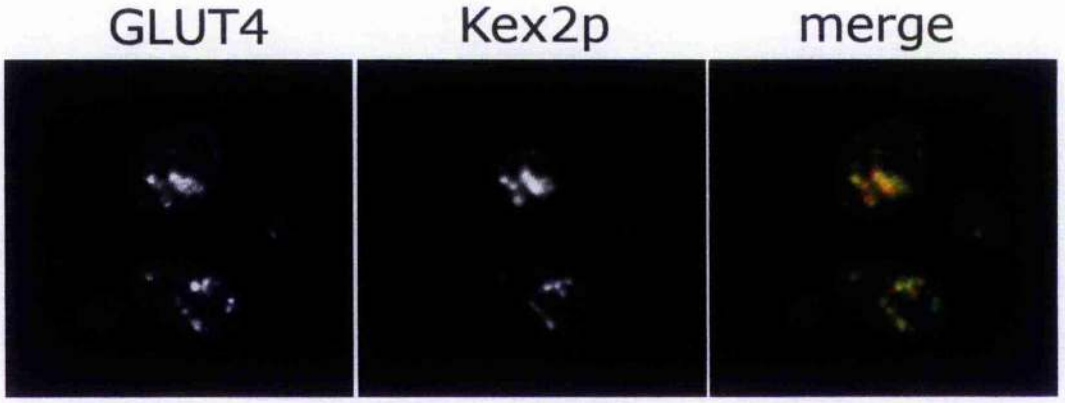

Figure 3.6. hGLUT4 colocalises with Kex2p (TGN) in yeast.
SF838-9Dα cells harbouring pWTG4 (hGLUT4 behind the CUP1 promoter) and pSN222 (encoding HA-tagged Kex2p) were grown in selective media (SD-ura-leu) containing 100μM $CuSO_4$, fixed in formaldehyde and double labelled with anti-HA and anti-GLUT4 antibodies. Rat anti-HA was visualised with alexa568-coupled secondary antibody (red in merged image) and rabbit anti-GLUT4 was visualised with alexa488-coupled secondary antibody (green in merged image).

3.5. hGLUT4 accumulates in the "class E" compartment in vps27 cells.

Like other yeast TGN proteins, Kex2p is retained in the yeast TGN by continually cycling through the endocytic system (Brickner and Fuller, 1997; Bryant and Stevens, 1997), and a similar phenomenon has been described for GLUT4 in adipocytes (Shewan et al., 2003). Resident TGN proteins such as Ste13p and Kex2p localise to the exaggerated

endosomal/prevacuolar compartment (PVC) that accumulates in Class E *vps* mutants such as *vps27Δ* cells (Piper et al., 1995). *VPS27* is one of 13 Class E vacuolar protein sorting (VPS) genes, that act together to regulate membrane traffic through the PVC (Raymond et al., 1992). Mutations in any one of these genes causes the accumulation of the "Class E compartment" which contains TGN proteins, as well as biosynthetic and endocytic traffic en route to the vacuole (Raymond et al., 1992). To further investigate the localisation of hGLUT4 in yeast, I set out to ask whether hGLUT4 also accumulates in the Class E compartment of *vps27Δ* mutant cells.

For this purpose a GFP(S65T)-tagged version of hGLUT4 was produced (the mutant GFP(S65T) emits a brighter fluorescence and acquires fluorescence up to four times faster than wild-type GFP (Heim et al., 1995)). Site-directed mutagenesis was used to replace the 'stop' codon of the hGLUT4 ORF in pRM2 with an *Sph*I site. Following digestion with *Sph*I to linearise the resulting plasmid, sequence encoding GFP(S65T)was introduced immediately after the last codon of hGLUT4 ORF by homologous recombination (for this, sequence encoding GFP(S65T) was amplified by PCR using oligos 365 and 366 (Table 2.2) as primers and pGO36 (Odorizzi et al., 2003) as a template, to carry ends homologous to the 3' end of the hGLUT4 ORF and the proximal region of the PHO8 3'UTR). The resulting plasmid, pRM34 therefore encodes a GFP(S65T)-tagged version of hGLUT4 from the copper-inducible CUP1 promoter. The construction of this plasmid was verified by DNA sequencing.

SF838-9Dα cells, producing a GFP(S65T)-tagged version of hGLUT4 show an intracellular punctate distribution for hGLUT4 that is reminiscent of the indirect immunofluorescence of hGLUT4, seen in Figure 3.6. Importantly, when expressed in *vps27Δ* mutant cells, the distribution of GFP(S65T)-tagged hGLUT4 is markedly different from that seen in wild-type cells, localizing to one or two tight spots. These were identified as the Class E compartment by their accumulation of the lipophilic styryl dye N-(3-triethylammoniumpropyl)-4-(p-diethylaminophenyl-hexatrienyl) pyridium dibromide (FM4-64; Molecular Probes, Oregon, USA). In wild-type cells FM4-64 is endocytosed and delivered to the limiting membrane of the vacuole (Vida and Emr, 1995), but becomes trapped in the Class E compartment of *vps27Δ* mutant cells (Bryant et al., 1998a). The data presented in Figure 3.7 are consistent with a model in which, like Kex2p, GLUT4

achieves localization to the yeast TGN by continually cycling through the endosomal system.

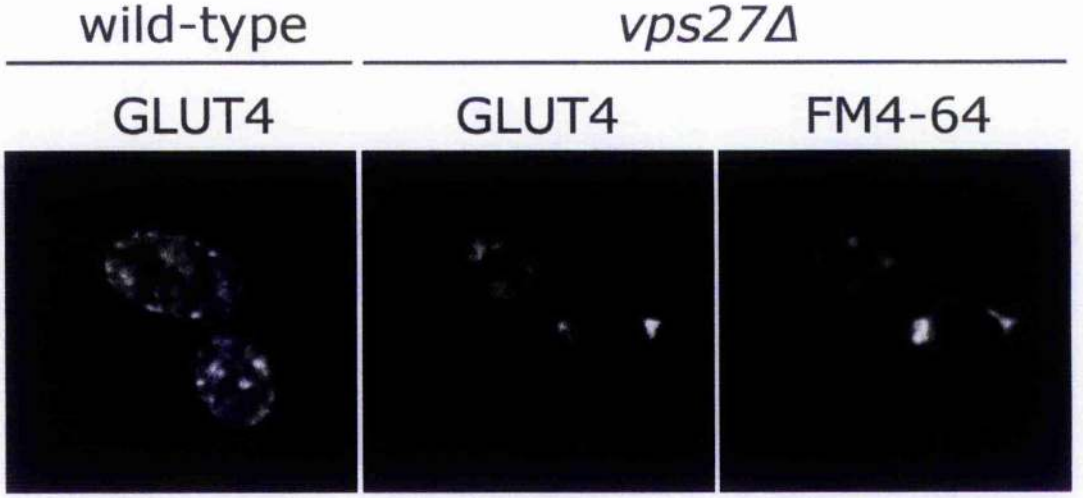

Figure 3.7. hGLUT4 accumulates in the class E compartment in vps27Δ cells
GFP(S65T) was visualised in SF838-9Dα (VPS27) and SGY73 (vps27Δ) cells harbouring pRM34 (GFP(S65T)-tagged hGLUT4 under the CUP1 promoter), which were grown in selective media (SD) with 100μM $CuSO_4$. SGY73 (vps27Δ) cells were also labelled with FM4-64 to mark the Class E compartment.

The data presented in Figures 3.6 and 3.7 indicate that, in yeast, as in adipocytes (Shewan et al., 2003), hGLUT4 localises to the TGN, and that this localisation is achieved by the transporter recycling through the PVC. Intriguingly, the Golgi-localised punctate staining observed for hGLUT4 in yeast (Figure 3.6) is reminiscent of that found for Gap1p under nutrient rich conditions (Roberg et al., 1997), and importantly Gap1p also localises to the PVC of Class E *vps* mutants (Nikko et al., 2003; Rubio-Texeira and Kaiser, 2006).

3.6. hGLUT4 is stabilised by growth on proline-containing media.

Mutant GLUT4 lacking its carboxyl-terminal tail fails to translocate to the plasma membrane of mammalian cells in response to insulin (Figure1.6, unpublished results; Nia Bryant and David James). This indicates that the trafficking information regarding the translocation of GLUT4 resides in the carboxyl-terminal tail. GLUT4 contains a carboxyl-terminal di-leucine motif and an acidic-cluster-based motif that have important

roles in the internalisation and subcellular targeting of GLUT4 (Cope et al., 2000; Shewan et al., 2000). When this region of GLUT4 is replaced with the carboxyl-terminal tail of the yeast general amino acid permease, Gap1p, the translocation of GLUT4 to the plasma membrane of mammalian cells in response to insulin is recovered (Figure1.6, unpublished results; Nia Bryant and David James). This demonstrates that the targeting motifs required for insulin-regulated GLUT4 trafficking are conserved between GLUT4 and Gap1p. Gap1p also contains a dileucine motif within its carboxyl-terminal tail that is required for its nitrogen-regulated transport (Hein and Andre, 1997).

As outlined in Section 1.8, the general amino acid permease, Gap1p, actively transports all naturally occurring amino acids across the plasma membrane of yeast (Grenson et al., 1970; Jauniaux and Grenson, 1990). When yeast cells are grown on non-preferred nitrogen sources such as proline or urea, Gap1p is mobilised from an intracellular storage pool to the plasma membrane, where it allows amino acids into the cell for use as a source of nitrogen (Roberg et al., 1997). However, when yeast cells are grown on preferred sources of nitrogen such as glutamate, Gap1p transported to the proteolytically active yeast endosomal system (Roberg et al., 1997). The parallels noted between the nitrogen-regulated transport of Gap1p in yeast and the insulin-responsive transport of GLUT4 in mammalian cells (Roberg et al., 1997) led me to investigate the hypothesis that GLUT4 would traffic in the same pathway as Gap1p when expressed in yeast.

In order to address this hypothesis, the effect of the nitrogen source in the growth media on hGLUT4 stabilisation was determined (Figure 3.8). KY73 (*PEP4*) and RMY1 (*pep4-3*) yeast cells harbouring pWTG4 were grown in media containing 100μM $CuSO_4$ and utilizing either, 0.5% ammonium chloride, 0.1% glutamate or 0.1% proline as the sole source of nitrogen. Proteins contained in lysates prepared from 10 OD_{600} equivalents of cells were separated using SDS-PAGE prior to immunoblot analysis, performed with anti-GLUT4 antibody.

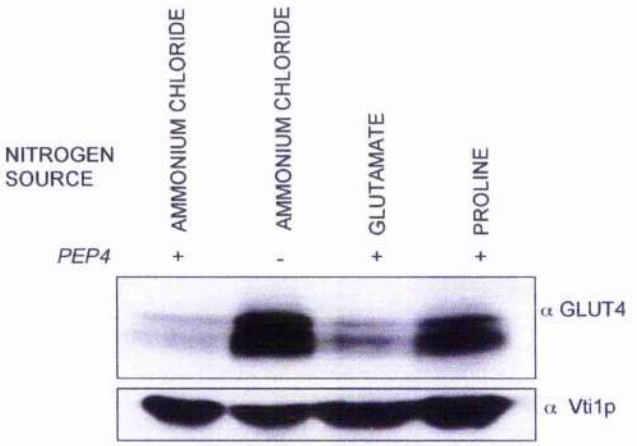

Figure 3.8. hGLUT4 is stabilised by growth on proline-containing media.
KY73 (PEP4) and RMY1 (pep4-3) yeast cells harbouring pWTG4 (hGLUT4 under CUP1 promoter) were grown in media containing 100μM $CuSO_4$ and, either, 0.5% ammonium chloride, 0.1% glutamate or 0.1% proline as the sole nitrogen source, as indicated above. The amount of hGLUT4 in 10 OD_{600} of cells was assessed using immunoblot analysis (the amount of Vti1p in each sample was similarly assessed to control for equal loading).

As in Figure 3.5, hGLUT4 could be detected in *pep4-3* strains (lane2) but not in *PEP4* strains (lane1) grown in media containing ammonium chloride. Interestingly, however, a greater amount of hGLUT4 could be detected in KY73 (*PEP4*) cells when grown in media that contained proline as the sole source of nitrogen, but not when grown in media with glutamate as the nitrogen source. hGLUT4 was, therefore, more stable in yeast grown with limited nutrients, which mirrors that found with Gap1p (Roberg et al., 1997) and led to the hypothesis that hGLUT4 was being directed away from the endosomal system when nutrients were limited and therefore prevented from degradation by active vacuolar proteases. This is reminiscent of the nitrogen-regulated trafficking of Gap1p and provides further indication that, when expressed in yeast, hGLUT4 traffics within the same transport pathway as Gap1p.

3.7. Chapter summary

This chapter describes how I expressed human GLUT4 (hGLUT4) in yeast in order to explore the possibility of using yeast as a model system in the study of insulin-regulated

GLUT4 trafficking. I determined that, when expressed in yeast, hGLUT4 shows significant colocalisation with the TGN marker Kex2p, and accumulates in the Class E compartment of *vps27Δ* mutant cells, consistent with a model in which GLUT4 localises to the TGN of yeast by continually cycling through the endosomal system. Furthermore, I show that hGLUT4 is stabilised when expressed in *pep4Δ* yeast lacking active vacuolar proteases, thus indicating the delivery of hGLUT4 to a proteolytically active compartment. These findings led me to further investigate the parallels between GLUT4 and Gap1p regulated trafficking by examining the trafficking of hGLUT4 when expressed in yeast grown with either a good, or poor, supply of nitrogen. Like Gap1p, hGLUT4 was transported away from a proteolytically active compartment when exposed to poor nutrients, thus supporting the hypothesis that hGLUT4 shares the same transport pathway as Gap1p when expressed in yeast.

Chapter 4: Examination of the ubiquitination of GLUT4

Chapter 4: Examination of the ubiquitination of GLUT4.

4.1. Introduction

The data presented in Chapter 3 demonstrates that, in yeast, hGLUT4 traffics in a nitrogen-regulated manner akin to that of Gap1p. The nitrogen-dependent trafficking of Gap1p is regulated, at least in part, by the ubiquitination of the transporter (Magasanik and Kaiser, 2002). Ubiquitination of Gap1p is required, not only for the endocytosis of Gap1p from the plasma membrane in response to favourable nutrient conditions (Springael and Andre, 1998; Springael et al., 1999) but also for the direct sorting of Gap1p from the TGN to the proteolytically active compartment (Helliwell et al., 2001). Therefore, in view of the similarities between Gap1p and GLUT4 trafficking, I set out to examine whether hGLUT4, like Gap1p, was also ubiquitinated in yeast.

This chapter presents data to show that hGLUT4 is ubiquitinated when expressed in yeast, and also outlines attempts made to determine the specific lysine residue(s) within hGLUT4 that is/are ubiquitinated. However, it is important to note that the purpose of investigating the trafficking of hGLUT4 in yeast was to provide a model system for understanding the insulin-regulated trafficking of GLUT4 in mammalian cells, and therefore, with this in mind, this chapter also presents data to show that GLUT4 is also ubiquitinated in the insulin-sensitive murine cell line 3T3-L1 adipocytes.

4.2. hGLUT4 is ubiquitinated in yeast.

As an initial approach to investigate whether, like Gap1p, GLUT4 is ubiquitinated in yeast, GLUT4 was immunoprecipitated from yeast cells that were also expressing an HA-tagged version of ubiquitin. These experiments were carried out in SF838-9Dα (*pep4-3)* yeast cells to minimize the possibility of degradation of any ubiquitin conjugates by vacuolar proteases, and pRM1 was used to express HA-Ub at high levels, in order to ensure a pool of free ubiquitin and also to provide an epitope tag for the easy detection of the ubiquitin conjugates. SF838-9Dα cells harbouring pWTG4 (pRM2) and also pRM1 (HA-tagged ubiquitin under control of the *CUP1* promoter), or not, were grown in selective media containing 100μM $CuSO_4$ to induce expression from the *CUP1* promoter. Immunoprecipitates formed from yeast cell lysates using rabbit anti-GLUT4 antibody were subject to immunoblot analysis with rat anti-HA antibody in order to detect any HA-Ub

that was conjugated to hGLUT4 and mouse anti-GLUT4 monoclonal antibody to verify that equal amounts of hGLUT4 and hGLUT4-7K/R were immunoprecipitated (Figure 4.1).

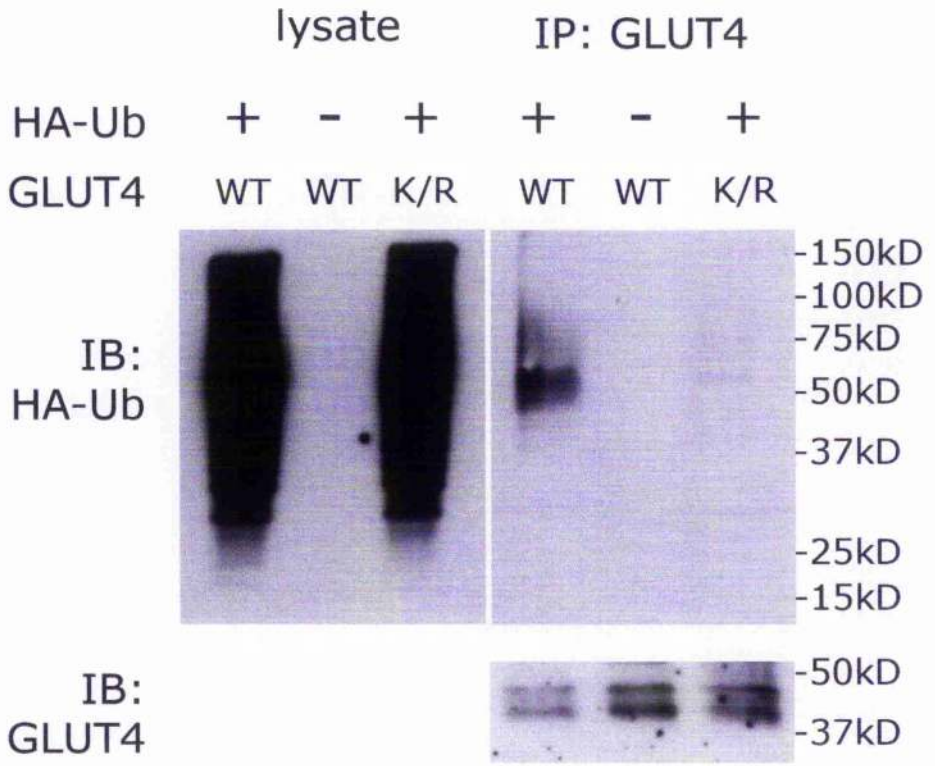

Figure 4.1. hGLUT4 is conjugated to HA-tagged ubiquitin in yeast

SF838-9Dα yeast cells harbouring either pWTG4 or p7KRG4 (as indicated above; WT or K/R, respectively) with HA-Ub or not (as indicated above +/-) were grown in selective media (SD) containing 100μM $CuSO_4$. Immunoprecipitates formed with 10μl anti-GLUT4 antibody were subject to immunoblot analysis with anti-HA antibody (to investigate whether HA-tagged ubiquitin was conjugated to hGLUT4 in yeast) and 1F8 antibody (a GLUT4 monoclonal antibody) to verify whether equal amounts of WT and 7K/R protein were immunoprecipitated.

Ubiquitination is the post-translational conjugation of the small molecule, ubiquitin, most commonly to specific lysine residues on a target protein (Hicke and Dunn, 2003). There are seven lysine residues in the sequence of hGLUT4 that are predicted to be cytosolically disposed (Figure 4.2): each one of these represents a potential site of ubiquitination. The first of these residues (K109) is predicted to be within the first intracellular loop, five of

these residues (K242, K245, K261, K264 and K266) have a predicted location within the large intracellular loop between transmembrane domains 6 and 7, and the final lysine residue (K495) is in the carboxyl-terminal tail (Figure 4.2).

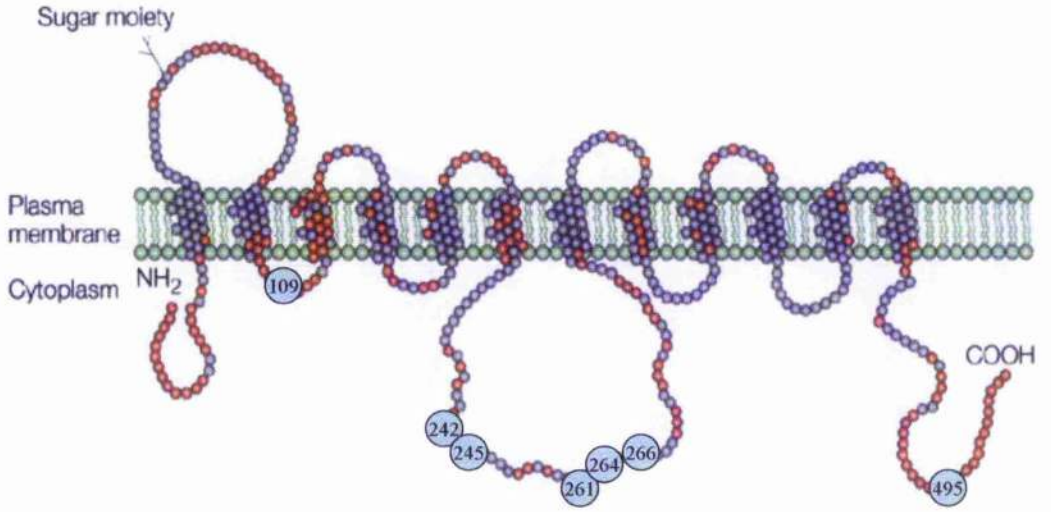

Figure 4.2. Schematic diagram of the predicted membrane topology of GLUT4 indicating the positions of cytoplasmic lysine residues
(adapted from (Bryant et al., 2002))

To characterise the ubiquitination of hGLUT4 observed using HA-tagged ubiquitin, I made a mutant version of hGLUT4 in which the 7 cytosolically-disposed lysines are mutated to arginine residues to serve as a non-ubiquitinated control. Both lysine and arginine residues contain basic side chains, but whereas lysine has a free amino group to which ubiquitin covalently attaches to target proteins, arginine does not: arginine is therefore routinely used to replace lysine in order to abolish ubiquitination without grossly altering the overall higher-order structure of the protein. Codons encoding the seven cytosolically-disposed lysine residues (K109, K242, K245, K261, K264, K266 and K495) of hGLUT4 were mutated in a series of SDM reactions using pRM2 as the original template. The pairs of oligonucleotides used (61 and 62, 73 and 74, 85 and 86, 77 and 78, 117 and 118, 119 and 120, 121 and 122), and the 'intermediate' plasmids created (pRM5, pRM11, pRM12, pRM13, pRM14, pRM15 and pRM3) in the process of making the final plasmid encoding the ubiquitin-deficient mutant (hGLUT4-7K/R) are listed in Tables 2.2 and 2.3,

respectively. The final plasmid pG47KR (pRM3) encodes hGLUT4 with all seven cytoplasmic lysines mutated to arginine residues from the *CUP1* promoter.

When hGLUT4-7K/R was immunoprecipitated from SF838-9Dα cells that were also producing HA-tagged ubiquitin, no ubiquitination was detected (Figure 4.1). Importantly, the bottom panel of this figure shows that hGLUT4-7K/R was precipitated just as efficiently as its wild-type counterpart (which clearly is ubiquitinated) in this experiment.

An immunoreactive band with an apparent molecular weight of ~50kDa was detected in the immunoprecipitate of those cells expressing both wild type hGLUT4 and HA-tagged ubiquitin, demonstrating that HA-Ub was conjugated to hGLUT4 in yeast. This band was absent from the immunoprecipitate of those cells expressing solely wild type hGLUT4 or those cells expressing the ubiquitination-deficient form of hGLUT4 (hGLUT4-7K/R) with HA-Ub, indicating the band was specific to cells carrying pWTG4 and HA-Ub. An immunoreactive band of ~42kDa could be detected in all immunoprecipitates when they were subject to immunoblot analysis with 1F8 antibody (a GLUT4 mouse monoclonal antibody) confirming that equal amounts of wild type hGLUT4 and hGLUT4-7K/R were immunoprecipitated. This increase of ~8kDa in the molecular weight between the 42kDa band detecting hGLUT4 and the 50kDa band detecting HA-Ub conjugated to hGLUT4 is consistent with the conjugation of one ubiquitin moiety to the hGLUT4 molecule, implying that hGLUT4 is monoubiquitinated.

It was necessary to confirm that the ubiquitination of hGLUT4 detected in Figure 4.1 was not due to the overexpression of HA-tagged ubiquitin in yeast. Therefore, an approach was taken to establish whether hGLUT4 expressed in yeast was ubiquitinated by endogenous ubiquitin (Figure 4.3). SF838-9Dα cells harbouring either pWTG4 (pRM2) or p7KRG4 (pRM3) were grown in selective media containing 100μM $CuSO_4$ to induce expression of hGLUT4 and hGLUT4-7K/R, respectively. Immunoprecipitates formed with rabbit anti-GLUT4 antibody were subject to immunoblot analysis with mouse anti-ubiquitin antibody, in order to detect whether endogenous ubiquitin was conjugated to hGLUT4, and mouse anti-GLUT4 monoclonal antibody to verify whether equal amounts of hGLUT4 and hGLUT4-7K/R were immunoprecipitated (Figure 4.3).

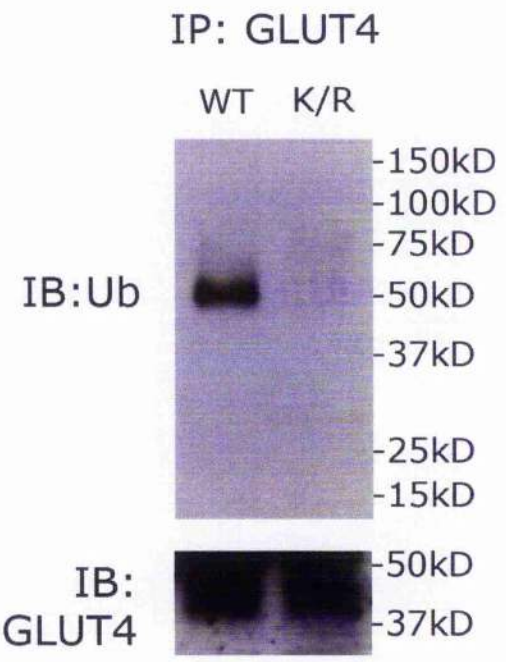

Figure 4.3 hGLUT4 is conjugated to endogenous ubiquitin in yeast

SF838-9Dα yeast cells harbouring either pWTG4 or p7KRG4 (as indicated above; WT or K/R, respectively) were grown in selective media containing 100μM $CuSO_4$. Immunoprecipitates formed with 10μl anti-GLUT4 antibody were immunoblotted with anti-Ub antibody to investigate whether endogenous ubiquitin was conjugated to hGLUT4 in yeast and 1F8 antibody (a GLUT4 monoclonal antibody) to verify whether equal amounts of wild type hGLUT4 (WT) and hGLUT4-7K/R (K/R) protein were immunoprecipitated.

In agreement with Figure 4.1, an immunoreactive band with an apparent molecular weight of ~50kDa was detected in the immunoprecipitate of those cells expressing wild-type hGLUT4 but not in those cells expressing the ubiquitination-deficient mutant hGLUT4-7K/R, with the levels of immunoprecipitated wild type hGLUT4 and hGLUT4-7K/R being approximately equal. Again, this is consistent with the addition of a single ubiquitin molecule to hGLUT4 and shows that hGLUT4 is bound to endogenous ubiquitin in yeast.

The above immunoprecipitation experiments establish that hGLUT4 is ubiquitinated in yeast, but this was always to be a model system for the study of the insulin-regulated

trafficking of GLUT4 and the end goal always to determine whether GLUT4 was ubiquitinated in mammalian cells. However, immunoprecipitation of 3T3-L1 adipocyte lysate with anti-GLUT4 antibody and subsequent immunoblot analysis with anti-ubiquitin antibody failed to yield any presentable data, and I therefore sought an alternative approach to investigate the possibility that GLUT4 is ubiquitinated in adipocytes. To this end, I utilised a GST fusion protein harbouring a ubiquitin-binding domain from the yeast protein Dsk2p.

Dsk2p is a member of a family of proteins that possess an N-terminal ubiquitin-like (Ubl) domain and a C-terminal ubiquitin-associated (UBA) domain (Jentsch and Pyrowolakis, 2000). This family of proteins plays an important role in protein degradation by the ubiquitin-proteasome pathway possibly as an adaptor between ubiquitinated proteins destined for proteasomal degradation and the proteasome complex (Funakoshi et al., 2002). The C-terminal UBA domain of Dsk2p binds to Lys^{48}-linked polyubiquitin chains while the N-terminal Ubl domain interacts with the proteasome (Funakoshi et al., 2002). It has been established that the C-terminal UBA domain alone (residues 328-373 of Dsk2p) binds, not only polyubiquitin but also monoubiquitin when produced as a GST-fusion protein (Funakoshi et al., 2002). I therefore sought to use this GST-fusion protein in 'pull-down' experiments to determine whether GLUT4 is ubiquitinated in adipocytes.

It was important to include a negative control for these experiments and I therefore set out to obtain a version of this protein whose ability to bind ubiquitin is impaired. The structure of the UBA domain of Dsk2p in complex with ubiquitin has been solved and identifies residues within the UBA domain as being important for the binding of ubiquitin (Ohno et al., 2005): Met^{342} mediates two contacts between the UBA domain and ubiquitin; it forms a hydrophobic contact with the Ile^{44}-centred pocket of ubiquitin and a hydrogen bond to Gly^{47} of ubiquitin. Phe^{344} makes hydrophobic contacts with Gly^{47} of ubiquitin (Ohno et al., 2005). These two residues were mutated by SDM to Arg^{342} and Ala^{344} in order to abolish ubiquitin binding of the Dsk2p-UBA domain (this was performed by Chris Lamb, a placement student in the lab).

This mutant was designed to act as a non-ubiquitin-binding control in the GST pull-down assays investigating GLUT4 ubiquitination. However, before using this new approach

with 3T3-L1 adipocytes, I set out to validate its effectiveness in specifically detecting ubiquitinated GLUT4 with the yeast system.

The recombinant fusion proteins, GST-UBA (GST fused to the UBA domain of Dsk2p; residues 328-373 (Funakoshi et al., 2002)) and GST-UBAmut (GST fused to the UBA domain of Dsk2p harbouring the two point mutations M342R and F344A) were expressed in BL-21(DE3) cells (Invitrogen) and purified using glutathione-Sepharose beads. The concentration of fusion proteins immobilised on the beads was estimated using SDS-PAGE and staining with Coomassie Blue, and comparison with a series of protein standards (2μg, 4μg and 10μg BSA) included on the same gel (Figure 4.4). Figure 4.4 shows bands of equal intensity for both GST-UBA and GST-UBAmut, with an apparent molecular weight of ~30kDa, around 5-6kDa larger than GST alone, consistent with the addition of the UBA and UBAmut domains.

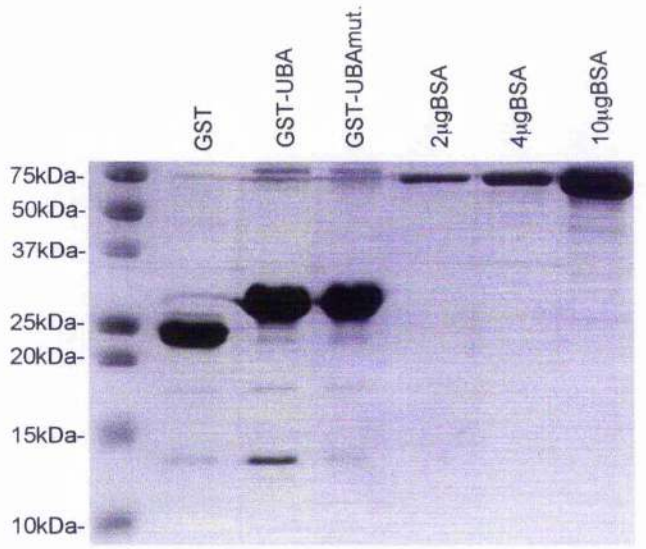

Figure 4.4. SDS-PAGE protein assay for immobilised GST fusion proteins

GST-fusion proteins, GST-UBA and GST-UBAmut were expressed in bacteria and purified with glutathione-Sepharose beads. Proteins eluted from the beads were separated by SDS-PAGE and the gel stained with Coomassie Blue. In order to estimate the quantity of protein bound to the beads, a series of protein standards; 2μg, 4μg and 10μg BSA were also loaded.

In order to validate the use of the GST fusion proteins in the detection of GLUT4 ubiquitination, lysates prepared from SF838-9Dα cells producing either hGLUT4 (from pRM30) or hGLUT4-7K/R (from pRM31), in addition to a GFP-tagged version of Gap1p (from p2313; to serve as a control) were incubated with either GST-UBA and GST-UBAmut immobilised on glutathione-Sepharose beads. Following the washes described in Section 2.2.19, proteins bound to the GST-fusion proteins were eluted and subject to SDS-PAGE and immunoblot analysis with anti-GFP antibody and anti-GLUT4 antibody (Figure 4.5). 0.25% of the input lysate was also subject to SDS-PAGE and immunoblot analysis with anti-GFP and anti-GLUT4 antibodies in order to check that equivalent amounts of Gap1pGFP, wild-type hGLUT4 or hGLUT4-7K/R proteins were added to the two different GST fusions.

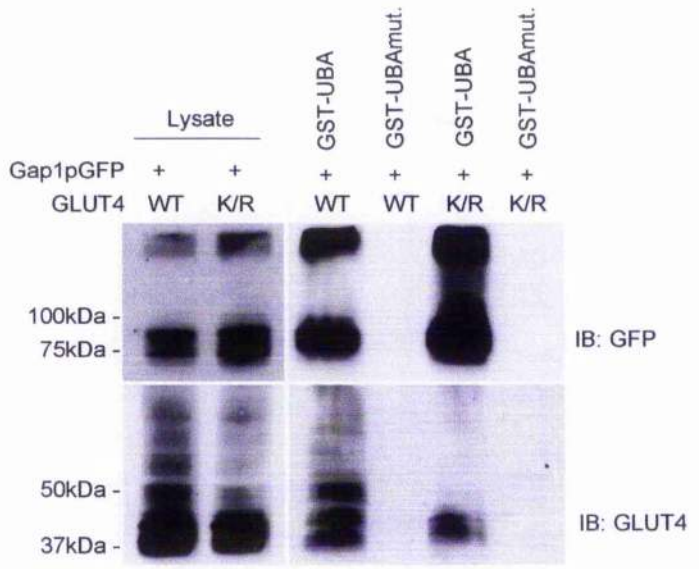

Figure 4.5. hGLUT4 interacts with GST-UBA in a GST pull down assay

Lysate prepared from SF838-9Dα yeast cells harbouring either pWTG4LEU2 (pRM30) or p7KRG4LEU2 (pRM31) (as indicated above; WT or K/R, respectively) and p2313 (GFP-tagged Gap1p) were incubated with glutathione-Sepharose beads that carried either of the GST-fusion proteins, GST-UBA and GST-UBAmut. Proteins eluted from the beads were subject to immunoblotting with anti-GFP antibody (top panel) and anti-GLUT4 antibody (bottom panel). 0.25% input (left panel; top and bottom) was also loaded as a control to verify whether equal amounts of proteins were expressed.

GFP-tagged Gap1p provided a control in this experiment as a protein known to be ubiquitinated in yeast (Hein and Andre, 1997; Helliwell et al., 2001; Springael and Andre, 1998; Springael et al., 1999). Immunoblot analysis with anti-GFP antibody detected an immunoreactive band of an apparent molecular weight of ~80kDa in the GST-UBA pull-down assays but not in the pull-down performed using the GST-UBAmut (Figure 4.5), indicating that, as predicted, the point mutations introduced here have indeed abolished the ability of the UBA domain to bind ubiquitin.

Immunoblot analysis with anti-GLUT4 antibody detects a band with an apparent molecular weight of ~50kDa in the GST-UBA pull down assay from a yeast cell lysate containing wild type hGLUT4, but not from a lysates prepared from cells expressing the ubiquitination-deficient hGLUT4-7K/R (Figure 4.5). The GLUT4 immunoreactive band is also absent from the pull down performed using the GST-UBAmut fusion with lysate prepared from cells expressing wild-type hGLUT4. The levels of wild type hGLUT4 and hGLUT4-7K/R added to the pull-down assays were comparable, as visualised by immunoblot analysis of the input lysate, which indicates immunoreactive bands of similar intensities with apparent molecular weights of ~42kDa in each case. GST-UBA binds ubiquitin, and therefore, ubiquitinated proteins are isolated in the GST pull-down assays. The detection of an immunoreactive band at ~50kDa in cells expressing wild-type hGLUT4, but not in cells with the ubiquitination-deficient hGLUT4-7K/R, thus indicates that hGLUT4 is ubiquitinated in yeast, probably by the addition of one ubiquitin moiety. This supports the data obtained with the immunoprecipitation experiments, and establishes this technique as a suitable method to investigate GLUT4 ubiquitination.

4.3. GLUT4 is ubiquitinated in adipocytes

The ubiquitination of GLUT4 in adipocytes was determined by incubating lysate prepared from 3T3-L1 adipocytes with glutathione-Sepharose beads carrying the GST fusion proteins, GST-UBA (ubiquitin-binding) and GST-UBAmut (non-ubiquitin binding). Proteins pulled-down by GST-UBA and GST-UBAmut were analysed by immunoblot analysis with anti-GLUT4 antibody (to detect any GLUT4 bound to the GST fusion proteins), anti-Syntaxin4 antibody (as a non-ubiquitinated protein control) and anti-IRS-1 antibody (as a ubiquitinated protein control) (Figure 4.6). 2.5% of the input lysate was also subject to SDS-PAGE and immunoblot analysis with the various antibodies to verify to

presence of the different proteins in the lysate. The coomassie staining of the purified GST-fusion proteins used is also shown in Figure 4.6 to confirm that equivalent amounts of the two fusion proteins were used in the pull-downs experiments.

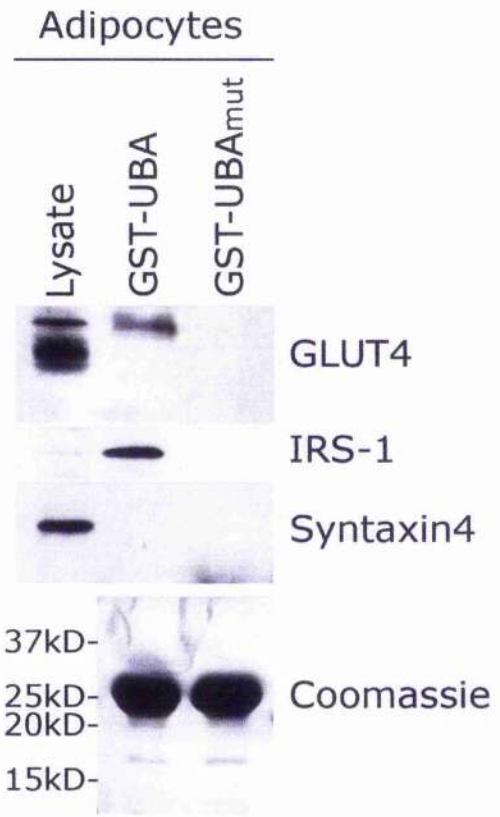

Figure 4.6. GLUT4 is ubiquitinated in 3T3-L1 adipocytes

Lysate prepared from 3T3-L1 adipocytes was incubated with glutathione-Sepharose beads that carried the GST-fusion proteins, GST-UBA and GST-UBAmut. Proteins eluted from the beads were subject to immunoblotting with anti-GLUT4, anti-IRS-1 and anti-Syntaxin4 antibodies. 2.5% input (lane 1) was also loaded as a control.

Immunoblot analysis with anti-GLUT4 antibody in Figure 4.6 shows an immunoreactive band only in proteins eluted from the beads carrying GST-UBA, not from those beads carrying an equivalent amount of the GST-UBAmut control. This immunoreactive band has a slightly larger molecular weight than the GLUT4 immunoreactive band detected in the input lysate, which is expected with ubiquitinated GLUT4. The binding of GLUT4 from adipocytes to the ubiquitin-binding UBA domain, but not to the non-ubiquitin

binding UBAmut domain, demonstrates that endogenous GLUT4 is ubiquitinated in adipocytes.

The protein levels of the insulin receptor substrate 1 (IRS-1) are regulated by its ubiquitination (Zhande et al., 2002) and subsequent proteasomal degradation (Sun et al., 1999). Therefore, the presence of IRS-1 in the pull-down assays was determined (as a protein known to be ubiquitinated in these cells) by immunoblot analysis with anti-IRS-1 antibody. Figure 4.6 demonstrates that IRS-1 is pulled out of the adipocytes lysates by GST-UBA, but not by the GST-UBAmut, confirming the specificity of binding of GST-UBA to ubiquitinated proteins. Syntaxin 4 is a target (t)-SNARE located at the plasma membrane of adipocytes (Tellam et al., 1997; Volchuk et al., 1996). As it is unlikely to be a target for ubiquitination it was used as a negative control for the GST pull-down assays. Input lysate subject to immunoblot analysis with anti-Syntaxin4 antibody detected an immunoreactive band of the predicted molecular weight of Syntaxin4, which was absent from the GST pull-downs: providing yet further evidence that the GST pull-down assays were specific for ubiquitinated protein.

Having confirmed that endogenous GLUT4 in adipocytes is ubiquitinated, I wanted to assess whether this ubiquitination was abolished by mutation of the 7 lysines of GLUT4 that are predicted to be cytosolically disposed (Figure 4.2). I therefore created a retroviral expression vector to drive the expression of the hGLUT4-7K/R mutant in 3T3-L1 adipocytes (the construction of this vector, production of retrovirus and the expression of wild-type HA-tagged GLUT4 and HA-tagged GLUT4-7K/R in infected adipocytes is outlined in the following chapter).

Lysates from 3T3-L1 adipocytes expressing either wild-type HA-tagged GLUT4 or HA-tagged GLUT4-7K/R were incubated with glutathione-Sepharose beads loaded with either GST-UBA and GST-UBAmut as described in materials and methods. Proteins eluted from the beads were subject to immunoblotting with anti-HA antibody to detect any HA-tagged GLUT4 bound to the GST fusion proteins (Figure 4.7). 2.5% of the input lysate was also subject to SDS-PAGE and immunoblot analysis with anti-HA antibody to verify equal levels of expression of wild type GLUT4 and GLUT4-7K/R (Figure 4.7).

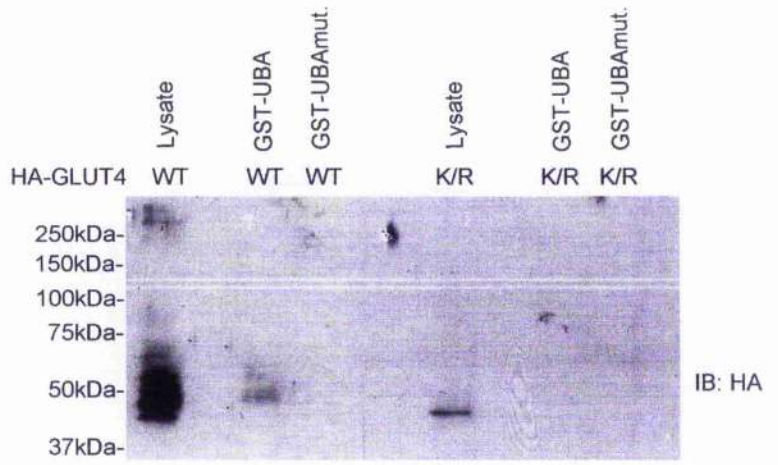

Figure 4.7. GST pull down with adipocytes expressing HA-GLUT4 or HA-GLUT4-7K/R
Lysate prepared from 3T3-L1 adipocytes expressing either HA-GLUT4 or HA-GLUT4-7K/R (as indicated above; WT and K/R respectively) was incubated with glutathione-Sepharose beads that carried the GST-fusion proteins, GST-UBA and GST-UBAmut. Proteins eluted from the beads were subject to immunoblotting with anti-HA antibody. 2.5% input lysate was also loaded as a control.

Immunoblot analysis with anti-HA antibody detected immunoreactive bands with apparent molecular weights of ~48kDa in the input lysate of adipocytes expressing either wild type or the ubiquitination-deficient form of HA-GLUT4. However, the immunoreactive band was a lot less pronounced in the case of HA-GLUT4-7K/R, likely due to poorer expression from the HA-GLUT4-7K/R retrovirus. An immunoreactive band can also be detected in the GST-UBA pull down from the lysates prepared from adipocytes expressing wild-type HA-GLUT4, indicating ubiquitinated HA-GLUT4 (as demonstrated in Figure 4.6). This band is absent from the GST-UBAmut control pull-down. No such band was detected in the GST-UBA pull-down from adipocytes lysates containing HA-GLUT4-7K/R. However, due to the low levels of expression of this mutant in this experiment it cannot be determined whether this control does, in fact, abolish ubiquitination. Unfortunately, due to time constraints, I was unable to fully optimise this experiment in order to acquire equal levels of wild-type HA-GLUT4 and HA-GLUT4-7K/R.

4.4. Mapping the ubiquitination sites of hGLUT4

Having determined that GLUT4 is modified by the addition of, at least one ubiquitin moiety, I set out to map the ubiquitination site(s) in the transporter. Having demonstrated that mutation of all 7 of the lysine residues within hGLUT4 that are predicted to be localised in the cytosol (Figure 4.2) abolishes the ubiquitination of GLUT4 (Figures 4.1 and 4.3), my first approach to mapping the site of ubiquitination was to create a series of lysine 'knock-out' mutants of GLUT4: with the 7 lysine residues mutated individually to arginines. The pairs of oligonucleotides; 61 and 62, 85 and 86, 87 and 88, 89 and 90, 91 and 92, 93 and 94, 73 and 74 (listed in Table 2.2) were used in a set of seven separate SDM reactions to individually mutate the lysine residues of hGLUT4, encoded by pWTG4 (pRM2), to arginines. This created the series of GLUT4 'knock-out' mutants under control of the *CUP1* promoter; pRM5 (K495R), pRM6 (K242R), pRM7 (K245R), pRM8 (K261R), pRM9 (K264R), pRM10 (K266R), pRM16 (K109R) (listed in Table 2.3). These mutants were used, along with pWTG4 (pRM2) and p7KRG4 (pRM3), to investigate which of the lysine residues in hGLUT4 was ubiquitinated. This was achieved by expressing the various forms of hGLUT4 in SF838-9Dα yeast, using anti-GLUT4 antibodies to immunoprecipitate the transporter, and then probe each of the precipitated versions of GLUT4 with anti-ubiquitin antibodies (in a manner similar to that presented in Figure 4.3). The rationale behind this experiment was that mutation of the ubiquitination acceptor site would abolish the ubiquitination of hGLUT4 (as seen for the hGLUT4-7K/R mutant in Figures 4.1 and 4.3).

SF838-9Dα cells harbouring either pWTG4 (pRM2), p7KRG4 (pRM3) or one of the 7 lysine 'knock-out' mutants, K109R (pRM16), K242R (pRM6), K245R (pRM7), K261R (pRM8), K264R (pRM9), K266R (pRM10) and K495R (pRM5) were grown in selective media (SD) containing 100μM $CuSO_4$ to induce expression of hGLUT4, hGLUT4-7K/R and the 7 mutants. Immunoprecipitates formed with rabbit anti-GLUT4 antibody were subject to immunoblot analysis with mouse anti-ubiquitin antibody, in order to detect whether endogenous ubiquitin, normally conjugated to hGLUT4, was prevented from ubiquitinating any of the 7 'knock-out' mutants. Immunoblot analysis with mouse anti-GLUT4 monoclonal antibody was used to ascertain whether equivalent amounts of hGLUT4, hGLUT4-7K/R and the seven 'knock-out' mutants were immunoprecipitated (Figure 4.8).

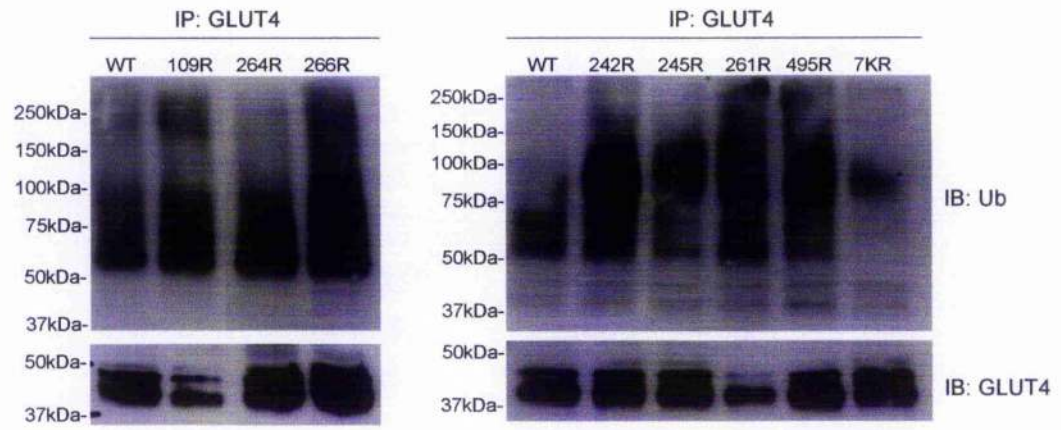

Figure 4.8. Investigation into the ubiquitination of GLUT4 lysine 'knock-out' mutants. *SF838-9Dα yeast cells harbouring any one of pWTG4, p7KRG4 or one of the 7 lysine 'knock-out' mutants (described in the text above) were grown in selective media containing 100μM $CuSO_4$. Immunoprecipitates formed with 10μl anti-GLUT4 antibody were immunoblotted with anti-Ub antibody and 1F8 (a GLUT4 monoclonal antibody).*

The data presented in Figure 4.8 are consistent with those presented in Figures 4.1 and 4.3, in that the anti-ubiquitin antibody detects a band with an apparent molecular weight of ~50kDa in the immunoprecipitate from cells expressing wild-type hGLUT4 but not in that obtained from cells expressing the hGLUT4-7K/R mutant. However, all of the seven 'knock-out' mutants showed a similar 50kDa immunoreactive band, indicating ubiquitin conjugation; none showed the removal of ubiquitin binding to hGLUT4 as seen with the ubiquitination-deficient mutant, as would have been expected had any of the 'knock-out' mutants abolished ubiquitination of hGLUT4.

Although the data presented thus far are consistent with hGLUT4 being monoubiquitinated (modified by a single ubiquitin molecule on one of its lysine residues), it is possible that the protein is multi-monoubiquitinated (modified by a single ubiquitin molecule on more than one lysine residue), as oppose to polyubiquitination, which refers to chains of ubiquitin molecules (Arnason and Ellison, 1994; Hicke and Dunn, 2003). This would explain the data presented in Figure 4.8, in that even if one of the ubiquitination sites had been knocked out, another one (at least) would still be ubiquitinated. I therefore undertook to make a series of 'knock-in' mutants where each of the 7 putative ubiquitination sites

were 'put back into' the ubiquitination-deficient (hGLUT4-7K/R) mutant, thus generating 7 individual mutants with only one lysine residue available for ubiquitination. The pairs of oligonucleotides; 233 and 234, 237 and 238, 231 and 232, 235 and 236, 239 and 240, 241 and 242, 243 and 244 (listed in Table 2.2) were used in a set of 7 separate SDM reactions to individually mutate the arginine residues at positions 109, 242, 245, 261, 264, 266 and 495 of hGLUT4-7K/R (in pRM3) back to lysine residues, thus making a series of 'knock-in' mutants under control of the *CUP1* promoter; pRM17 (7KRK242), pRM18 (7KRK261), pRM19 (7KRK109), pRM20 (7KRK245), pRM21 (7KRK264), pRM22 (7KRK266), pRM23 (7KRK495) (listed in Table 2.3). As described for the 'knock-out' mutants, these 'knock-in' mutants were used, along with pWTG4 (pRM2) and p7KRG4 (pRM3), to examine which of the lysine residues was subject to ubiquitination.

SF838-9Dα cells harbouring either pWTG4 (pRM2), p7KRG4 (pRM3) or one of the 7 lysine 'knock-in' mutants, were grown in selective media containing 100μM $CuSO_4$ to induce expression of hGLUT4, hGLUT4-7K/R and the 7 mutants. Immunoprecipitates formed with rabbit anti-GLUT4 antibody were subject to immunoblot analysis with mouse anti-ubiquitin antibody, in order to detect whether endogenous ubiquitin was conjugated to any of the individual lysine residues within the hGLUT4 'knock-in' mutants. Immunoblot analysis with mouse anti-GLUT4 monoclonal antibody was used to ascertain whether equivalent amounts of hGLUT4, hGLUT4-7K/R and the seven 'knock-in' mutants were immunoprecipitated (Figure 4.9).

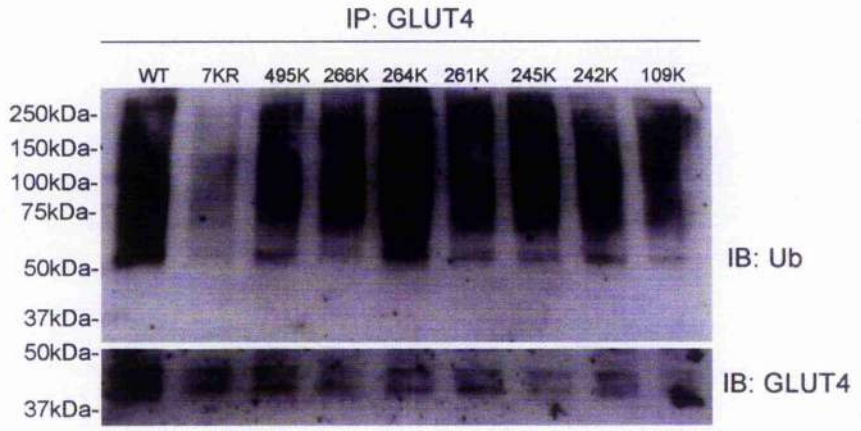

Figure 4.9. Investigation into the ubiquitination of GLUT4 lysine 'knock-in' mutants. *SF838-9Dα yeast cells harbouring any one of pWTG4, p7KRG4 or one of the 7 lysine 'knock-in' mutants (as described in the text above) were grown in selective media containing 100μM $CuSO_4$. Immunoprecipitates formed with 10μl anti-GLUT4 antibody were immunoblotted with anti-Ub antibody, to investigate whether ubiquitin conjugation was retained in any of the 'knock-in' mutants, and 1F8 antibody (a GLUT4 monoclonal antibody).*

The data presented above in Figure 4.9 is consistent with that seen in Figures 4.1, 4.3 and 4.8, in that an immunoreactive band with apparent molecular weight of ~50kDa is detected by the anti-ubiquitin antibody in the immunoprecipitate from cells producing wild-type hGLUT4 but not from those cells producing the ubiquitin-deficient mutant hGLUT4-7K/R. Disappointingly however, all of the 7 'knock-in' mutants still showed the presence of similar 50kDa immunoreactive band, with the exception of, perhaps, hGLUT4-7K/RK266. However, this experiment was repeated on a number of occasions, without any consistency in the results.

This knock-in/knock-out approach to mapping the site of hGLUT4 ubiquitination was unsuccessful. This has also been the case in other studies attempting to map ubiquitination sites. Lysine to arginine mutants of the three ubiquitination substrates; c-Jun (Treier et al., 1994), the T-cell receptor ζ subunit (Hou et al., 1994) and the encephalomyocarditis (EMC) virus 3C protease (Lawson et al., 1999), showed every single mutant to retain nearly wild-type susceptibility to ubiquitination. Therefore, it would seem that E3 ligases

can be rather nonselective with respect to which lysine in the target protein is ubiquitinated. If a particular lysine residue is unavailable for modification by ubiquitination, it is probable the E3 ligase moves along the protein until it finds a lysine that can be ubiquitinated. This would explain why all of the GLUT4 'knock-in' and 'knock-out' mutants created appeared to be ubiquitinated.

4.5. Chapter summary

In view of the finding that, when expressed in yeast, hGLUT4 traffics in a nitrogen-regulated manner analogous to the regulated trafficking of Gap1p, the aim of this chapter was to address whether, also like Gap1p, GLUT4 was subject to ubiquitination. By way of a series of immunoprecipitation experiments and pull-down assays, I show that hGLUT4 is indeed ubiquitinated in yeast, and importantly, also in the insulin-sensitive, murine cell line 3T3-L1 adipocytes, most likely by monoubiquitination. This chapter also outlines efforts made towards identifying the specific lysine residue(s) of GLUT4 that is/are subject to ubiquitination.

Chapter 5: Analysis of the role of ubiquitination in GLUT4 trafficking

Chapter 5: Analysis of the role of ubiquitination in GLUT4 trafficking.

5.1. Introduction

The finding that GLUT4 is subject to ubiquitination adds to the similarities between the regulated trafficking of GLUT4 in insulin-sensitive cells and the general amino acid permease, Gap1p in yeast. Given that hGLUT4, when expressed in yeast, follows the same nitrogen-regulated trafficking pathway as Gap1p, and the sorting of Gap1p to the proteolytically active compartment in nutrient-rich conditions is regulated by its ubiquitination (Hein and Andre, 1997; Helliwell et al., 2001; Springael and Andre, 1998; Springael et al., 1999), I set out to test the hypothesis that ubiquitination plays a role in the nitrogen-regulated trafficking of GLUT4 in yeast.

By using yeast that produce either a ubiquitination-deficient mutant of hGLUT4 (hGLUT4-7K/R), or a constitutively-ubiquitinated hGLUT4 fusion protein (hGLUT4-7K/R-HAUb), I set out to address whether, like Gap1p, the ubiquitination of hGLUT4 in yeast serves as a signal to direct the transporter to the proteolytically active compartment for degradation. This chapter presents data to support the above hypothesis, and also presents experiments directed towards defining a role for ubiquitination in the regulated trafficking of GLUT4 in the insulin-sensitive murine cell line, 3T3-L1 adipocytes. Through a series of experiments studying the trafficking of either wild type HA-GLUT4, the ubiquitin-deficient mutant HA-GLUT4-7K/R or the constitutively-ubiquitinated hGLUT4-7K/R-HAUb in adipocytes, I propose a model in which the ubiquitination of GLUT4 is required for its exit from the TGN into the GLUT4 storage vesicles (GSVs) from where it can be mobilised to the plasma membrane in response to insulin.

5.2. Ubiquitination of hGLUT4 in yeast targets it for degradation by active vacuolar proteases

In order to build on the findings presented in Chapters 3 and 4: namely that when expressed in yeast, hGLUT4 traffics in a nitrogen-regulated manner analogous to Gap1p; and, again like Gap1p, GLUT4 is ubiquitinated, I set out to determine whether the ubiquitination of GLUT4 is determined for its nitrogen-regulated trafficking in yeast. To this end, I asked whether the ubiquitination-deficient mutant hGLUT4-7K/R (Figures 4.1,

4.3 and 4.5) is subject to the same nitrogen-regulated trafficking as its wild-type counterpart in yeast.

KY73 cells (*PEP4*; wild-type, i.e. containing active vacuolar proteases) expressing either wild-type hGLUT4 or the ubiquitination-deficient hGLUT4-7K/R were grown in media containing either 0.5% ammonium chloride or 0.1% proline as the sole source of nitrogen (Figure 5.1). Proteins contained in lysates prepared from 10 OD_{600} equivalents of cells were separated using SDS-PAGE prior to immunoblot analysis, performed with anti-GLUT4 antibody (and also anti-Vti1p as a loading control).

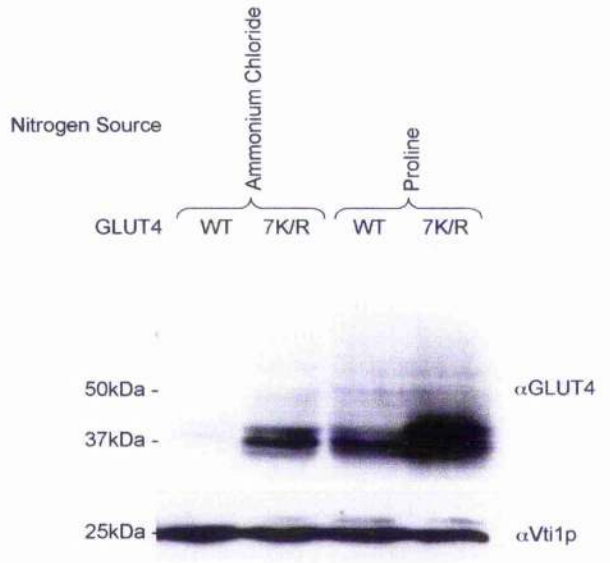

Figure 5.1. hGLUT4–7K/R is stabilised in PEP4 cells.

KY73(PEP4) yeast cells harbouring either pWTG4 (pRM2; hGLUT4 under control of the CUP1 promoter) or pG47KR (pRM3; hGLUT4-7K/R under control of the CUP1 promoter) were grown in media containing 100μM $CuSO_4$ and, either, 0.5% ammonium chloride or 0.1% proline as the sole nitrogen source, as indicated above. The amount of hGLUT4 or hGLUT4-7K/R in 10 OD_{600} equivalents of cells was assessed using immunoblot analysis with anti-GLUT4 antibody (the amount of Vti1p in each sample was similarly assessed to control for equal loading).

Consistent with the data presented in Figure 3.8, wild type hGLUT4 can be detected in KY73(*PEP4*) cells grown in media providing proline as the sole source of nitrogen (a poor nitrogen source), but not when grown in media containing ammonium chloride (a rich

nitrogen source) (Figure 5.1). This indicates that wild-type hGLUT4 is more stable in yeast grown with limited nutrients, such as proline, likely due to the fact that it is being directed away from the proteolytically active endosomal system (as seen for Gap1p).

In contrast to its wild-type counterpart, the ubiquitination-deficient hGLUT4-7K/R mutant was easily detectable in cells containing active vacuolar proteases and grown on ammonium chloride (Figure 5.1). This indicates that hGLUT4-7K/R is being prevented from degradation, likely due to it being directed away from the endosomal system, thus avoiding vacuolar proteases, even under conditions where the wild type hGLUT4 is being transported to a proteolytically active compartment. As hGLUT4-7K/R lacks modification by ubiquitin, this adds further weight to the hypothesis that the ubiquitination of hGLUT4 subsequently causes its transport to the proteolytically active endosomal system.

To further investigate the role that ubiquitin modification plays in hGLUT4 trafficking, I created a translational fusion of hGLUT4-7K/R with an HA-tagged ubiquitin moiety. This fusion protein was produced by using site directed mutagenesis to replace the 'stop' codon of the hGLUT4-7K/R ORF in pRM3 with an *Sph*I site. Following digestion with *Sph*I to linearise the resulting plasmid, sequence encoding HA-tagged ubiquitin (which had been amplified using PCR to carry homologous to the hGLUT4-7K/R ORF and the *PHO8* 3'*UTR*) was introduced to the carboxy-terminal end of hGLUT4-7K/R by homologous recombination (see Section 2.2.2 for details). The resulting plasmid, pG47KRHAUb (pRM24) encodes constitutively-ubiquitinated fusion protein hGLUT4-7K/R-HAUb from the copper-inducible *CUP1* promoter. The construction of this plasmid was verified by DNA sequencing.

KY73(*PEP4)* and RMY1(*pep4-3)* cells expressing the constitutively-ubiquitinated hGLUT4-7K/R-HAUb fusion protein were grown in media containing 0.5% ammonium chloride or 0.1% proline as the sole source of nitrogen (Figure 5.2). Proteins contained in lysates prepared from 10 OD_{600} equivalents of cells were separated using SDS-PAGE prior to immunoblot analysis, performed with anti-HA antibody to detect the hGLUT4-7K/R-HAUb fusion protein and anti-Vti1p as a loading control.

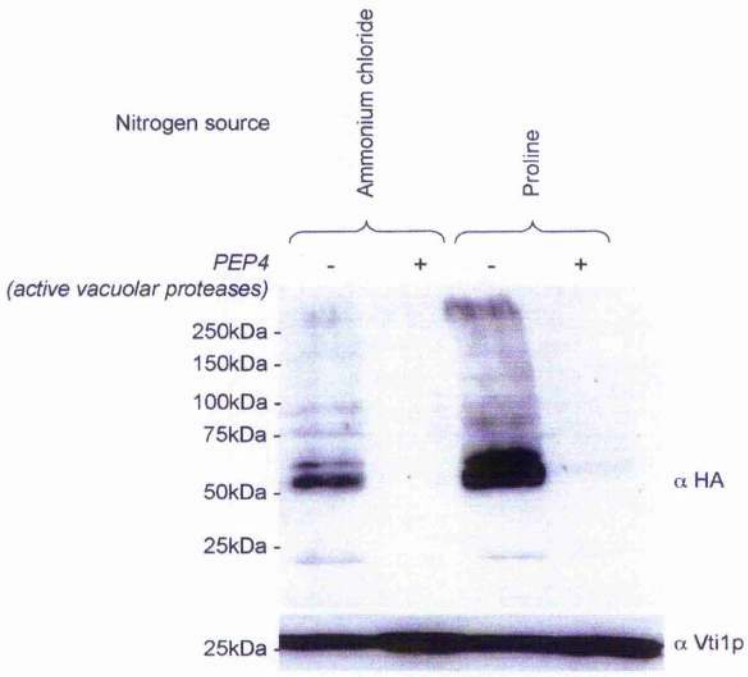

Figure 5.2. hGLUT4–7K/R-HAUb is degraded by vacuolar proteases regardless of the nitrogen source.

KY73(PEP4; containing active vacuolar proteases) and RMY1(pep4-3; without active vacuolar proteases) yeast cells harbouring pRM24 (hGLUT4-7K/R-HAUb fusion protein under control of the CUP1 promoter) were grown in media containing 100μM $CuSO_4$ and either 0.5% ammonium chloride or 0.1% proline as the sole nitrogen source, as indicated. The amount of hGLUT4-7K/R-HAUb fusion protein in 10 OD_{600} equivalents of cells was assessed by immunoblot analysis with anti-HA antibody (the amount of Vti1p in each sample was similarly assessed to control for equal loading).

Immunoblot analysis with anti-HA antibody detects an immunoreactive band with an apparent molecular weight of ~50kDa in the lysate produced from cells that lack active vacuolar proteases (Figure 5.2). This is consistent with the predicted molecular weight of the hGLUT4-7K/R-HAUb fusion protein, as it accounts for the addition of one 8kDa ubiquitin moiety to the ~42kDa hGLUT4-7K/R protein. Importantly, no such band was detected in the lysate prepared from cells, expressing the fusion protein, that contain active vacuolar proteases. These data are consistent with a model in which the hGLUT4-7K/R-HAUb fusion protein is delivered to the proteolytically active endosomal system where it

is degraded by active vacuolar proteases (as only in cells that lack vacuolar proteases is the fusion protein stabilised).

As shown in Figures 3.8 and 5.1, wild-type hGLUT4 is degraded in cells grown in ammonium chloride but not in cells grown in proline. I have interpreted this as reflecting the diversion of hGLUT4 away from the proteolytically active endosomal system under nitrogen-limiting conditions, as observed for Gap1p (Roberg et al., 1997). In contrast, the ubiquitination-deficient mutant hGLUT4-7K/R is stabilised, not only in cells grown using the poor nitrogen source proline, but also in the presence of the rich nitrogen source ammonium chloride (Figure 5.1); indicating that ubiquitination of GLUT4 is required for its nitrogen-regulated sorting to the endosomal system. The constitutively-ubiquitinated hGLUT4-7K/R-HAUb fusion protein is degraded regardless of the nitrogen source, and is only stablilised upon inactivation of vacuolar proteases (Figure 5.2). Thus it appears that the in-frame ubiquitin fusion protein is trafficked to the proteolytically active endosomal system regardless of nitrogen source. These data indicate that the addition of a ubiquitin moiety to hGLUT4 is sufficient to direct the transporter to the endosomal system in yeast.

5.3. Expression of recombinant GLUT4 proteins in 3T3-L1 adipocytes

Having characterised the trafficking of both the ubiquitin-deficient mutant hGLUT4-7K/R and the constitutively ubiquitinated hGLUT4-7K/R-HAUb fusion protein in the yeast model system, I moved on to use these proteins to investigate the role of ubiquitination in the trafficking of GLUT4 in insulin-sensitive cells. For this purpose, I set out to create two retroviral expression vectors that would drive the expression of the hGLUT4-7K/R mutant and the hGLUT4-7K/R-HAUb fusion protein in the insulin-sensitive murine cell line 3T3-L1 adipocytes.

For these experiments, it was necessary for the retrovirally expressed GLUT4 molecules to carry an HA-epitope tag in order to distinguish them from endogenous GLUT4 expressed by 3T3-L1 adipocytes. I obtained a retroviral expression construct that drives the expression of wild-type GLUT4 harbouring an HA tag in the first exofacial loop of GLUT4, from Professor David James. This molecule is subject to insulin-regulated trafficking in 3T3-L1 adipocytes in a manner indistinguishable from the endogenous protein (Shewan et al., 2003). To create an HA-tagged version of the hGLUT4-7K/R mutant I used an approach that involved 'splicing' two gene fragments together by the

gene splicing by overlap extension (SOEing) PCR technique (Horton et al., 1990). This technique is a method of recombining DNA sequences without depending on restriction sites or the use of restriction endonucleases or ligase, allowing the precise design of junctions between DNA sequences. In brief, gene SOEing relies on the gene fragments to be recombined sharing a complimentary sequence at one end, allowing the DNA strands from the two different fragments to form an overlap. The extension of this overlap by DNA polymerase yields a recombinant molecule in which the original DNA fragments are 'spliced' together.

To construct an HA-tagged version of the hGLUT4-7K/R mutant, cDNA encoding amino acid residues 1 to 75 of wild type HA-GLUT4 (with the exofacial HA-tag between residues 67 and 68) was 'spliced' together with cDNA encoding amino acid residues 69 to 509 of the hGLUT4-7K/R mutant, which includes all of the lysine to arginine changes. Therefore two fragments of DNA were generated in two separate PCRs with pairs of oligos 260, 263 and 261, 264 (Table 2.2) using pMEXHAGLUT4 (Benito et al., 1991; Shewan et al., 2000) and pG47KR (pRM3) as templates, respectively. These two fragments contain overlapping regions of identical sequence between the cDNA encoding amino acids 69 to 75 of GLUT4 and were used together as template DNA in a final PCR to extend the overlap (using oligos 260 and 261) to produce a final recombinant molecule encoding an HA-tagged version of the mutant GLUT4-7K/R.

In order to construct retroviral expression vectors that will drive the expression of HA-GLUT4-7K/R and the hGLUT4-7K/R-HAUb fusion protein in adipocytes, PCR products encoding HA-tagged GLUT4-7K/R and hGLUT4-7K/R-HAUb were introduced into the pBABE-puro retroviral expression vector (Morgenstern and Land, 1990). Note that the hGLUT4-7K/R-HAUb fusion protein already contains an HA-tag between the carboxyl terminal of the GLUT4 molecule and the first methionine of ubiquitin; therefore there was no need to engineer a tag into this sequence.

In addition to producing the final recombinant HA-GLUT4-7K/R encoding DNA, oligos 260 and 261 were designed to add *Eco*RI and *Sal*I restriction sites at the 5' and 3' ends, respectively, of the HA-GLUT4-7K/R molecule. This allowed for the subcloning of the HA-GLUT4-7K/R mutant as an *Eco*RI-*Sal*I fragment into the pBABE-puro retroviral

expression vector (Morgenstern and Land, 1990). Similarly, the hGLUT4-7K/R-HAUb encoding DNA was amplified using PCR with oligos 260 and 262; also designed to add *Eco*RI and *Sal*I restriction sites at the 5' and 3' ends, respectively, of the PCR product, again enabling it to be subcloned into the pBABE-puro retroviral expression vector. The resulting plasmids, pRM4 and pRM25 thus encode HA-GLUT4-7K/R and hGLUT4-7K/R-HAUb, respectively, in the retroviral expression vector, pBABE-puro (Morgenstern and Land, 1990).

The production of infectious retrovirus containing the constructs, pRM4, pRM25 and pHA-GLUT4; encoding HA-tagged wild type GLUT4 in pBABE-puro (Shewan et al., 2000), was carried out with the use of the packaging cell line, Platinum-E (Plat-E) (Morita et al., 2000). The Plat-E cells constitutively express the viral structural genes, *gag*, *pol* and *env*, which encode essential protein components for the production of infectious retrovirus, including the viral reverse transcriptase and retroviral coat proteins (Morita et al., 2000). As fully described in Section 2.2.8c, the Plat-E cell line was stably transfected with the retroviral expression vectors using liposome-mediated transfection. The Plat-E packaging cell line produces retroviral particles (containing the retroviral expression vectors), which are released into the media surrounding the packaging cells. This media, containing the relevant retrovirus, can then be added directly to the media of 3T3-L1 fibroblasts to allow infection of these cells and consequent uptake of the recombinant GLUT4 cDNA. The pBABE-puro retroviral expression vector contains a drug selectable marker that confers resistance to infected cells in medium containing puromycin (Morgenstern and Land, 1990). Subsequent differentiation of infected 3T3-L1 fibroblasts thus generated 3T3-L1 adipocytes that stably express each of the 3 GLUT4 constructs (wild-type HA-GLUT4; the ubiquitin deficient HA-GLUT4-7K/R; and the GLUT4-7K/R mutant carrying an in-frame ubiquitin fusion hGLUT4-7K/R-HAUb), which were used to analyse the role of ubiquitination in insulin-regulated GLUT4 trafficking.

5.4. Ubiquitination of GLUT4 is required for its exit from the Syntaxin16 positive compartment into insulin responsive GSVs.

As described for Gap1p, the conjugation of ubiquitin to transmembrane proteins can act as a sorting signal for their transport into vesicles that bud into the lumen of multivesicular bodies (MVB) (Katzmann et al., 2002). MVBs subsequently fuse with the mammalian lysosome, or the yeast vacuole, resulting in the eventual proteolysis of the MVB contents

(Katzmann et al., 2002).

The ubiquitination of proteins at the cell surface also acts as a signal for their internalisation (Urbe, 2005). This was first described in yeast where Ste6p, an ABC (ATP-binding cassette) transporter accumulates in a ubiquitinated form in *end* (endocytosis-defective) mutant cells (Kolling and Hollenberg, 1994). The ubiquitination of many proteins has subsequently been shown to be required for their internalisation from the cell surface (Urbe, 2005). In mammalian cells, the ubiquitination of the renal aquaporin-2 (AQP2) water channel at the apical membrane of the kidney-collecting duct upon removal of the hormone arginine-vasopressin triggers its internalisation and subsequent delivery to the lysosome (Kamsteeg et al., 2006). Conversely, the ubiquitination of major histocompatibility complex class II molecules (MHC II) ceases upon dendritic cell maturation, allowing for its accumulation at the plasma membrane (Shin et al., 2006). A ubiquitination-deficient mutant of MHC II is retained at the plasma membrane of immature dendritic cells, while a constitutively ubiquitinated MHC II molecule is retained intracellularly (Shin et al., 2006). Likewise, a ubiquitination-deficient mutant of AQP2 localised mainly to the apical membrane of kidney cells while a constitutively ubiquitinated form of AQP2 localised primarily to the internal vesicles of MVBs (Kamsteeg et al., 2006). In light of the above studies, and the data presented thus far in this thesis, demonstrating that ubiquitination of hGLUT4 in yeast acts as a signal to direct the transporter to the proteolytically active endosomal system, I embarked on a series of experiments to study the role that ubiquitination plays in the trafficking of GLUT4 in 3T3-L1 adipocytes.

To assess whether ubiquitination was required for the insulin-dependent delivery of GLUT4 from an intracellular store to the plasma membrane of adipocytes, I utilised an assay that takes advantage of the exofacial HA-tag carried by wild-type HA-GLUT4 and the ubiquitin-deficient HA-GLUT4-7K/R mutant. Antibodies that specifically recognise the HA-epitope (in the first exofacial loop of the two retrovirally expressed GLUT4 constructs) were used to visualise GLUT4 molecules present at the cell surface of adipocytes that had either been treated with insulin, or not. This experiment (presented in Figure 5.3) was carried out in collaboration with Jacqueline Stöeckli at the Garvan Institute of Medical Research, Australia. The labelling of surface GLUT4 was carried out in the

absence of any cell permeabilisation (see Section 2.2.13c for details), but was followed by a second round of labelling with anti-HA antibody after subsequent permeabilisation with saponin. This allowed for the labelling of total HA-tagged GLUT4 and was used as a control to check that absence of HA staining at the cell surface was not due to lack of expression (Figure 5.3). Due to the fact that the HA tag present in the constitutively-ubiquitinated hGLUT4-7K/R-HAUb is in the cytosolically-disposed carboxyl terminal tail of the GLUT4-7K/R molecule, rather than in an exofacial HA-tag, I was unable to include hGLUT4-7K/R-HAUb in this experiment.

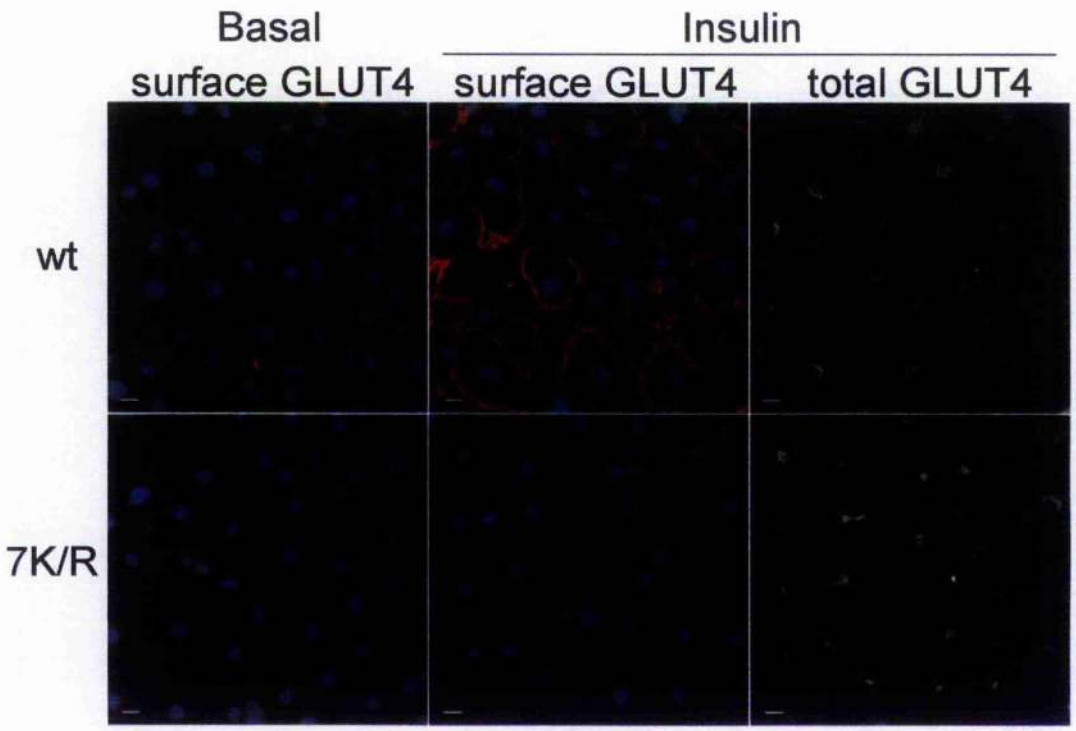

Figure 5.3. HA-GLUT4-7K/R fails to translocate to the plasma membrane in response to insulin.

3T3-L1 adipocytes expressing wild-type HA-tagged GLUT4 (wt) or HA-GLUT4-7K/R (7K/R), incubated for 20mins in the presence (Insulin) or absence (Basal) of 200nM insulin, were fixed and processed for surface and internal GLUT4 staining as described in Section 2.2.13c. Surface GLUT4 (labelled with anti-HA antibody) is shown in red, DAPI in blue and total HA staining is shown in white. Scale bar = 10μm.

The insulin-stimulated translocation of wild-type HA-GLUT4 to the plasma membrane of adipocytes is evident in Figure 5.3, as indicated by the surface labelling of HA-GLUT4 (shown in red) following treatment of adipocytes expressing wild type HA-GLUT4 with insulin. If the ubiquitination of GLUT4 acted as a signal to direct its internalisation from the plasma membrane of adipocytes, I would have expected the ubiquitination-deficient HA-GLUT4-7K/R to be constitutively localised to the adipocyte plasma membrane. However, Figure 5.3 shows a lack of surface labelling of the ubiquitination-deficient HA-GLUT4-7K/R in adipocytes regardless of whether they were treated with insulin or not. This is despite there being approximately equal levels of internal GLUT4 (shown in white) between adipocytes expressing wild type HA-GLUT4 or ubiquitination-deficient HA-GLUT4-7K/R. The low levels of HA-GLUT4-7K/R surface labelling compared to the wild-type protein following insulin treatment, demonstrates a failure of the ubiquitination-deficient HA-GLUT4-7K/R to translocate to the plasma membrane in response to insulin. Therefore, rather than indicating a role for ubiquitination in the internalisation of GLUT4 from the plasma membrane of adipocytes, it would appear that ubiquitination of GLUT4 may be required for its insulin-stimulated translocation to the plasma membrane.

To further investigate these findings, I used differential centrifugation to perform subcellular fractionation on adipocytes expressing HA-GLUT4, HA-GLUT4-7K/R or GLUT4-7K/R-HAUb to determine the subcellular distribution of the three GLUT4 molecules, before and after insulin treatment. This technique yields four membrane fractions that have previously been characterised in detail (Piper et al., 1991) and are designated as; the high-density microsomal fraction (HDM), containing large endosomal components and the endoplasmic reticulum (ER), the low-density microsomal fraction (LDM), enriched in GLUT4 storage vesicles (Millar et al., 1999), the plasma membrane fraction (PM) and the mitochondria/nuclei fraction (M/N). Proteins contained within the PM, LDM and HDM fractions were separated by SDS-PAGE and subjected to immunoblot analysis with anti-HA antibody (Figure 5.4).

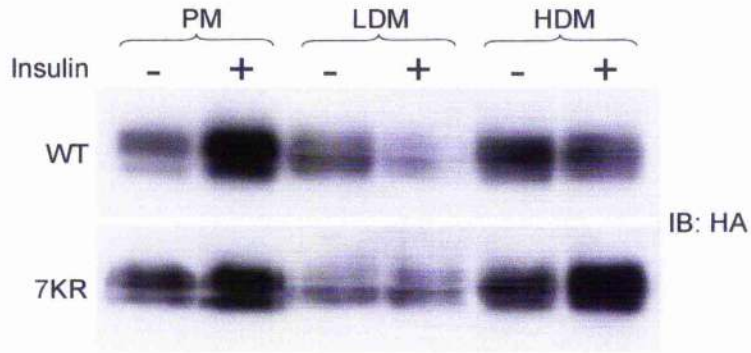

Figure 5.4. HA-GLUT4-7K/R fails to translocate to the plasma membrane in response to insulin.

3T3-L1 adipocytes expressing either wild-type HA-GLUT4 (WT), or HA-GLUT4-7K/R (7KR) were incubated in the absence (-) or presence (+) of 200nM insulin for 20 min. Cells were then fractionated into PM, LDM and HDM fractions as described in materials and methods. Aliquots of each fraction (10μg of protein) were then immunoblotted with anti-HA antibody.

As previously demonstrated (Shewan et al., 2000), the amount of wild type HA-GLUT4 in the PM fraction increases in response to insulin treatment, with a corresponding decrease in the LDM fraction. This demonstrates the translocation of wild type HA-GLUT4 from the GLUT4 storage vesicles, contained within the LDM fraction, to the PM. Although the amount of HA-GLUT4-7K/R in the PM does increase slightly following insulin stimulation, there is no corresponding decrease of HA-GLUT4-7K/R in the LDM fraction. This suggests that the small increase of HA-GLUT4-7K/R at the PM, in response to insulin, is unlikely due to its translocation from GLUT4 storage vesicles.

The data presented in Figures 5.3 and 5.4 indicate that ubiquitination of GLUT4 is required for the insulin-stimulated translocation of the transporter to the plasma membrane of adipocytes. One possibility is that an insulin signal might result in the ubiquitination of GLUT4 and cause GLUT4 to traffic to the plasma membrane. If this were the case, I would expect to see an increase in GLUT4 ubiquitination upon treatment of the adipocytes with insulin. To address this, I prepared lysate from adipocytes that were either treated with 200nM insulin or not and investigated the ubiquitin status of the endogenous GLUT4

from these adipocytes. This was achieved by incubating the lysates with glutathione-Sepharose beads carrying the GST fusion protein, GST-UBA (ubiquitin-binding) and, as a control, GST alone. Proteins pulled-down by GST-UBA and GST were analysed by immunoblot analysis with anti-GLUT4 antibody (to detect any GLUT4 bound to GST alone or to the GST fusion protein), anti-Syntaxin4 antibody (as a non-ubiquitinated protein control) and anti-IRS-1 antibody (as a ubiquitinated protein control) (Figure 5.5). 2.5% of the input lysate was also subject to SDS-PAGE and immunoblot analysis with the various antibodies to verify to presence of the proteins in the lysate.

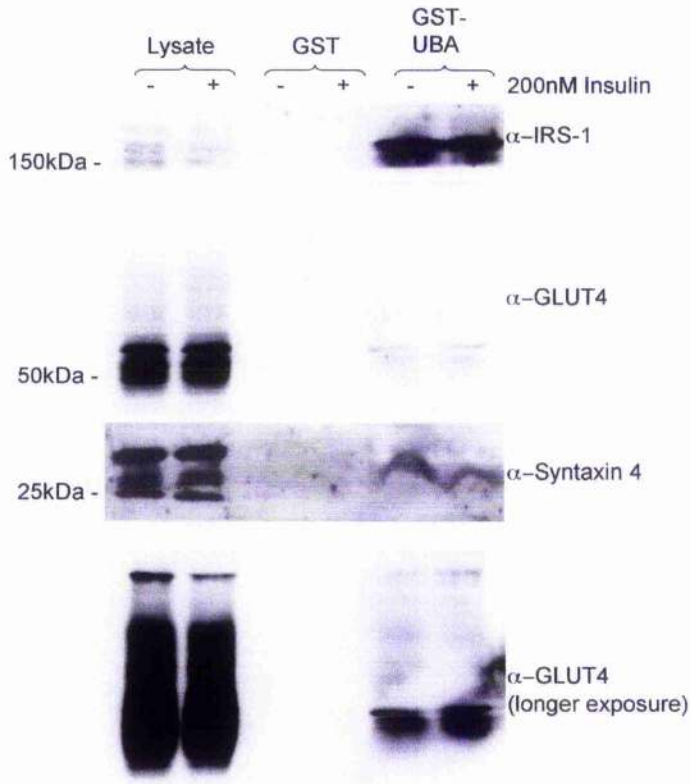

Figure 5.5. GLUT4 is ubiquitinated in 3T3-L1 adipocytes with and without insulin stimulation

Lysate prepared from 3T3-L1 adipocytes, treated with 200nM insulin or not for 15mins (+/- respectively) was incubated with glutathione-Sepharose beads that carried the GST-fusion protein GST-UBA or GST alone. Proteins eluted from the beads were subject to immunoblotting with anti-GLUT4, anti-IRS-1 and anti-Syntaxin4 antibodies. 2.5% input (lanes 1 and 2) was also loaded as a control.

Consistent with the data shown in Figure 4.6, immunoblot analysis with anti-GLUT4 antibody in Figure 5.5 reveals that GLUT4 binds selectively to the GST-UBA fusion protein. Immunoreactive bands of approximately equal intensity and with the expected larger molecular weight to represent ubiquitinated GLUT4 (as compared to the input lysate) were detected from adipocytes that were, or were not, treated with insulin. This indicates that GLUT4 is ubiquitinated in adipocytes regardless of whether the cells are stimulated with insulin, or not.

I next performed a series of indirect immunofluorescence experiments to further characterise the HA-GLUT4-7K/R mutant in adipocytes. Adipocytes expressing wild-type HA-GLUT4, HA-GLUT4-7K/R or GLUT4-7K/R-HAUb were incubated for 20 mins either with, or without 200nM insulin before being processed for indirect immunofluorescence, as described in Section 2.2.13c. Cells were double labelled with antibodies specific for the HA-epitope tag (to label the recombinant GLUT4 molecules) and either antibody specific for the TGN marker Syntaxin16 (Figure 5.6), or antibody specific for early endosomal antigen 1 protein (EEA1), a marker of early endosomes (Mu et al., 1995) (Figure 5.7).

Figure 5.6. HA-GLUT4-7K/R and GLUT4-7K/R-HAUb co-localise with the Syntaxin16 positive compartment.

3T3-L1 adipocytes expressing wild-type HA-GLUT4 (WT), HA-GLUT4-7K/R (7K/R) or GLUT4-7K/R-HAUb (7K/R-HAUb) were incubated in the presence or absence of 200nM insulin for 15min. Cells were then fixed in 3% paraformaldehyde and double labelled with anti-HA antibody and an antibody specific for Syntaxin16. Mouse anti-HA was visualised with Cy3-coupled secondary antibody, rabbit anti-Syntaxin 16 was visualised by alexa488-coupled secondary antibody.

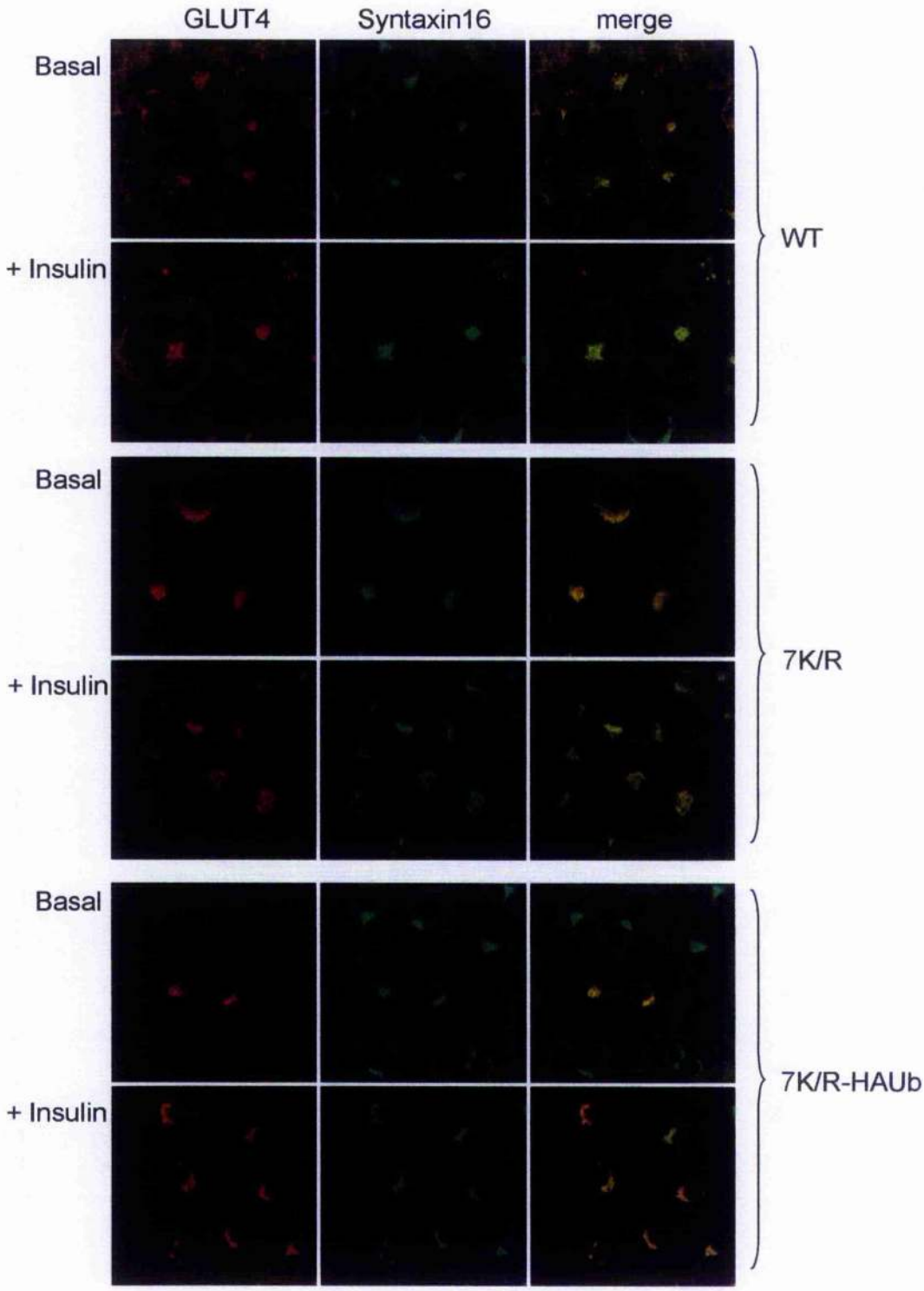
GLUT4
Syntaxin16
merge
Basal
+ Insulin
WT
Basal
+ Insulin
7K/R
Basal
+ Insulin
7K/R-HAUb

Figure 5.7. HA-GLUT4-7K/R and GLUT4-7K/R-HAUb do not colocalise with EEA1. *3T3-L1 adipocytes expressing wild-type HA-GLUT4 (WT), HA-GLUT4-7K/R (7K/R) or GLUT4-7K/R-HAUb (7K/R-HAUb) were incubated in the presence or absence of 200nM insulin for 15min. Cells were then fixed in 3% paraformaldehyde and double labelled with anti-HA antibody and an antibody specific for EEA1. Mouse anti-HA was visualised with Cy3-coupled secondary antibody, rabbit anti-EEA1 was visualised with alexa488-coupled secondary antibody.*

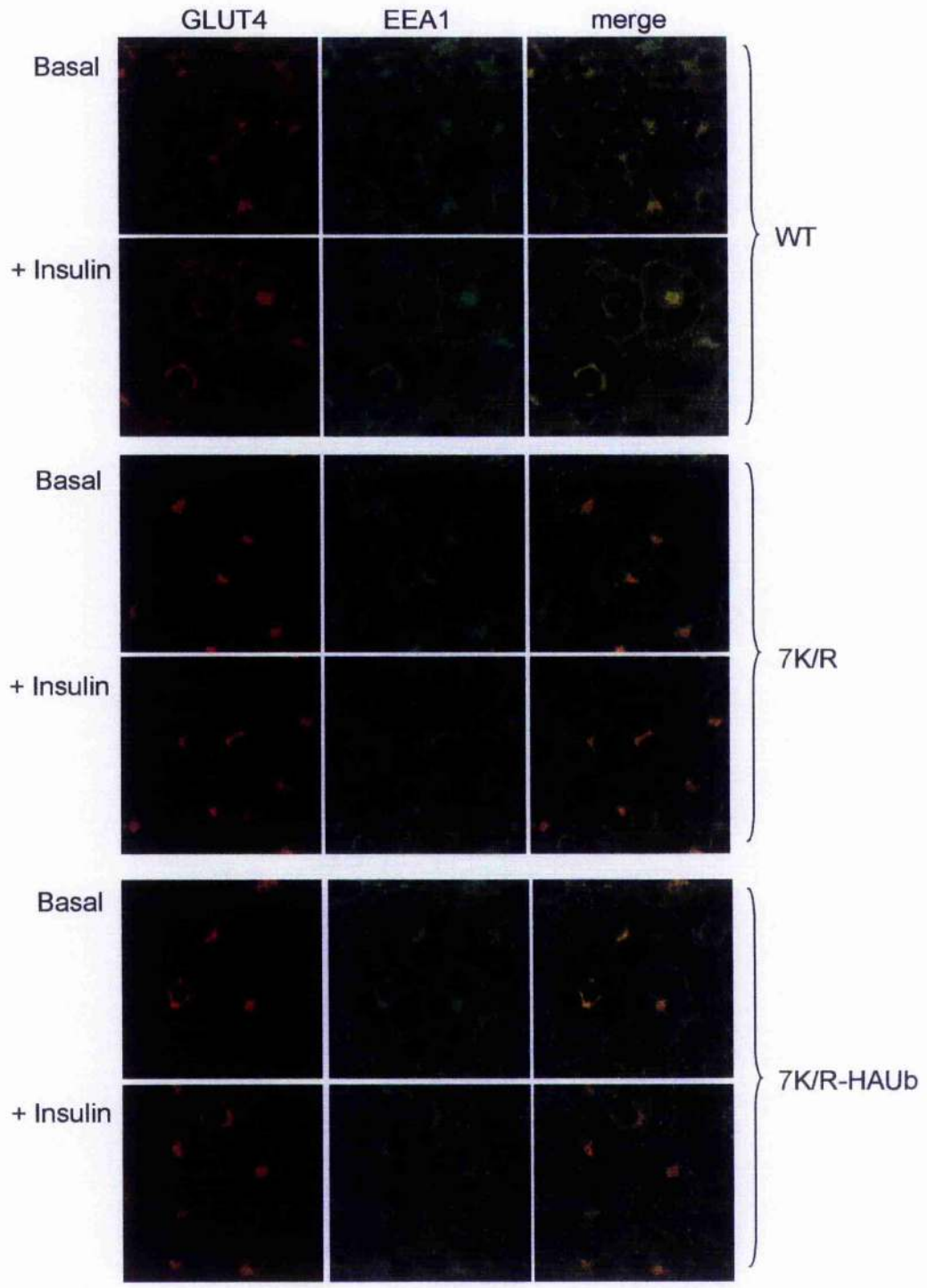
GLUT4
EEA1
merge
Basal
+ Insulin
WT
Basal
+ Insulin
7K/R
Basal
+ Insulin
7K/R-HAUb

Consistent with previous studies (Martin et al., 2000a; Shewan et al., 2000; Shewan et al., 2003), Figure 5.6 demonstrates that wild-type HA-GLUT4 (shown in red), localises to the peri-nuclear region of basal adipocytes, co-localising with the TGN marker Syntaxin16 (shown in green), and also to small punctate structures throughout the cytoplasm, thought to represent GSVs (Martin et al., 2000a). Although HA-GLUT4-7K/R also shows colocalisation with Syntaxin16 in the perinuclear region of the cell, it is striking that there is a distinct lack of labelling of the cytosolic vesicles with this mutant, which shows a less dispersed staining compared to the wild-type (Figure 5.6). The labelling of these peripheral punctate structures by wild-type HA-GLUT4 is also evident in Figure 5.7, where again the HA-GLUT4-7K/R mutant shows less diffuse labelling throughout the cytoplasm of the adipocytes. In addition, to further support that seen in Figures 5.3 and 5.4, wild-type HA-GLUT4 displays a marked translocation to the plasma membrane in response to insulin, whereas the HA-GLUT4-7K/R mutant does not respond to insulin in this manner.

The observation that HA-GLUT4-7K/R is excluded from punctate, GSV-like, structures in adipocytes and is not insulin responsive, supports a model in which the ubiquitination of GLUT4 facilitates its entry into GSVs from where it is mobilised to the cell surface in response to insulin. As the HA-GLUT4-7K/R mutant lacks ubiquitin modification, it is prevented from entering the GSVs, and hence does not translocate to the plasma membrane in response to insulin.

One prediction of the above model is that the constitutively-ubiquitinated GLUT4-7K/R-HAUb fusion protein would have a subcellular localisation that mirrors that seen for wild-type GLUT4. However, indirect immunofluorescence performed on adipocytes expressing the GLUT4-7K/R-HAUb fusion protein (Figures 5.6 and 5.7) show it to have the same subcellular localisation as the ubiquitination-deficient HA-GLUT-7K/R in basal cells (note that that the GLUT4-7K/R-HAUb is also absent from the peripheral GSV-like structures), and also demonstrate that this mutant is not responsive to insulin. Although I found that this method of attaching ubiquitin to GLUT4 was sufficient to direct its trafficking to the endosomal system in yeast (Figure 5.2) it does not appear to be sufficient to direct the entry of GLUT4 into GSVs in adipocytes. It is possible that the specific site of ubiquitin attachment to the GLUT4 molecule is important for this function.

5.5. GGAs are required for ubiquitin-dependent hGLUT4 trafficking

Gga proteins are essential for the nitrogen-regulated trafficking of Gap1p in yeast (Scott et al., 2004). The interaction between ubiquitin on Gap1p and the GAT domain of the Gga proteins is an absolute requirement, as Gap1p remains stable in yeast expressing Gga2p lacking its GAT domain (*gga2-ΔGAT*) as the sole Gga protein, under conditions where it is normally degraded (Scott et al., 2004).

GGA proteins have also been implicated in regulating the entry of GLUT4 into its insulin-responsive location in 3T3-L1 adipocytes (Li and Kandror, 2005; Watson et al., 2004b). The entry of newly synthesised GLUT4 into its insulin-sensitive pool was blocked in adipocytes expressing a 'dominant-negative' GGA mutant (containing only the VHS and GAT domains) (Watson et al., 2004b). This mutant also selectively inhibited the *in vitro* budding of GLUT4-containing vesicles (while having no effect on the generation of vesicles containing GLUT1 and/or the transferrin receptor) (Watson et al., 2004b). In addition, the GGA2 isoform shows significant colocalisation with GLUT4 in the perinuclear region of adipocytes (Li and Kandror, 2005).

The involvement of GGA proteins in the regulated sorting of both Gap1p (in yeast) and GLUT4 (in adipocytes) adds to the parallels between these two systems and makes it tempting to speculate that the ubiquitination of GLUT4 might control its association with GGA proteins, an interaction which may be involved in the biogenesis of the insulin-sensitive pool of GLUT4.

To explore this possibility, I set out to investigate whether, as with Gap1p, Gga proteins were required for the trafficking of hGLUT4 to the yeast endosomal system. hGLUT4 and hGLUT4-7K/R were expressed in the yeast strains MBY004 *(gga)*, deficient in Gga proteins, and the congenic, wild-type *GGA* strain, SEY6210 (Black and Pelham, 2000; Robinson et al., 1988). Proteins contained in lysates prepared from 10 OD_{600} equivalents of cells were separated using SDS-PAGE prior to immunoblot analysis, performed with anti-GLUT4 antibody (Figure 5.8; carried out in conjunction with Nia Bryant).

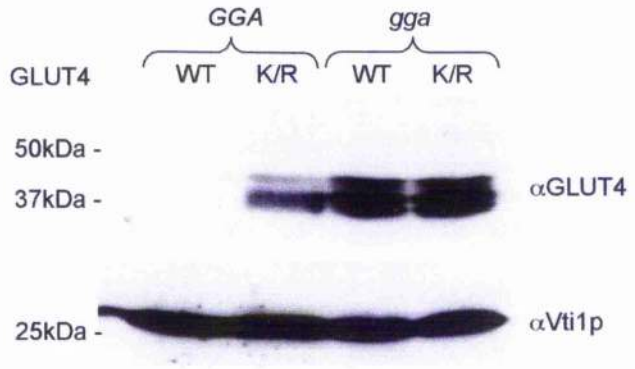

Figure 5.8. GGAs are required for ubiquitin-dependent hGLUT4 trafficking
SEY6210 (GGA) and MBY004 (gga) yeast cells harbouring either pWTG4 or pG47KR (as indicated above; WT and K/R, respectively) were grown in selective media (SD) containing 100μM $CuSO_4$. The amount of wild type hGLUT4 and hGLUT4-7K/R in 10 OD_{600} equivalents of cells was assessed using immunoblot analysis (the amount of Vti1p in each sample was similarly assessed to control for equal loading).

As shown previously (Figure 3.5), steady state levels of wild-type GLUT4 in wild-type (*GGA*) yeast (containing active vacuolar proteases) grown under the nitrogen-rich conditions used here are low, due to the delivery of the transporter to the proteolytically active endosomal system (Figure 5.8). In contrast, the ubiquitin-deficient mutant hGLUT4-7K/R is not delivered to the endosomal system and remains stable under the same conditions (Figure 5.8). Importantly, levels of wild-type GLUT4 expressed in cells lacking Gga proteins (*ggaΔ*) were similar to those seen for hGLUT4-7K/R expressed in both wild-type (*GGA*) and *ggaΔ* mutant cells. Note that it was not possible to look at the nitrogen dependency of this observation since the *ggaΔ* cells would not grow when supplied with unfavourable nitrogen sources such as proline. This is presumably due to a failure of Gap1p to reach the cell surface under these conditions (since this trafficking step required the Gga proteins). The data presented in Figure 5.8 are consistent with the model in which the Gga proteins are required to sort ubiquitinated GLUT4 into the proteolytically active endosomal system in yeast.

Since the interaction between the Gga GAT domain and ubiquitin is an absolute requirement for Gap1p sorting in yeast (Scott et al., 2004), I set out to investigate whether there was a similar interaction with the ubiquitin conjugated to hGLUT4. GLUT4 was

immunoprecipitated from yeast expressing either wild-type hGLUT4 or ubiquitin-deficient hGLUT4-7K/R, with either HA-tagged wild-type Gga2p or a version lacking the ubiquitin-binding GAT domain (HA-tagged GGA2Δgat). The Gga constructs used here were those used in (Scott et al., 2004); obtained from Rob Piper, University of Iowa. Immunoprecipitates were subject to immunoblot analysis with rat anti-HA antibody (to detect whether any HA-tagged GGA2 had coprecipitated with hGLUT4), and mouse anti-GLUT4 monoclonal antibody to assess whether equal amounts of hGLUT4 and hGLUT4 7K/R were immunoprecipitated (Figure 5.9).

If there were an interaction between hGLUT4 and Gga2p, I would expect the immunoblot analysis with anti-HA antibody to detect a band in the immunoprecipitate from yeast expressing both wild-type hGLUT4 and HA-tagged Gga2p. If this interaction was between the ubiquitin, bound to hGLUT4, and the GAT domain of Gga2p, I would predict that this band would not be present in the immunoprecipitate prepared from yeast expressing hGLUT4-7K/R or HA-tagged GGA2Δgat. Figure 5.9 shows no evidence for an interaction between HA-tagged Gga2p and hGLUT4. However, this experiment was flawed since immunoblot analysis with anti-GLUT4 monoclonal antibody demonstrates that equal amounts of wild-type hGLUT4 or hGLUT4-7K/R were not immunoprecipitated. Indeed, the lack of a band representing GLUT4 in the lysates indicates that neither the wild-type not the 7K/R mutant were even expressed in these cells (although a band was detected in one of the immunoprecipitates). Unfortunately, due to time constraints I was unable to repeat this experiment in order to acquire equal levels of wild-type hGLUT4 and hGLUT4-7K/R and am therefore not able to conclude whether, like Gap1p, ubiquitinated GLUT4 interacts with the Gga GAT domain in yeast. Another problem with this approach is that I do not know whether the putative interaction between the Gga protein and the ubiquitin on GLUT4 would survive the conditions used in this experiment.

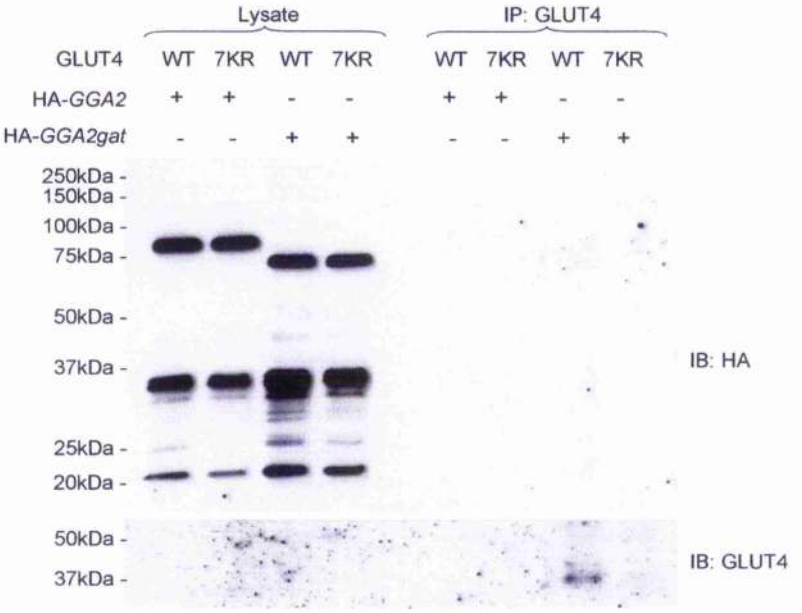

Figure 5.9. Immunoprecipitation to determine an interaction between hGLUT4 and HA-tagged GGA2, in yeast.

SF838-9Dα yeast cells producing either wild-type hGLUT4 (from pRM2) or the ubiquitination-deficient hGLUT4-7K/R mutant (from pRM3) and either HA-tagged Gga2p (from p2256) or HA-tagged GGA2Δ gat (from p2309) were grown in selective media (SD) containing 100μM $CuSO_4$. Immunoprecipitates formed with 10μl anti-GLUT4 antibody were subject to immunoblot analysis with rat anti-HA antibody and mouse anti-GLUT4 monoclonal antibody (1F8).

I also performed experiments to examine whether GLUT4 associates with any of the three GGA isoforms expressed in adipocytes. To investigate an interaction with GGA2, previously implicated in GLUT4 sorting into GSVs (Li and Kandror, 2005; Watson et al., 2004b), GLUT4 was immunoprecipitated from 3T3-L1 adipocytes. This immunoprecipitate was subsequently subject to immunoblot analysis using an anti-GGA2 antibody, obtained from Juan Bonifacino, National Institutes of Health, Bethesda. (Figure 5.10).

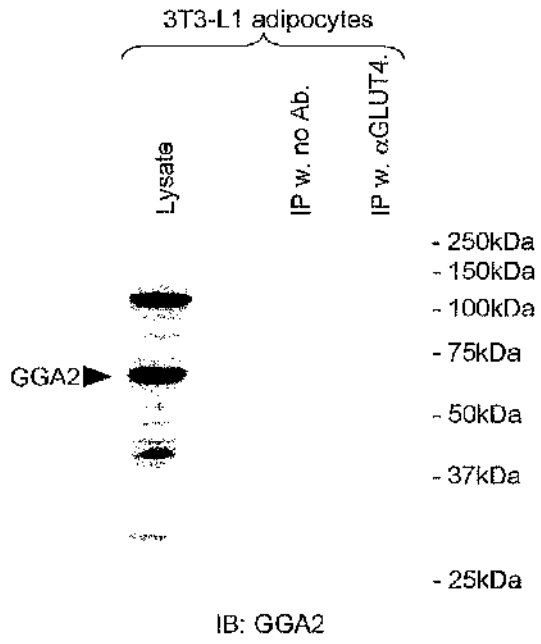

Figure 5.10. Immunoprecipitation to determine an interaction between endogenous GLUT4 and GGA2, in adipocytes.

Immunoprecipitates formed with 10µl anti-GLUT4 antibody from lysate prepared from 3T3-L1 adipocytes were subject to immunoblot analysis with anti-GGA2 antibody (to investigate whether GGA2 interacted with endogenous GLUT4 in adipocytes). 2.5% input (lane 1) was also loaded as a control.

Immunoblot analysis with anti-GGA2 antibody detects an immunoreactive band of ~67kDa (the predicted MW of GGA2) in the adipocyte lysate (Figure 5.10). However, GGA2 appears not to have coprecipitated with GLUT4, as a similar immunoreactive band cannot be detected above background levels in the immunoprecipitate formed with anti-GLUT4 antibody. It is possible that the levels of GGA2 bound to GLUT4 at any one time are too low for detection by this approach, particularly if GGA2 interacts only with ubiquitinated GLUT4. As with the experiment presented in Figure 5.9, another caveat here is that the conditions used for the immunoprecipitation may have disrupted an interaction between ubiquitin and the Gga proteins. Further experiments carried out under different conditions will be required to investigate this. Yet another problem with this experiment is that I was unable to probe the immunoprecipitates with anti-GLUT4 antibody since the GGA2 antibody was also a mouse monoclonal.

To investigate an interaction between GLUT4 and the other GGA isoforms expressed by adipocytes, I took another approach where I utilised GST fusion proteins containing the GAT and VHS domains of GGA1 and GGA3, GST-GGA1-GAT-VHS and GST-GGA3-GAT-VHS, respectively (obtained from Rob Piper, University of Iowa). Lysate prepared from 3T3-L1 adipocytes was incubated with glutathione-Sepharose beads carrying the GST fusion proteins, GST-GGA1-GAT-VHS and GST-GGA3-GAT-VHS and, as a control, GST alone. Proteins pulled-down by the GST fusion proteins or by GST alone were analysed by immunoblot analysis with anti-GLUT4 antibody (to detect any GLUT4 bound to the GST fusion proteins) (Figure 5.11). 2.5% of the input lysate was also subject to SDS-PAGE and immunoblot analysis with anti-GLUT4 antibody to verify the presence of GLUT4.

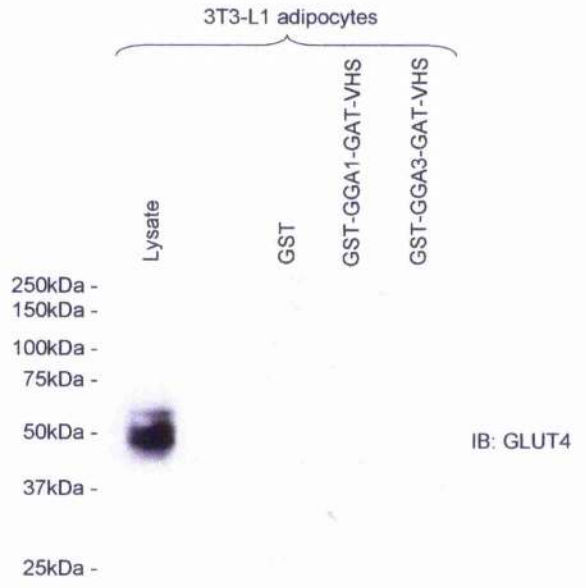

Figure 5.11. GST pull down assays to determine an interaction between endogenous GLUT4 and GGA proteins, in adipocytes.

Lysate prepared from 3T3-L1 adipocytes was incubated with glutathione-Sepharose beads that carried GST alone or the GST-fusion proteins, GST-GGA1-GAT-VHS and GST-GGA3-GAT-VHS. Proteins eluted from the beads were subject to immunoblot analysis with anti-GLUT4 antibody. 2.5% input (lane 1) was also loaded as a control.

Immunoblot analysis with anti-GLUT4 antibody detects an immunoreactive band with an apparent molecular weight of ~48kDa in the adipocyte lysate, thus indicating the presence of GLUT4 (Figure 5.11). However, no such band was detected in the proteins pulled-down by either of the GST fusion proteins, presenting no evidence for an interaction of GLUT4 with either GGA1 or GGA3. However, this experiment lacks a positive control. To substantiate this experiment, I would need to perform immunoblot analysis of proteins known to interact with GGA1 and GGA3, such as the cation-independent mannose 6-phosphate receptor (CI-MPR) or the cation-dependent mannose 6-phosphate receptor (CD-MPR) (Puertollano et al., 2001).

Although GGA2 has been implicated in the sorting of GLUT4 in adipocytes, no direct interaction between GGA2 and GLUT4 has been previously detected (Li and Kandror, 2005). Consistent with this, I was unable to coprecipitate GGA2 and GLUT4 from 3T3-L1 adipocytes (Figure 5.10), or demonstrate binding of GLUT4 from an adipocyte lysate to either GST-GGA1 or GST-GGA3 fusion proteins (Figure 5.11). However, I am aware that these results are preliminary due to the caveats discussed.

5.6. Chapter summary

In this chapter I aimed to address the role that ubiquitin plays in the nitrogen-regulated trafficking of GLUT4 when expressed in yeast, as well as in the insulin-regulated trafficking of GLUT4 in the murine cell line 3T3-L1 adipocytes. By investigating the intracellular trafficking of a ubiquitination-deficient mutant of hGLUT4 (hGLUT4-7K/R), or a constitutively-ubiquitinated hGLUT4 fusion protein (hGLUT4-7K/R-HAUb), I determined that, in yeast, the ubiquitination of GLUT4 is both necessary and sufficient to direct it to the proteolytically active endosomal system. Furthermore, through a series of experiments studying the trafficking of wild-type HA-GLUT4, the ubiquitin-deficient mutant HA-GLUT4-7K/R and the constitutively- ubiquitinated hGLUT4-7K/R-HAUb in adipocytes, I have presented data to support a model in which ubiquitination of GLUT4 is required for its exit from the TGN into the GLUT4 storage vesicles (GSVs) from where it can be mobilised to the plasma membrane in response to insulin.

Chapter 6: Final Discussion

Chapter 6: Final Discussion

The overall goal of this thesis was to further our understanding of the insulin-regulated trafficking of the facilitative glucose transporter GLUT4 in fat and muscle cells. One of the major consequences of insulin binding to its receptor on fat and muscle cells is the translocation of GLUT4 from an intracellular store to the plasma membrane (Bryant et al., 2002). This allows the uptake of glucose into muscle and adipose tissue, thereby reducing levels of plasma glucose (Bryant et al., 2002). The insulin-resistant state associated with Type-2 diabetes and obesity is characterised by an insufficient recruitment of GLUT4 to the plasma membrane in response to insulin, despite there being normal levels of GLUT4 expression (Bjornholm and Zierath, 2005). Therefore, understanding the molecular mechanisms that control the insulin-regulated trafficking of GLUT4 is of high priority as it has the potential to aid us in the development of therapeutic interventions to treat and/or prevent Type-2 diabetes.

Despite the fact that the intracellular trafficking of GLUT4 has been intensely studied for nearly 20 years, two fundamental questions remain largely unanswered (Bryant et al., 2002):

How is GLUT4 sorted into its insulin-sensitive pool?
How is GLUT4 mobilised to the plasma membrane in response to insulin?

One of the major problems with the study of insulin-regulated GLUT4 trafficking is that, as they are terminally differentiated, insulin-responsive cells are hard to work with experimentally (Quon et al., 1993). A common approach used to circumvent such a problem in cell biology is to use an experimentally tractable eukaryote system, such as the budding yeast *Saccharomyces cerevisiae* (Baker's yeast) (Broach et al., 1991; Guthrie and Fink, 1991). There is a high degree of conservation in some of the major signalling pathways and basic cellular processes between *S.cerevisiae* and mammalian cells (Broach et al., 1991; Guthrie and Fink, 1991). This has led to *S.cerevisiae* becoming a well-established and powerful tool that has greatly furthered the knowledge of many aspects of cell biology, such as membrane trafficking, cell cycle control, cell signalling and DNA repair (Broach et al., 1991; Guthrie and Fink, 1991). However, given that yeast neither

respond to insulin, nor express GLUT4, it is not immediately apparent how yeast might be a good system in which to study the insulin-regulated trafficking of GLUT4.

Despite their lack of insulin-responsiveness, it is clear that yeast do possess a regulated membrane trafficking step that bears remarkable similarity to the insulin-regulated trafficking of GLUT4, namely the nitrogen-regulated trafficking of the general amino acid permease, Gap1p (Roberg et al., 1997). Gap1p is retained intracellularly under nutrient-rich conditions but when nutrients are limited, Gap1p is trafficked to the plasma membrane, where it facilitates the uptake of amino acids from the extracellular media (Roberg et al., 1997). Like GLUT4, Gap1p is predicted to span the membrane twelve times (Jauniaux and Grenson, 1990) and interestingly, contains motifs in its cytosolic carboxyl terminal tail that are analogous to those required for GLUT4 trafficking (Hein and Andre, 1997). Furthermore, when a chimeric protein, in which the carboxyl terminal tail of GLUT4 was replaced with the analogous portion of Gap1p, is expressed in adipocytes, it localises to the TGN and translocates to the cell surface in response to insulin, similar to endogenous GLUT4 (Nia Bryant and David James; unpublished data; Figure 1.6).

To build on these observations, and to assess the suitability of using yeast as a model system in the study of the insulin-regulated GLUT4 trafficking, I expressed human GLUT4 (hGLUT4) in yeast to further explore the parallels between GLUT4 and Gap1p regulated trafficking. In Chapter 3, I describe how I expressed hGLUT4 in yeast and presented data to demonstrate that hGLUT4 traffics in yeast in a nitrogen-regulated manner analogous to that observed for Gap1p.

I used indirect immunofluorescence to demonstrate that, like Gap1p (Roberg et al., 1997), hGLUT4 shows an intracellular punctate staining, which co-localises significantly with Kex2p, a marker of the yeast TGN (Redding et al., 1991; Wilcox and Fuller, 1991; Wilcox et al., 1992). This observation is in contrast to previous studies expressing mammalian GLUT4 in yeast (Kasahara and Kasahara, 1997; Wieczorke et al., 2003), which reported that the transporter localises to the endoplasmic reticulum (ER). This is likely due to the high levels of expression used in these studies, as they expressed GLUT4 at very high levels from the *GAL1/10* promoter (Kasahara and Kasahara, 1997; Wieczorke et al., 2003).

It is likely that when expressed at such high levels a large proportion of GLUT4 is misfolded and therefore fails to exit the ER. In order to produce GLUT4 at more modest levels in yeast I used the regulatable *CUP1* promoter, which allows gene expression to be tightly modulated (Mascorro-Gallardo et al., 1996). The colocalisation of GLUT4 with Kex2p was encouraging as GLUT4 colocalises with the TGN marker Syntaxin16 in mammalian cells (Figure 5.6) (Shewan et al., 2003).

Kex2p is retained in the yeast TGN by continually cycling through the endocytic system (Brickner and Fuller, 1997) and a similar phenomenon has been described for GLUT4 in adipocytes (Shewan et al., 2003). The yeast endocytic system is proteolytically active (Bryant and Stevens, 1997) and so my finding that I can only detect hGLUT4 at steady state levels in yeast cells devoid of active vacuolar proteases (Figures 3.5 and 3.8) supports the immunofluorescence data and indicates that hGLUT4 localises to the yeast TGN by continually cycling through the endosomal system.

Importantly, Chapter 3 demonstrates that hGLUT4 traffics in yeast in a nitrogen-regulated manner akin to Gap1p. When yeast producing hGLUT4 were grown in media containing ammonium chloride as the sole nitrogen source (a good source of nitrogen), hGLUT4 was directed to the proteolytically active endosomal system and degraded. However, when the same cells were provided with proline (a poor source of nitrogen) as their sole nitrogen source, hGLUT4 was stabilised, indicating that it had been directed away from the endosomal system and therefore not degraded. This mirroring of the nitrogen-regulated trafficking of Gap1p (Roberg et al., 1997) indicates the two transporters are similarly trafficked in yeast, further advances the parallels between GLUT4/Gap1p trafficking, and firmly establishes the use of yeast as a suitable model system to study GLUT4 trafficking.

Gap1p moves to plasma membrane in response to limited nutrients (Roberg et al., 1997). Unfortunately I was unable to assess whether hGLUT4 also traffics to the plasma membrane in yeast grown with limited nutrients. With more time, I could have taken a number of approaches to address this. I could have used indirect immunofluorescence (or a GFP-tagged version of hGLUT4) to localise hGLUT4 in yeast grown in proline-containing media. In addition, another approach would be to utilise the *hexΔ* yeast strains, KY73 and RMY1, which are normally unable to grow on glucose-containing media due to

the fact that they lack endogenous hexose transporters and instead must be supplied with an alternative carbon source (such as maltose). If hGLUT4 does indeed traffic to the plasma membrane in response to limited nutrients, it should enable the growth of *hexΔ* yeast in proline-containing, glucose-containing media.

Nonetheless, the data presented in Chapter 3 clearly demonstrate that hGLUT4 is trafficked away from the endosomal system under poor nitrogen conditions, but enters proteolytically active compartments when nitrogen is plentiful. The nitrogen-regulated trafficking of Gap1p is regulated by the ubiquitination of the transporter, targeting it for degradation by active vacuolar proteases as a mechanism to control nitrogen uptake under nutrient rich conditions (Hein and Andre, 1997; Helliwell et al., 2001; Springael and Andre, 1998; Springael et al., 1999). With this in mind, and noting the similarities that exist between Gap1p and GLUT4, I demonstrated that hGLUT4 was also subject to ubiquitination when expressed in yeast.

This was presented in Chapter 4 through a series of immunoprecipitation experiments and pull-down assays. The initial indications from these studies point towards hGLUT4 being monoubiquitinated, as a prominent immunoreactive band at ~50kDa detected in both the immunoprecipitation experiments and the GST-UBA pull down assays suggest the addition of one ubiquitin moiety to the transporter. The modification of a protein by monoubiquitin can be a signal for the targeting of transmembrane proteins, from both endocytic and biosynthetic pathways, into vesicles budding into the lumen of the multivesicular body (MVB), which subsequently fuses with, and consequently delivers its contents to, the mammalian lysosome or yeast vacuole (Katzmann et al., 2002).

Having provided evidence that hGLUT4 is ubiquitinated in the yeast model system, and having established the suitability of the GST-UBA pull down assay as a technique to determine whether a particular protein is ubiquitinated (Figures 4.1, 4.3 and 4.5), I went on to use the pull-down approach to demonstrate that endogenous GLUT4 is ubiquitinated in the insulin-sensitive, murine cell line 3T3-L1 adipocytes (Figure 4.6). Unfortunately, I was not able to definitively ascertain whether the mutant HA-GLUT4-7K/R is, as predicted, not ubiquitinated when expressed in adipocytes. This was due to inadequate levels of expression from the retrovirus in the cells used for this experiment. With more

time, I would have optimised this expression either by infecting more adipocytes or producing a fresh preparation of virus with a higher titre of infectivity. However, given that the 7K/R mutant was not ubiquitinated in yeast, it seems reasonable to assume that it will not be in adipocytes either.

I also presented efforts made towards identifying the specific lysine residue(s) in the GLUT4 molecule that is (are) ubiquitinated. Frustratingly, these studies were unsuccessful at identifying definitive sites of ubiquitination and due to time constraints I was unable to explore an alternative approach. One possible avenue that could have been taken to address this issue would be to use tandem mass spectrometry (MS/MS) to identify the precise site of ubiquitination (Peng et al., 2003). This would require substantial work as I would need to optimise conditions to purify sufficient quantities of GLUT4 for these experiments, and given that the transporter has 12 transmembrane domains this would be no small undertaking. However, establishing that hGLUT4 is ubiquitinated is a very novel and exciting finding that has opened up new avenues of research and furthered our understanding of the insulin-regulated trafficking of GLUT4.

As a first step towards understanding the role of GLUT4 ubiquitination I followed the trafficking of the ubiquitination-deficient mutant GLUT4-7K/R, and also a constitutively-ubiquitinated GLUT4 fusion protein (GLUT4-7K/R-HAUb) in yeast and in adipocytes (Chapter 5). I determined that ubiquitination is both necessary and sufficient to direct hGLUT4 to the proteolytically active endosomal system in yeast, and in adipocytes, I observed that ubiquitination of GLUT4 is required for its insulin-stimulated translocation to the plasma membrane. This observation suggests that ubiquitination is either required for the delivery of GLUT4 from GSVs to the cell surface, or into GSVs in the first place. I favour a model in which ubiquitination is required for the sorting of GLUT4 into GSVs (rather than from GSVs to the cell surface) for the following reasons; firstly, if ubiquitination was the insulin-regulated signal that allows GLUT4 to exit from GSVs to the cell surface, I would expect to see an increase in the ubiquitination of the transporter in response to insulin. This was not observed (Figure 5.5) and instead I detected that GLUT4 is constitutively ubiquitinated in basal adipocytes (Figures 5.5). In addition, immunofluorescence microscopy indicates that wild-type HA-GLUT4 localises, not only to the TGN (colocalising with Syntaxin16), but also to cytosolic puncta, previously

identified as GSVs (Martin et al., 2000a). The HA-GLUT4-7K/R localised only to the TGN with the punctate staining being conspicuously absent.

I had hoped to use the constitutively ubiquitinated version of GLUT4 (GLUT4-7K/R-HAUb) to distinguish between the two models proposed above. If ubiquitination is required for the delivery of GLUT4 from GSVs to the cell surface, then I would predict that this mutant would localise to the cell surface of adipocytes even in the absence of insulin-stimulation. If, on the other hand, ubiquitination is required for GLUT4's delivery into GSVs then I would predict that this mutant would behave like wild-type GLUT4, requiring insulin-stimulation for translocation to the plasma membrane. Unfortunately, this mutant proved hard to characterise in that, when expressed in basal adipocytes it showed the same localisation as the ubiquitin-defective HA-GLUT4-7K/R mutant: localising to the peri-nuclear TGN region of the cell, but lacking the cytosolic punctate staining observed for wild-type HA-GLUT4. No plasma membrane staining was detected either in basal adipocytes or following insulin-stimulation (Figures 5.6 and 5.7). It is possible that the ubiquitin moeity fused onto GLUT4 is not correctly folded in adipocytes and thus GLUT4-7K/R-HAUb behaves like HA-GLUT4-7K/R.

GGA proteins are a family of clathrin adaptors that facilitate protein sorting in the TGN/endosomal system (Pelham, 2004). They have been found to play a role in both the nitrogen-regulated trafficking of Gap1p in yeast (Scott et al., 2004) and in the regulated trafficking of GLUT4 in insulin-sensitive cells (Li and Kandror, 2005; Watson et al., 2004b). The ubiquitination of Gap1p, caused when yeast are grown on rich sources of nitrogen (e.g. ammonium), regulates its interaction with the yeast GGAs (through the ubiquitin-binding GAT domain) (Scott et al., 2004), which deliver Gap1p to the endosomal system and divert it away from the plasma membrane (Scott et al., 2004). Under poor nitrogen conditions (e.g. proline) however, Gap1p is not ubiquitinated, does not bind GGAs, and is therefore trafficked to the cell surface (Soetens et al., 2001). This finding provides a link between the ubiquitination of Gap1p under nitrogen-rich conditions and the transporter's regulated trafficking.

Intriguingly, over-expression of a dominant-interfering GGA mutant (VHS-GAT) in adipocytes inhibits the sorting of newly synthesised GLUT4 into an insulin-sensitive pool,

but it does not inhibit the movement of GLUT4 from GSVs to the cell surface (Watson et al., 2004b). The finding that the ubiquitination-deficient GLUT4 mutant (GLUT4-7K/R) displays defective entry into the regulated cell surface recycling pathway could reflect a role for GGAs in binding to ubiquitinated GLUT4, a step that would be impaired with the GLUT4-7K/R mutant. Indeed, wild-type hGLUT4 was stabilised when expressed in mutant yeast cells lacking GGA proteins (*ggaΔ;* Figure 5.8), grown under the nitrogen-rich conditions that normally deliver hGLUT4 to the proteolytically active endosomal system for degradation (Figure 3.5), thus indicating a requirement for GGA proteins in this trafficking step. The steady-state levels of hGLUT4-7K/R were similar when expressed in either wild-type or *ggaΔ* cells, and not significantly different to that observed for wild-type hGLUT4 in *ggaΔ* cells (Figure 5.8). This is consistent with a model in which the ubiquitination of hGLUT4 facilitates its trafficking within the endosomal/TGN system in concert with the GGA proteins. By analogy with the regulated trafficking of Gap1p, it is tempting speculate that the ubiquitination of GLUT4 might control its association with GGA proteins (Scott et al., 2004). However, although GGA2 has been implicated in the sorting of GLUT4 in adipocytes, no direct interaction between GGA2 and GLUT4 has been detected (Li and Kandror, 2005). Furthermore, I was unable to demonstrate, by either coprecipitating any of the GGA isoforms with GLUT4 or by GST fusion protein pull-down assay, any interaction between GLUT4 and any of the GGA isoforms, in yeast, or in adipocytes (Figures 5.9, 5.10 and 5.11). However, I am aware that these studies are preliminary and require further work for the results to be substantiated.

Ubiquitination has been implicated as a signal in the regulated trafficking of a number of other molecules, including MHC class II and aquaporin-2 (Kamsteeg et al., 2006; Shin et al., 2006). In these instances, a loss of the ubiquitin modification results in the accumulation of the protein at the cell surface, implying a role for ubiquitination in controlling endocytosis. Similarly, a loss of the ubiquitin modification of Gap1p results in its accumulation at the cell surface (Helliwell et al., 2001; Soetens et al., 2001). Notably however, this is not the case for GLUT4, as the ubiquitination-deficient GLUT4-7K/R mutant did not accumulate at the cell surface, but rather in the TGN area of adipocytes and was rendered insulin insensitive. This is consistent with the model for GLUT4 transport proposed in (Bryant et al., 2002), which suggests that GLUT4 is selectively targeted into an intracellular transport loop between endosomes and the TGN and is therefore

consequently excluded from the cell-surface recycling pathway. Within this intracellular transport loop GLUT4 is packaged into insulin responsive GSVs from where it can move to the cell surface in response to insulin. The lack of insulin responsiveness, and the absence from peripheral punctate GSV-like structures in adipocytes, of the ubiquitination-deficient GLUT4-7K/R mutant supports a role for ubiquitination in the trafficking of GLUT4 from the TGN/endosomal system into GSVs. Overall, this model bears remarkable similarities to that proposed for the sorting of Gap1p in yeast, and the finding that certain elements of this regulated pathway can be transferred to GLUT4 represents yet another example of the conservation between these essential trafficking pathways and the machinery that controls them.

Future Work

This study has been successful in implicating a role for ubiquitination in the insulin-regulated trafficking of GLUT4 in adipocytes. This finding has opened up a new area of research that can now be directed towards understanding more about this process. Of high priority will be to determine precisely which of the 7 cytosolically disposed lysine residues are ubiquitinated in adipocytes. In addition, since the E3 ubiquitin ligase is often regarded as the key regulatory determinant of the ubiquitination process (Hicke and Dunn, 2003), it would be of great interest to identify which ligase transfers the ubiquitin moiety onto GLUT4 in adipocytes.

Bibliography

Adams, B.G. 1972. Induction of galactokinase in Saccharomyces cerevisiae: kinetics of induction and glucose effects. J Bacteriol. 111:308-15.

Ammerer, G., C.P. Hunter, J.H. Rothman, G.C. Saari, L.A. Valls, and T.H. Stevens. 1986. PEP4 gene of Saccharomyces cerevisiae encodes proteinase A, a vacuolar enzyme required for processing of vacuolar precursors. Mol Cell Biol. 6:2490-9.

Amos, A.F., D.J. McCarty, and P. Zimmet. 1997. The rising global burden of diabetes and its complications: estimates and projections to the year 2010. Diabet Med. 14 Suppl 5:S1-85.

Andre, B. 1995. An overview of membrane transport proteins in Saccharomyces cerevisiae. Yeast. 11:1575-611.

Arnason, T., and M.J. Ellison. 1994. Stress resistance in Saccharomyces cerevisiae is strongly correlated with assembly of a novel type of multiubiquitin chain. Mol Cell Biol. 14:7876-83.

Benito, M., A. Porras, A.R. Nebreda, and E. Santos. 1991. Differentiation of 3T3-L1 fibroblasts to adipocytes induced by transfection of ras oncogenes. Science. 253:565-8.

Birnbaum, M.J., H.C. Haspel, and O.M. Rosen. 1986. Cloning and characterization of a cDNA encoding the rat brain glucose-transporter protein. Proc Natl Acad Sci U S A. 83:5784-8.

Bjornholm, M., and J.R. Zierath. 2005. Insulin signal transduction in human skeletal muscle: identifying the defects in Type II diabetes. Biochem Soc Trans. 33:354-7.

Black, M.W., and H.R. Pelham. 2000. A selective transport route from Golgi to late endosomes that requires the yeast GGA proteins. J Cell Biol. 151:587-600.

Boeke, J.D., J. Trueheart, G. Natsoulis, and G.R. Fink. 1987. 5-Fluoroorotic acid as a selective agent in yeast molecular genetics. Methods Enzymol. 154:164-75.

Bogan, J.S., N. Hendon, A.E. McKee, T.S. Tsao, and H.F. Lodish. 2003. Functional cloning of TUG as a regulator of GLUT4 glucose transporter trafficking. Nature. 425:727-33.

Bonifacino, J.S. 2004. The GGA proteins: adaptors on the move. Nat Rev Mol Cell Biol. 5:23-32.

Brant, A.M., S. McCoid, H.M. Thomas, S.A. Baldwin, A. Davies, J.C. Parker, E.M. Gibbs, and G.W. Gould. 1992. Analysis of the glucose transporter content of islet cell lines: implications for glucose-stimulated insulin release. Cell Signal. 4:641-50.

Brickner, J.H., and R.S. Fuller. 1997. SOI1 encodes a novel, conserved protein that promotes TGN-endosomal cycling of Kex2p and other membrane proteins by modulating the function of two TGN localization signals. J Cell Biol. 139:23-36.

Broach, J.R., J.R. Pringle, and E.W. Jones. 1991. The Molecular and Cellular Biology of the Yeast Saccharomyces. Cold Spring Laboratory Press, Cold Spring Harbor, NY.

Brownlee, M. 2001. Biochemistry and molecular cell biology of diabetic complications. Nature. 414:813-20.

Bryant, N.J., and A. Boyd. 1993. Immunoisolation of Kex2p-containing organelles from yeast demonstrates colocalisation of three processing proteinases to a single Golgi compartment. J Cell Sci. 106 (Pt 3):815-22.

Bryant, N.J., R. Govers, and D.E. James. 2002. Regulated transport of the glucose transporter GLUT4. Nat Rev Mol Cell Biol. 3:267-77.

Bryant, N.J., R.C. Piper, S.R. Gerrard, and T.H. Stevens. 1998a. Traffic into the prevacuolar/endosomal compartment of Saccharomyces cerevisiae: a VPS45-dependent intracellular route and a VPS45-independent, endocytic route. Eur J Cell Biol. 76:43-52.

Bryant, N.J., R.C. Piper, L.S. Weisman, and T.H. Stevens. 1998b. Retrograde traffic out of the yeast vacuole to the TGN occurs via the prevacuolar/endosomal compartment. J Cell Biol. 142:651-63.

Bryant, N.J., and T.H. Stevens. 1997. Two separate signals act independently to localize a yeast late Golgi membrane protein through a combination of retrieval and retention. J Cell Biol. 136:287-97.

Butt, T.R., E.J. Sternberg, J.A. Gorman, P. Clark, D. Hamer, M. Rosenberg, and S.T. Crooke. 1984. Copper metallothionein of yeast, structure of the gene, and regulation of expression. Proc Natl Acad Sci U S A. 81:3332-6.

Chau, V., J.W. Tobias, A. Bachmair, D. Marriott, D.J. Ecker, D.K. Gonda, and A. Varshavsky. 1989. A multiubiquitin chain is confined to specific lysine in a targeted short-lived protein. Science. 243:1576-83.

Chen, E.J., and C.A. Kaiser. 2002. Amino acids regulate the intracellular trafficking of the general amino acid permease of Saccharomycescerevisiae. Proc Natl Acad Sci U S A. 99:14837-42.

Coe, J.G., A.C. Lim, J. Xu, and W. Hong. 1999. A role for Tlg1p in the transport of proteins within the Golgi apparatus of Saccharomyces cerevisiae. Mol Biol Cell. 10:2407-23.

Cope, D.L., S. Lee, D.R. Melvin, and G.W. Gould. 2000. Identification of further important residues within the Glut4 carboxy-terminal tail which regulate subcellular trafficking. FEBS Lett. 481:261-5.

Czech, M.P., and S. Corvera. 1999. Signaling mechanisms that regulate glucose transport. J Biol Chem. 274:1865-8.

DeFronzo, R.A. 1992. Pathogenesis of type 2 (non-insulin dependent) diabetes mellitus: a balanced overview. Diabetologia. 35:389-97.

Di Fiore, P.P., S. Polo, and K. Hofmann. 2003. When ubiquitin meets ubiquitin receptors: a signalling connection. Nat Rev Mol Cell Biol. 4:491-7.

Douglas, H.C., and D.C. Hawthorne. 1964. Enzymatic Expression and Genetic Linkage of Genes Controlling Galactose Utilization in Saccharomyces. Genetics. 49:837-44.

Dupre, S., D. Urban-Grimal, and R. Haguenauer-Tsapis. 2004. Ubiquitin and endocytic internalization in yeast and animal cells. Biochim Biophys Acta. 1695:89-111.

Fisk, H.A., and M.P. Yaffe. 1999. A role for ubiquitination in mitochondrial inheritance in Saccharomyces cerevisiae. J Cell Biol. 145:1199-208.

Fukumoto, H., T. Kayano, J.B. Buse, Y. Edwards, P.F. Pilch, G.I. Bell, and S. Seino. 1989. Cloning and characterization of the major insulin-responsive glucose transporter expressed in human skeletal muscle and other insulin-responsive tissues. J Biol Chem. 264:7776-9.

Fuller, R.S., A. Brake, and J. Thorner. 1989. Yeast prohormone processing enzyme (KEX2 gene product) is a Ca2+-dependent serine protease. Proc Natl Acad Sci U S A. 86:1434-8.

Funakoshi, M., T. Sasaki, T. Nishimoto, and H. Kobayashi. 2002. Budding yeast Dsk2p is a polyubiquitin-binding protein that can interact with the proteasome. Proc Natl Acad Sci U S A. 99:745-50.

Galan, J.M., and R. Haguenauer-Tsapis. 1997. Ubiquitin lys63 is involved in ubiquitination of a yeast plasma membrane protein. Embo J. 16:5847-54.

Garippa, R.J., A. Johnson, J. Park, R.L. Petrush, and T.E. McGraw. 1996. The carboxyl terminus of GLUT4 contains a serine-leucine-leucine sequence that functions as a potent internalization motif in Chinese hamster ovary cells. J Biol Chem. 271:20660-8.

Garippa, R.J., T.W. Judge, D.E. James, and T.E. McGraw. 1994. The amino terminus of GLUT4 functions as an internalization motif but not an intracellular retention signal when substituted for the transferrin receptor cytoplasmic domain. J Cell Biol. 124:705-15.

Gerrard, S.R., N.J. Bryant, and T.H. Stevens. 2000. VPS21 controls entry of endocytosed and biosynthetic proteins into the yeast prevacuolar compartment. Mol Biol Cell. 11:613-26.

Giorgino, F., O. de Robertis, L. Laviola, C. Montrone, S. Perrini, K.C. McCowen, and R.J. Smith. 2000. The sentrin-conjugating enzyme mUbc9 interacts with GLUT4 and GLUT1 glucose transporters and regulates transporter levels in skeletal muscle cells. Proc Natl Acad Sci U S A. 97:1125-30.

Gould, G.W., and G.I. Bell. 1990. Facilitative glucose transporters: an expanding family. Trends Biochem Sci. 15:18-23.

Grenson, M. 1983a. Inactivation-reactivation process and repression of permease formation regulate several ammonia-sensitive permeases in the yeast Saccharomyces cerevisiae. Eur J Biochem. 133:135-9.

Grenson, M. 1983b. Study of the positive control of the general amino-acid permease and other ammonia-sensitive uptake systems by the product of the NPR1 gene in the yeast Saccharomyces cerevisiae. Eur J Biochem. 133:141-4.

Grenson, M., C. Hou, and M. Crabeel. 1970. Multiplicity of the amino acid permeases in Saccharomyces cerevisiae. IV. Evidence for a general amino acid permease. J Bacteriol. 103:770-7.

Guthrie, C., and G.R. Fink. 1991. Guide to Yeast Genetics and Molecular Cell Biology. Academic Press, Orlando, FL USA.

Hanahan, D. 1983. Studies on transformation of Escherichia coli with plasmids. J Mol Biol. 166:557-80.

Haney, P.M., M.A. Levy, M.S. Strube, and M. Mueckler. 1995. Insulin-sensitive targeting of the GLUT4 glucose transporter in L6 myoblasts is conferred by its COOH-terminal cytoplasmic tail. J Cell Biol. 129:641-58.

Hashiramoto, M., and D.E. James. 2000. Characterization of insulin-responsive GLUT4 storage vesicles isolated from 3T3-L1 adipocytes. Mol Cell Biol. 20:416-27.

Hay, R.T. 2005. SUMO: a history of modification. Mol Cell. 18:1-12.

Heim, R., A.B. Cubitt, and R.Y. Tsien. 1995. Improved green fluorescence. Nature. 373:663-4.

Hein, C., and B. Andre. 1997. A C-terminal di-leucine motif and nearby sequences are required for NH4(+)-induced inactivation and degradation of the general amino acid permease, Gap1p, of Saccharomyces cerevisiae. Mol Microbiol. 24:607-16.

Hein, C., J.Y. Springael, C. Volland, R. Haguenauer-Tsapis, and B. Andre. 1995. NPI1, an essential yeast gene involved in induced degradation of Gap1 and Fur4 permeases, encodes the Rsp5 ubiquitin-protein ligase. Mol Microbiol. 18:77-87.

Helliwell, S.B., S. Losko, and C.A. Kaiser. 2001. Components of a ubiquitin ligase complex specify polyubiquitination and intracellular trafficking of the general amino acid permease. J Cell Biol. 153:649-62.

Hershko, A., and A. Ciechanover. 1998. The ubiquitin system. Annu Rev Biochem. 67:425-79.

Hertzel, A.V., M.A. Sanders, and D.A. Bernlohr. 2000. Adenovirus-mediated gene transfer in primary murine adipocytes. J Lipid Res. 41:1082-6.

Hicke, L. 2001. Protein regulation by monoubiquitin. Nat Rev Mol Cell Biol. 2:195-201.

Hicke, L., and R. Dunn. 2003. Regulation of membrane protein transport by ubiquitin and ubiquitin-binding proteins. Annu Rev Cell Dev Biol. 19:141-72.

Hicke, L., H.L. Schubert, and C.P. Hill. 2005. Ubiquitin-binding domains. Nat Rev Mol Cell Biol. 6:610-21.

Hochstrasser, M., M.J. Ellison, V. Chau, and A. Varshavsky. 1991. The short-lived MAT alpha 2 transcriptional regulator is ubiquitinated in vivo. Proc Natl Acad Sci U S A. 88:4606-10.

Hoege, C., B. Pfander, G.L. Moldovan, G. Pyrowolakis, and S. Jentsch. 2002. RAD6-dependent DNA repair is linked to modification of PCNA by ubiquitin and SUMO. Nature. 419:135-41.

Holman, G.D., L. Lo Leggio, and S.W. Cushman. 1994. Insulin-stimulated GLUT4 glucose transporter recycling. A problem in membrane protein subcellular trafficking through multiple pools. J Biol Chem. 269:17516-24.

Horak, J. 1986. Amino acid transport in eucaryotic microorganisms. Biochim Biophys Acta. 864:223-56.

Horak, J. 2003. The role of ubiquitin in down-regulation and intracellular sorting of membrane proteins: insights from yeast. Biochim Biophys Acta. 1614:139-55.

Horton, R.M., Z.L. Cai, S.N. Ho, and L.R. Pease. 1990. Gene splicing by overlap extension: tailor-made genes using the polymerase chain reaction. Biotechniques. 8:528-35.

Hou, D., C. Cenciarelli, J.P. Jensen, H.B. Nguygen, and A.M. Weissman. 1994. Activation-dependent ubiquitination of a T cell antigen receptor subunit on multiple intracellular lysines. J Biol Chem. 269:14244-7.

Huibregtse, J.M., M. Scheffner, S. Beaudenon, and P.M. Howley. 1995. A family of proteins structurally and functionally related to the E6-AP ubiquitin-protein ligase. Proc Natl Acad Sci U S A. 92:2563-7.

Hurley, J.H., S. Lee, and G. Prag. 2006. Ubiquitin-binding domains. Biochem J. 399:361-72.

Ito, H., Y. Fukuda, K. Murata, and A. Kimura. 1983. Transformation of intact yeast cells treated with alkali cations. J Bacteriol. 153:163-8.

James, D.E., R. Brown, J. Navarro, and P.F. Pilch. 1988. Insulin-regulatable tissues express a unique insulin-sensitive glucose transport protein. Nature. 333:183-5.

Jauniaux, J.C., and M. Grenson. 1990. GAP1, the general amino acid permease gene of Saccharomyces cerevisiae. Nucleotide sequence, protein similarity with the other bakers yeast amino acid permeases, and nitrogen catabolite repression. Eur J Biochem. 190:39-44.

Jentsch, S., and G. Pyrowolakis. 2000. Ubiquitin and its kin: how close are the family ties? Trends Cell Biol. 10:335-42.

Joost, H.G., and B. Thorens. 2001. The extended GLUT-family of sugar/polyol transport facilitators: nomenclature, sequence characteristics, and potential function of its novel members (review). Mol Membr Biol. 18:247-56.

Kamsteeg, E.J., G. Hendriks, M. Boone, I.B. Konings, V. Oorschot, P. van der Sluijs, J. Klumperman, and P.M. Deen. 2006. Short-chain ubiquitination mediates the regulated endocytosis of the aquaporin-2 water channel. Proc Natl Acad Sci U S A. 103:18344-9.

Kandror, K.V., and P.F. Pilch. 1996a. Compartmentalization of protein traffic in insulin-sensitive cells. Am J Physiol. 271:E1-14.

Kandror, K.V., and P.F. Pilch. 1996b. The insulin-like growth factor II/mannose 6-phosphate receptor utilizes the same membrane compartments as GLUT4 for insulin-dependent trafficking to and from the rat adipocyte cell surface. J Biol Chem. 271:21703-8.

Kao, A.W., B.P. Ceresa, S.R. Santeler, and J.E. Pessin. 1998. Expression of a dominant interfering dynamin mutant in 3T3L1 adipocytes inhibits GLUT4 endocytosis without affecting insulin signaling. J Biol Chem. 273:25450-7.

Kasahara, T., and M. Kasahara. 1996. Expression of the rat GLUT1 glucose transporter in the yeast Saccharomyces cerevisiae. Biochem J. 315 (Pt 1):177-82.

Kasahara, T., and M. Kasahara. 1997. Characterization of rat Glut4 glucose transporter expressed in the yeast Saccharomyces cerevisiae: comparison with Glut1 glucose transporter. Biochim Biophys Acta. 1324:111-9.

Katzmann, D.J., G. Odorizzi, and S.D. Emr. 2002. Receptor downregulation and multivesicular-body sorting. Nat Rev Mol Cell Biol. 3:893-905.

Kawanishi, M., Y. Tamori, H. Okazawa, S. Araki, H. Shinoda, and M. Kasuga. 2000. Role of SNAP23 in insulin-induced translocation of GLUT4 in 3T3-L1 adipocytes. Mediation of complex formation between syntaxin4 and VAMP2. J Biol Chem. 275:8240-7.

Khan, A.H., E. Capilla, J.C. Hou, R.T. Watson, J.R. Smith, and J.E. Pessin. 2004. Entry of newly synthesized GLUT4 into the insulin-responsive storage compartment is dependent upon both the amino terminus and the large cytoplasmic loop. J Biol Chem. 279:37505-11.

King, H., R.E. Aubert, and W.H. Herman. 1998. Global burden of diabetes, 1995-2025: prevalence, numerical estimates, and projections. Diabetes Care. 21:1414-31.

Kolling, R., and C.P. Hollenberg. 1994. The ABC-transporter Ste6 accumulates in the plasma membrane in a ubiquitinated form in endocytosis mutants. Embo J. 13:3261-71.

Laemmli, U.K. 1970. Cleavage of structural proteins during the assembly of the head of bacteriophage T4. Nature. 227:680-5.

Lalioti, V., S. Vergarajauregui, and I.V. Sandoval. 2001. Targeting motifs in GLUT4 (review). Mol Membr Biol. 18:257-64.

Lalioti, V.S., S. Vergarajauregui, D. Pulido, and I.V. Sandoval. 2002. The insulin-sensitive glucose transporter, GLUT4, interacts physically with Daxx. Two proteins with capacity to bind Ubc9 and conjugated to SUMO1. J Biol Chem. 277:19783-91.

Lasko, P.F., and M.C. Brandriss. 1981. Proline transport in Saccharomyces cerevisiae. J Bacteriol. 148:241-7.

Lawson, T.G., D.L. Gronros, P.E. Evans, M.C. Bastien, K.M. Michalewich, J.K. Clark, J.H. Edmonds, K.H. Graber, J.A. Werner, B.A. Lurvey, and J.M. Cate. 1999. Identification and characterization of a protein destruction signal in the encephalomyocarditis virus 3C protease. J Biol Chem. 274:9871-80.

Lee, J., and P.F. Pilch. 1994. The insulin receptor: structure, function, and signaling. Am J Physiol. 266:C319-34.

Li, L.V., and K.V. Kandror. 2005. Golgi-localized, gamma-ear-containing, Arf-binding protein adaptors mediate insulin-responsive trafficking of glucose transporter 4 in 3T3-L1 adipocytes. Mol Endocrinol. 19:2145-53.

Livingstone, C., D.E. James, J.E. Rice, D. Hanpeter, and G.W. Gould. 1996. Compartment ablation analysis of the insulin-responsive glucose transporter (GLUT4) in 3T3-L1 adipocytes. Biochem J. 315 (Pt 2):487-95.

Magasanik, B., and C.A. Kaiser. 2002. Nitrogen regulation in Saccharomyces cerevisiae. Gene. 290:1-18.

Mallard, F., B.L. Tang, T. Galli, D. Tenza, A. Saint-Pol, X. Yue, C. Antony, W. Hong, B. Goud, and L. Johannes. 2002. Early/recycling endosomes-to-TGN transport involves two SNARE complexes and a Rab6 isoform. J Cell Biol. 156:653-64.

Marsh, B.J., R.A. Alm, S.R. McIntosh, and D.E. James. 1995. Molecular regulation of GLUT-4 targeting in 3T3-L1 adipocytes. J Cell Biol. 130:1081-91.

Marsh, B.J., S. Martin, D.R. Melvin, L.B. Martin, R.A. Alm, G.W. Gould, and D.E. James. 1998. Mutational analysis of the carboxy-terminal phosphorylation site of GLUT-4 in 3T3-L1 adipocytes. Am J Physiol. 275:E412-22.

Marshall, B.A., H. Murata, R.C. Hresko, and M. Mueckler. 1993. Domains that confer intracellular sequestration of the Glut4 glucose transporter in Xenopus oocytes. J Biol Chem. 268:26193-9.

Martin, L.B., A. Shewan, C.A. Millar, G.W. Gould, and D.E. James. 1998. Vesicle-associated membrane protein 2 plays a specific role in the insulin-dependent trafficking of the facilitative glucose transporter GLUT4 in 3T3-L1 adipocytes. J Biol Chem. 273:1444-52.

Martin, S., C.A. Millar, C.T. Lyttle, T. Meerloo, B.J. Marsh, G.W. Gould, and D.E. James. 2000a. Effects of insulin on intracellular GLUT4 vesicles in adipocytes: evidence for a secretory mode of regulation. J Cell Sci. 113 Pt 19:3427-38.

Martin, S., G. Ramm, C.T. Lyttle, T. Meerloo, W. Stoorvogel, and D.E. James. 2000b. Biogenesis of insulin-responsive GLUT4 vesicles is independent of brefeldin A-sensitive trafficking. Traffic. 1:652-60.

Martin, S., J. Tellam, C. Livingstone, J.W. Slot, G.W. Gould, and D.E. James. 1996. The glucose transporter (GLUT-4) and vesicle-associated membrane protein-2 (VAMP-2) are segregated from recycling endosomes in insulin-sensitive cells. J Cell Biol. 134:625-35.

Martinez-Arca, S., V.S. Lalioti, and I.V. Sandoval. 2000. Intracellular targeting and retention of the glucose transporter GLUT4 by the perinuclear storage compartment involves distinct carboxyl-tail motifs. J Cell Sci. 113 (Pt 10):1705-15.

Mascorro-Gallardo, J.O., A.A. Covarrubias, and R. Gaxiola. 1996. Construction of a CUP1 promoter-based vector to modulate gene expression in Saccharomyces cerevisiae. Gene. 172:169-70.

Mattera, R., R. Puertollano, W.J. Smith, and J.S. Bonifacino. 2004. The trihelical bundle subdomain of the GGA proteins interacts with multiple partners through overlapping but distinct sites. J Biol Chem. 279:31409-18.

Mazumder, B., V. Seshadri, and P.L. Fox. 2003. Translational control by the 3'-UTR: the ends specify the means. Trends Biochem Sci. 28:91-8.

Melvin, D.R., B.J. Marsh, A.R. Walmsley, D.E. James, and G.W. Gould. 1999. Analysis of amino and carboxy terminal GLUT-4 targeting motifs in 3T3-L1 adipocytes using an endosomal ablation technique. Biochemistry. 38:1456-62.

Millar, C.A., A. Shewan, G.R. Hickson, D.E. James, and G.W. Gould. 1999. Differential regulation of secretory compartments containing the insulin-responsive glucose transporter 4 in 3T3-L1 adipocytes. Mol Biol Cell. 10:3675-88.

Mitsumoto, Y., and A. Klip. 1992. Development regulation of the subcellular distribution and glycosylation of GLUT1 and GLUT4 glucose transporters during myogenesis of L6 muscle cells. J Biol Chem. 267:4957-62.

Morgenstern, J.P., and H. Land. 1990. Advanced mammalian gene transfer: high titre retroviral vectors with multiple drug selection markers and a complementary helper-free packaging cell line. Nucleic Acids Res. 18:3587-96.

Morita, S., T. Kojima, and T. Kitamura. 2000. Plat-E: an efficient and stable system for transient packaging of retroviruses. Gene Ther. 7:1063-6.

Mu, F.T., J.M. Callaghan, O. Steele-Mortimer, H. Stenmark, R.G. Parton, P.L. Campbell, J. McCluskey, J.P. Yeo, E.P. Tock, and B.H. Toh. 1995. EEA1, an early endosome-associated protein. EEA1 is a conserved alpha-helical peripheral membrane protein flanked by cysteine "fingers" and contains a calmodulin-binding IQ motif. J Biol Chem. 270:13503-11.

Mueckler, M. 1994. Facilitative glucose transporters. Eur J Biochem. 219:713-25.

Mueckler, M., C. Caruso, S.A. Baldwin, M. Panico, I. Blench, H.R. Morris, W.J. Allard, G.E. Lienhard, and H.F. Lodish. 1985. Sequence and structure of a human glucose transporter. Science. 229:941-5.

Nikko, E., A.M. Marini, and B. Andre. 2003. Permease recycling and ubiquitination status reveal a particular role for Bro1 in the multivesicular body pathway. J Biol Chem. 278:50732-43.

Nothwehr, S.F., E. Conibear, and T.H. Stevens. 1995. Golgi and vacuolar membrane proteins reach the vacuole in vps1 mutant yeast cells via the plasma membrane. J Cell Biol. 129:35-46.

Odorizzi, G., D.J. Katzmann, M. Babst, A. Audhya, and S.D. Emr. 2003. Bro1 is an endosome-associated protein that functions in the MVB pathway in Saccharomyces cerevisiae. J Cell Sci. 116:1893-903.

Ohno, A., J. Jee, K. Fujiwara, T. Tenno, N. Goda, H. Tochio, H. Kobayashi, H. Hiroaki, and M. Shirakawa. 2005. Structure of the UBA domain of Dsk2p in complex with ubiquitin molecular determinants for ubiquitin recognition. Structure. 13:521-32.

Olson, A.L., and J.E. Pessin. 1996. Structure, function, and regulation of the mammalian facilitative glucose transporter gene family. Annu Rev Nutr. 16:235-56.

Palacios, S., V. Lalioti, S. Martinez-Arca, S. Chattopadhyay, and I.V. Sandoval. 2001. Recycling of the insulin-sensitive glucose transporter GLUT4. Access of surface internalized GLUT4 molecules to the perinuclear storage compartment is mediated by the Phe5-Gln6-Glu7-Ile8 motif. J Biol Chem. 276:3371-83.

Pelham, H.R. 2004. Membrane traffic: GGAs sort ubiquitin. Curr Biol. 14:R357-9.

Peng, J., D. Schwartz, J.E. Elias, C.C. Thoreen, D. Cheng, G. Marsischky, J. Roelofs, D. Finley, and S.P. Gygi. 2003. A proteomics approach to understanding protein ubiquitination. Nat Biotechnol. 21:921-6.

Pessin, J.E., and G.I. Bell. 1992. Mammalian facilitative glucose transporter family: structure and molecular regulation. Annu Rev Physiol. 54:911-30.

Piper, R.C., N.J. Bryant, and T.H. Stevens. 1997. The membrane protein alkaline phosphatase is delivered to the vacuole by a route that is distinct from the VPS-dependent pathway. J Cell Biol. 138:531-45.

Piper, R.C., A.A. Cooper, H. Yang, and T.H. Stevens. 1995. VPS27 controls vacuolar and endocytic traffic through a prevacuolar compartment in Saccharomyces cerevisiae. J Cell Biol. 131:603-17.

Piper, R.C., L.J. Hess, and D.E. James. 1991. Differential sorting of two glucose transporters expressed in insulin-sensitive cells. Am J Physiol. 260:C570-80.

Piper, R.C., C. Tai, P. Kulesza, S. Pang, D. Warnock, J. Baenziger, J.W. Slot, H.J. Geuze, C. Puri, and D.E. James. 1993. GLUT-4 NH2 terminus contains a phenylalanine-based targeting motif that regulates intracellular sequestration. J Cell Biol. 121:1221-32.

Piper, R.C., C. Tai, J.W. Slot, C.S. Hahn, C.M. Rice, H. Huang, and D.E. James. 1992. The efficient intracellular sequestration of the insulin-regulatable glucose transporter (GLUT-4) is conferred by the NH2 terminus. J Cell Biol. 117:729-43.

Piper, R.C., E.A. Whitters, and T.H. Stevens. 1994. Yeast Vps45p is a Sec1p-like protein required for the consumption of vacuole-targeted, post-Golgi transport vesicles. Eur J Cell Biol. 65:305-18.

Puertollano, R., R.C. Aguilar, I. Gorshkova, R.J. Crouch, and J.S. Bonifacino. 2001. Sorting of mannose 6-phosphate receptors mediated by the GGAs. Science. 292:1712-6.

Quon, M.J., M.J. Zarnowski, M. Guerre-Millo, M. de la Luz Sierra, S.I. Taylor, and S.W. Cushman. 1993. Transfection of DNA into isolated rat adipose cells by electroporation: evaluation of promoter activity in transfected adipose cells which are highly responsive to insulin after one day in culture. Biochem Biophys Res Commun. 194:338-46.

Ramm, G., J.W. Slot, D.E. James, and W. Stoorvogel. 2000. Insulin recruits GLUT4 from specialized VAMP2-carrying vesicles as well as from the dynamic endosomal/trans-Golgi network in rat adipocytes. Mol Biol Cell. 11:4079-91.

Raymond, C.K., I. Howald-Stevenson, C.A. Vater, and T.H. Stevens. 1992. Morphological classification of the yeast vacuolar protein sorting mutants: evidence for a prevacuolar compartment in class E vps mutants. Mol Biol Cell. 3:1389-402.

Rea, S., and D.E. James. 1997. Moving GLUT4: the biogenesis and trafficking of GLUT4 storage vesicles. Diabetes. 46:1667-77.

Redding, K., C. Holcomb, and R.S. Fuller. 1991. Immunolocalization of Kex2 protease identifies a putative late Golgi compartment in the yeast Saccharomyces cerevisiae. J Cell Biol. 113:527-38.

Reifenberger, E., K. Freidel, and M. Ciriacy. 1995. Identification of novel HXT genes in Saccharomyces cerevisiae reveals the impact of individual hexose transporters on glycolytic flux. Mol Microbiol. 16:157-67.

Roberg, K.J., N. Rowley, and C.A. Kaiser. 1997. Physiological regulation of membrane protein sorting late in the secretory pathway of Saccharomyces cerevisiae. J Cell Biol. 137:1469-82.

Robinson, J.S., D.J. Klionsky, L.M. Banta, and S.D. Emr. 1988. Protein sorting in Saccharomyces cerevisiae: isolation of mutants defective in the delivery and processing of multiple vacuolar hydrolases. Mol Cell Biol. 8:4936-48.

Robinson, L.J., S. Pang, D.S. Harris, J. Heuser, and D.E. James. 1992. Translocation of the glucose transporter (GLUT4) to the cell surface in permeabilized 3T3-L1 adipocytes: effects of ATP insulin, and GTP gamma S and localization of GLUT4 to clathrin lattices. J Cell Biol. 117:1181-96.

Rothman, J.H., I. Howald, and T.H. Stevens. 1989. Characterization of genes required for protein sorting and vacuolar function in the yeast Saccharomyces cerevisiae. Embo J. 8:2057-65.

Rubio-Texeira, M., and C.A. Kaiser. 2006. Amino acids regulate retrieval of the yeast general amino acid permease from the vacuolar targeting pathway. Mol Biol Cell. 17:3031-50.

Salghetti, S.E., A.A. Caudy, J.G. Chenoweth, and W.P. Tansey. 2001. Regulation of transcriptional activation domain function by ubiquitin. Science. 293:1651-3.

Saltiel, A.R., and C.R. Kahn. 2001. Insulin signalling and the regulation of glucose and lipid metabolism. Nature. 414:799-806.

Saltiel, A.R., and J.E. Pessin. 2003. Insulin signaling in microdomains of the plasma membrane. Traffic. 4:711-6.

Sambrook, D.W.R.J. 2001. Molecular Cloning: A Laboratory Manual. Cold Spring Harbor Laboratory Press.

Sano, H., S. Kane, E. Sano, C.P. Miinea, J.M. Asara, W.S. Lane, C.W. Garner, and G.E. Lienhard. 2003. Insulin-stimulated phosphorylation of a Rab GTPase-activating protein regulates GLUT4 translocation. J Biol Chem. 278:14599-602.

Schwartz, D.C., and M. Hochstrasser. 2003. A superfamily of protein tags: ubiquitin, SUMO and related modifiers. Trends Biochem Sci. 28:321-8.

Scott, P.M., P.S. Bilodeau, O. Zhdankina, S.C. Winistorfer, M.J. Hauglund, M.M. Allaman, W.R. Kearney, A.D. Robertson, A.L. Boman, and R.C. Piper. 2004. GGA proteins bind ubiquitin to facilitate sorting at the trans-Golgi network. Nat Cell Biol. 6:252-9.

Sesti, G. 2006. Pathophysiology of insulin resistance. Best Pract Res Clin Endocrinol Metab. 20:665-79.

Sherman, F., Fink, G.R. and Hinks, J. 1986. Methods in Yeast Genetics. Cold Spring Laboratory Press, Cold Spring Harbor, NY:pp. 146-153.

Shewan, A.M., B.J. Marsh, D.R. Melvin, S. Martin, G.W. Gould, and D.E. James. 2000. The cytosolic C-terminus of the glucose transporter GLUT4 contains an acidic cluster endosomal targeting motif distal to the dileucine signal. Biochem J. 350 Pt 1:99-107.

Shewan, A.M., E.M. van Dam, S. Martin, T.B. Luen, W. Hong, N.J. Bryant, and D.E. James. 2003. GLUT4 recycles via a trans-Golgi network (TGN) subdomain enriched in Syntaxins 6 and 16 but not TGN38: involvement of an acidic targeting motif. Mol Biol Cell. 14:973-86.

Shin, J.S., M. Ebersold, M. Pypaert, L. Delamarre, A. Hartley, and I. Mellman. 2006. Surface expression of MHC class II in dendritic cells is controlled by regulated ubiquitination. Nature. 444:115-8.

Sikorski, R.S., and P. Hieter. 1989. A system of shuttle vectors and yeast host strains designed for efficient manipulation of DNA in Saccharomyces cerevisiae. Genetics. 122:19-27.

Slot, J.W., H.J. Geuze, S. Gigengack, D.E. James, and G.E. Lienhard. 1991a. Translocation of the glucose transporter GLUT4 in cardiac myocytes of the rat. Proc Natl Acad Sci U S A. 88:7815-9.

Slot, J.W., H.J. Geuze, S. Gigengack, G.E. Lienhard, and D.E. James. 1991b. Immuno-localization of the insulin regulatable glucose transporter in brown adipose tissue of the rat. J Cell Biol. 113:123-35.

Soetens, O., J.O. De Craene, and B. Andre. 2001. Ubiquitin is required for sorting to the vacuole of the yeast general amino acid permease, Gap1. J Biol Chem. 276:43949-57.

Sophianopoulou, V., and G. Diallinas. 1995. Amino acid transporters of lower eukaryotes: regulation, structure and topogenesis. FEMS Microbiol Rev. 16:53-75.

Springael, J.Y., and B. Andre. 1998. Nitrogen-regulated ubiquitination of the Gap1 permease of Saccharomyces cerevisiae. Mol Biol Cell. 9:1253-63.

Springael, J.Y., J.M. Galan, R. Haguenauer-Tsapis, and B. Andre. 1999. NH4+-induced down-regulation of the Saccharomyces cerevisiae Gap1p permease involves its ubiquitination with lysine-63-linked chains. J Cell Sci. 112 (Pt 9):1375-83.

Stanbrough, M., and B. Magasanik. 1995. Transcriptional and posttranslational regulation of the general amino acid permease of Saccharomyces cerevisiae. J Bacteriol. 177:94-102.

Stanbrough, M., D.W. Rowen, and B. Magasanik. 1995. Role of the GATA factors Gln3p and Nil1p of Saccharomyces cerevisiae in the expression of nitrogen-regulated genes. Proc Natl Acad Sci U S A. 92:9450-4.

Sun, X.J., J.L. Goldberg, L.Y. Qiao, and J.J. Mitchell. 1999. Insulin-induced insulin receptor substrate-1 degradation is mediated by the proteasome degradation pathway. Diabetes. 48:1359-64.

Sychrova, H., and M.R. Chevallier. 1993. Cloning and sequencing of the Saccharomyces cerevisiae gene LYP1 coding for a lysine-specific permease. Yeast. 9:771-82.

Tanaka, J., and G.R. Fink. 1985. The histidine permease gene (HIP1) of Saccharomyces cerevisiae. Gene. 38:205-14.

Tanner, L.I., and G.E. Lienhard. 1987. Insulin elicits a redistribution of transferrin receptors in 3T3-L1 adipocytes through an increase in the rate constant for receptor externalization. J Biol Chem. 262:8975-80.

Tellam, J.T., S.L. Macaulay, S. McIntosh, D.R. Hewish, C.W. Ward, and D.E. James. 1997. Characterization of Munc-18c and syntaxin-4 in 3T3-L1 adipocytes. Putative role in insulin-dependent movement of GLUT-4. J Biol Chem. 272:6179-86.

Thorens, B. 1996. Glucose transporters in the regulation of intestinal, renal, and liver glucose fluxes. Am J Physiol. 270:G541-53.

Thorens, B., H.K. Sarkar, H.R. Kaback, and H.F. Lodish. 1988. Cloning and functional expression in bacteria of a novel glucose transporter present in liver, intestine, kidney, and beta-pancreatic islet cells. Cell. 55:281-90.

Thrower, J.S., L. Hoffman, M. Rechsteiner, and C.M. Pickart. 2000. Recognition of the polyubiquitin proteolytic signal. Embo J. 19:94-102.

Thurmond, D.C., and J.E. Pessin. 2001. Molecular machinery involved in the insulin-regulated fusion of GLUT4-containing vesicles with the plasma membrane (review). Mol Membr Biol. 18:237-45.

Treier, M., L.M. Staszewski, and D. Bohmann. 1994. Ubiquitin-dependent c-Jun degradation in vivo is mediated by the delta domain. Cell. 78:787-98.

Urbe, S. 2005. Ubiquitin and endocytic protein sorting. Essays Biochem. 41:81-98.

Vandenbol, M., J.C. Jauniaux, and M. Grenson. 1989. Nucleotide sequence of the Saccharomyces cerevisiae PUT4 proline-permease-encoding gene: similarities between CAN1, HIP1 and PUT4 permeases. Gene. 83:153-9.

Verhey, K.J., S.F. Hausdorff, and M.J. Birnbaum. 1993. Identification of the carboxy terminus as important for the isoform-specific subcellular targeting of glucose transporter proteins. J Cell Biol. 123:137-47.

Verhey, K.J., J.I. Yeh, and M.J. Birnbaum. 1995. Distinct signals in the GLUT4 glucose transporter for internalization and for targeting to an insulin-responsive compartment. J Cell Biol. 130:1071-9.

Vida, T.A., and S.D. Emr. 1995. A new vital stain for visualizing vacuolar membrane dynamics and endocytosis in yeast. J Cell Biol. 128:779-92.

Volchuk, A., Q. Wang, H.S. Ewart, Z. Liu, L. He, M.K. Bennett, and A. Klip. 1996. Syntaxin 4 in 3T3-L1 adipocytes: regulation by insulin and participation in insulin-dependent glucose transport. Mol Biol Cell. 7:1075-82.

Watson, R.T., M. Kanzaki, and J.E. Pessin. 2004a. Regulated membrane trafficking of the insulin-responsive glucose transporter 4 in adipocytes. Endocr Rev. 25:177-204.

Watson, R.T., A.H. Khan, M. Furukawa, J.C. Hou, L. Li, M. Kanzaki, S. Okada, K.V. Kandror, and J.E. Pessin. 2004b. Entry of newly synthesized GLUT4 into the insulin-responsive storage compartment is GGA dependent. Embo J. 23:2059-70.

Watson, R.T., and J.E. Pessin. 2006. Bridging the GAP between insulin signaling and GLUT4 translocation. Trends Biochem Sci. 31:215-22.

Weissman, A.M. 2001. Themes and variations on ubiquitylation. Nat Rev Mol Cell Biol. 2:169-78.

Wieczorke, R., S. Dlugai, S. Krampe, and E. Boles. 2003. Characterisation of mammalian GLUT glucose transporters in a heterologous yeast expression system. Cell Physiol Biochem. 13:123-34.

Wilcox, C.A., and R.S. Fuller. 1991. Posttranslational processing of the prohormone-cleaving Kex2 protease in the Saccharomyces cerevisiae secretory pathway. J Cell Biol. 115:297-307.

Wilcox, C.A., K. Redding, R. Wright, and R.S. Fuller. 1992. Mutation of a tyrosine localization signal in the cytosolic tail of yeast Kex2 protease disrupts Golgi retention and results in default transport to the vacuole. Mol Biol Cell. 3:1353-71.

Wolf, D.H., and G.R. Fink. 1975. Proteinase C (carboxypeptidase Y) mutant of yeast. J Bacteriol. 123:1150-6.

Woolford, C.A., L.B. Daniels, F.J. Park, E.W. Jones, J.N. Van Arsdell, and M.A. Innis. 1986. The PEP4 gene encodes an aspartyl protease implicated in the posttranslational regulation of Saccharomyces cerevisiae vacuolar hydrolases. Mol Cell Biol. 6:2500-10.

Yashiroda, H., D. Kaida, A. Toh-e, and Y. Kikuchi. 1998. The PY-motif of Bul1 protein is essential for growth of Saccharomyces cerevisiae under various stress conditions. Gene. 225:39-46.

Yashiroda, H., T. Oguchi, Y. Yasuda, E.A. Toh, and Y. Kikuchi. 1996. Bul1, a new protein that binds to the Rsp5 ubiquitin ligase in Saccharomyces cerevisiae. Mol Cell Biol. 16:3255-63.

Yu, C., J. Cresswell, M.G. Loffler, and J.S. Bogan. 2007. The GLUT4 regulating protein TUG is essential for highly insulin responsive glucose uptake in 3T3-L1 adipocytes. J Biol Chem.

Zerial, M., and H. McBride. 2001. Rab proteins as membrane organizers. Nat Rev Mol Cell Biol. 2:107-17.

Zhande, R., J.J. Mitchell, J. Wu, and X.J. Sun. 2002. Molecular mechanism of insulin-induced degradation of insulin receptor substrate 1. Mol Cell Biol. 22:1016-26.

Zimmet, P., K.G. Alberti, and J. Shaw. 2001. Global and societal implications of the diabetes epidemic. Nature. 414:782-7.